Chapter 14

Experimental astronomy and astrophysics

	page
Attenuation of electromagnetic radiation	291
Extrapolated absorption and absorption-jump ratios	292
Mass attenuation coefficients, ranges, cross-sections	292
Fluorescence yields	304
Passage of charged particles through matter	304
Total ionization loss by electrons or positrons	304
Radiative loss for non-relativistic electrons	305
Ionization and radiative loss for highly relativistic electrons	306
Total ionization loss by heavy charged particles	307
Approximate range–energy relationships	307
Charged particles in silicon	309
Radioactive sources	311
X-ray sources	311
Alpha sources	312
Gamma-ray energy standards	312
Electron energy standards	313
Characteristics of synchrotron radiation	314
Practical formulae for electron storage rings	316
X-ray spectroscopy	318
Crystal spectroscopy	318
Crystal properties	319
Useful characteristic lines for X-ray spectroscopy	320
Grating spectroscopy	320
Reflection of X-rays	322
Optical constants at soft X-ray wavelengths	325
Reflectivity vs. wavelength (energy)	326
Wolter type I mirror system	332

© Cambridge University Press • Provided by the NASA Astrophysics Data System

Vacuum technology 333
Equivalents for various cryogenic fluids 334
Optical point spread function 334
The line spread function 335
The edge trace 335
The modulation transfer function 335
The full-width half maximum 336
The root mean square radius 336
The encircled energy function 336
The half-power radius 336
Point spread function for a circular aperture 337
Optical telescopes 339
Photometry 341
Spectral luminous efficiency 341
Summary of typical sources/parameters 343
Conversion table for various photometric units 343
Luminance values for various sources 344
Typical values of natural scene illuminance 344
Radiant responsivity 345
Standard units, symbols, and defining equations 346
Detectors 348
Visible and ultraviolet light detectors 348
X-ray and gamma-ray detectors 358
Microcomputer topics 370
ASCII character code 370
Boolean algebra 373
Logic gates 374
The RS-232-C standard 375
Parallel interface 376
IEEE 488 interface 377
Data transmission 378
Bibliography 378

© Cambridge University Press • Provided by the NASA Astrophysics Data System

$I = I_0 e^{-(\mu/\rho)\rho t}$,

I_0 = initial intensity of a collimated photon beam,

I = intensity of beam after traversing a thickness t of material density ρ,

(μ/ρ) = total mass attenuation coefficient

$= \sigma/\rho + \tau/\rho + k/\rho$,

σ/ρ = total Compton mass attenuation coefficient,

τ/ρ = photoelectric mass absorption coefficient

$(\sim \frac{Z^4}{A} E^{-8/3}$ between absorption edges),

k/ρ = pair production mass attenuation coefficient.

Mixtures of materials:

$$\mu/\rho = \sum_i (\mu_i/\rho_i)\omega_i,$$

where

μ_i/ρ_i = mass attenuation coefficient of element i,

ω_i = fraction by weight of element i.

Photon mean free path $= [(\mu/\rho)\rho]^{-1}$.

Relative importance of the three major types of electromagnetic interactions. The lines show the values of Z and $h\nu$ for which the two neighboring effects are just equal. (Evans, R. D., *The Atomic Nucleus*, McGraw-Hill, 1955, with permission.)

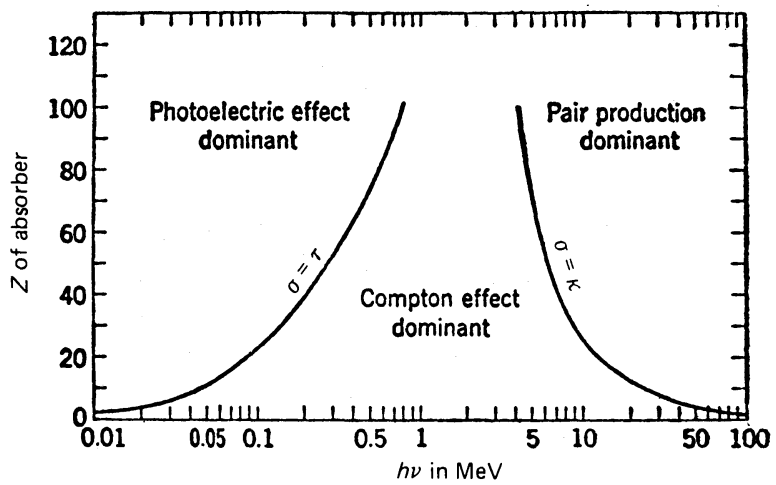

© Cambridge University Press • Provided by the NASA Astrophysics Data System

Extrapolated absorption and absorption-jump ratios (r) ***at the K-edge***

Z	element	Atomic weight	Density ($g\,cm^{-3}$)	λ_k (Å)	E_k (keV)	Fluor. yield ω_k	$(\mu/\rho)^-$ ($cm^2\,g^{-1}$)	$(\mu/\rho)^+$ ($cm^2\,g^{-1}$)	r
4	Be	9.01	1.85	112	0.111		179 000	(5000)	(35)
5	B	10.81	2.34	66.0	0.188		88 400	3130	28.3
6	C	12.01	2.26	43.7	0.284		53 900	2230	24.2
7	N	14.01	0.001 25	30.9	0.402		32 800	1540	21.4
8	O	16.00	0.001 43	23.3	0.532		22 400	1160	19.3
9	F	19.00	0.001 70	18.1	0.685		14 800	846	17.5
10	Ne	20.18	0.000 90	14.3	0.867		10 950	687	15.94
11	Na	22.99	0.97	11.56	1.072		7760	525	14.78
12	Mg	24.31	1.74	9.50	1.305		6000	440	13.63
13	Al	26.98	2.70	7.95	1.560	0.036	4500	355	12.68
14	Si	28.09	2.33	6.74	1.839	0.047	3640	307	11.89
15	P	30.97	1.82	5.77	2.146	0.060	2800	251	11.18
16	S	32.06	2.07	5.01	2.472	0.076	2340	222	10.52
17	Cl	35.45	0.003 17	4.38	2.822	0.094	1840	185	9.92
18	Ar	39.95	0.001 78	3.87	3.203	0.115	1440	154	9.34
19	K	39.10	0.86	3.44	3.607	0.138	1300	148	8.79
20	Ca	40.08	1.55	3.07	4.038	0.163	1120	135	8.28

(After Henke, B. L. & Elgin, R. L. in *Advances in X-ray Analysis*, Vol. 13, Plenum Press, New York, 1970.)

Mass attenuation coefficients ($cm^2\,g^{-1}$)

Wavelength (Å)	Polypropylene (CH_2)	Mylar ($C_{10}H_8O_4$)	Teflon (CF_2)	Air 0 = 21 % N = 78 % Ar = 1 %	P 10 CH_4 = 10 % Ar = 90 %	Methane (CH_4)	Energy (eV)
2.0	8	14	28	21	230	7	6199.0
4.0	69	116	220	148	162	60	3099.5
6.0	234	384	700	481	467	205	2066.3
8.0	550	870	1540	1090	1020	479	1549.8
10.0	1040	1630	2800	2020	1850	910	1239.8
12.0	1740	2680	4250	3310	3010	1520	1033.2
14.0	2660	4040	6700	4980	4500	2330	885.6
16.0	3830	5800	9400	7100	6400	3350	774.9
18.0	5200	7800	12 600	9500	8400	4570	688.8
20.0	6900	10 200	2780	12 400	10 900	6100	619.9
22.0	8800	12 900	3540	15 700	13 500	7700	563.5
24.0	11 000	8500	4430	14 100	16 400	9700	516.6
26.0	13 500	10 400	5400	17 100	19 600	11 800	476.8
28.0	16 200	12 400	6500	20 400	22 800	14 100	442.8
30.0	19 200	14 700	7800	24 000	26 300	16 800	413.3
32.0	22 400	17 200	9100	2290	29 700	19 600	387.4
34.0	25 900	19 900	10 600	2650	33 300	22 700	364.6

© Cambridge University Press • Provided by the NASA Astrophysics Data System

Mass attenuation coefficients (*cont.*)

Wavelength (Å)	Polypropylene (CH_2)	Mylar ($C_{10}H_8O_4$)	Teflon (CF_2)	Air O = 21% N = 78% Ar = 1%	P 10 CH_4 = 10% Ar = 90%	Methane (CH_4)	Energy (eV)
36.0	29 600	22 800	12 100	3040	36 900	25 900	344.4
38.0	33 600	25 800	13 800	3460	40 500	29 300	326.3
40.0	37 800	29 100	15 600	3810	37 600	33 000	309.9
42.0	42 200	32 500	17 500	4270	40 900	36 900	295.2
44.0	1940	3350	6900	4780	42 600	1700	281.8
46.0	2180	3760	7800	5300	45 600	1910	269.5
48.0	2430	4170	8600	5900	48 900	2130	258.3
50.0	2690	4590	9500	6400	52 000	2350	248.0
52.0	2960	5100	10 500	6300		2590	238.4
54.0	3240	5600	11 500	7000		2840	229.6
56.0	3540	6100	12 500	7600		3100	221.4
58.0	3860	6600	13 600	8200		3380	213.8
60.0	4190	7200	14 800	8900		3660	206.6
62.0	4540	7800	16 000	9700		3970	200.0
64.0	4880	8400	17 300	10 400		4270	193.7
66.0	5200	9000	18 600	11 200		4570	187.8
68.0	5700	9700	19 900	12 100		4940	182.3
70.0	6000	10 300	21 300	12 900		5200	177.1
72.0	6400	11 100	22 700	13 800		5600	172.2
74.0	6800	11 800	24 200	14 700		6000	167.5
76.0	7300	12 500	25 700	15 600		6400	163.1
78.0	7700	13 300	27 200	16 600		6700	158.9
80.0	8100	14 100	28 800	17 600		7100	155.0
82.0	8600	14 900	30 500	18 600		7600	151.2
84.0	9100	15 800	32 100	19 700		7900	147.6
86.0	9600	16 600	33 800	20 800		8400	144.2
88.0	10 100	17 500	35 500	21 900		8800	140.9
90.0	10 600	18 400	37 300	23 100		9300	137.8
92.0	11 100	19 400	39 100	24 200		9700	134.8
94.0	11 700	20 300	40 900	25 400		10 300	131.9
96.0	12 200	21 300	43 000	26 700		10 700	129.1
98.0	12 800	22 300	44 600	28 000		11 200	126.5
100.0	13 400	23 300	46 300	29 200		11 800	124.0
105.0	15 000	26 000	51 000	32 700		13 100	118.1
110.0	16 600	28 800	56 000	36 200		14 500	112.7
115.0	18 200	31 600	61 000	39 900		15 900	107.8
120.0	20 000	34 600	67 000	43 800		17 500	103.3
125.0	21 900	38 000	72 000	48 000		19 200	99.2
130.0	23 900	41 100	78 000	52 000		20 900	95.4
135.0	25 900	44 600	83 000	57 000		22 700	91.8
140.0	28 100	48 200	89 000	61 000		24 600	88.6
145.0	30 300	52 000	95 000	65 000		26 500	85.5
150.0	32 600	55 000	101 000	71 000		28 500	82.7

(Adapted from *The Handbook of Chemistry and Physics*, CRC Press, Cleveland, 1976.)

© Cambridge University Press • Provided by the NASA Astrophysics Data System

Mass attenuation coefficients (*cont.*)

Total mass-absorption coefficients for gamma-rays in all elements from Be to U. Energy range 1.8 keV–10 MeV. (From *Nucleonics*, **19**, 62, 1961.)

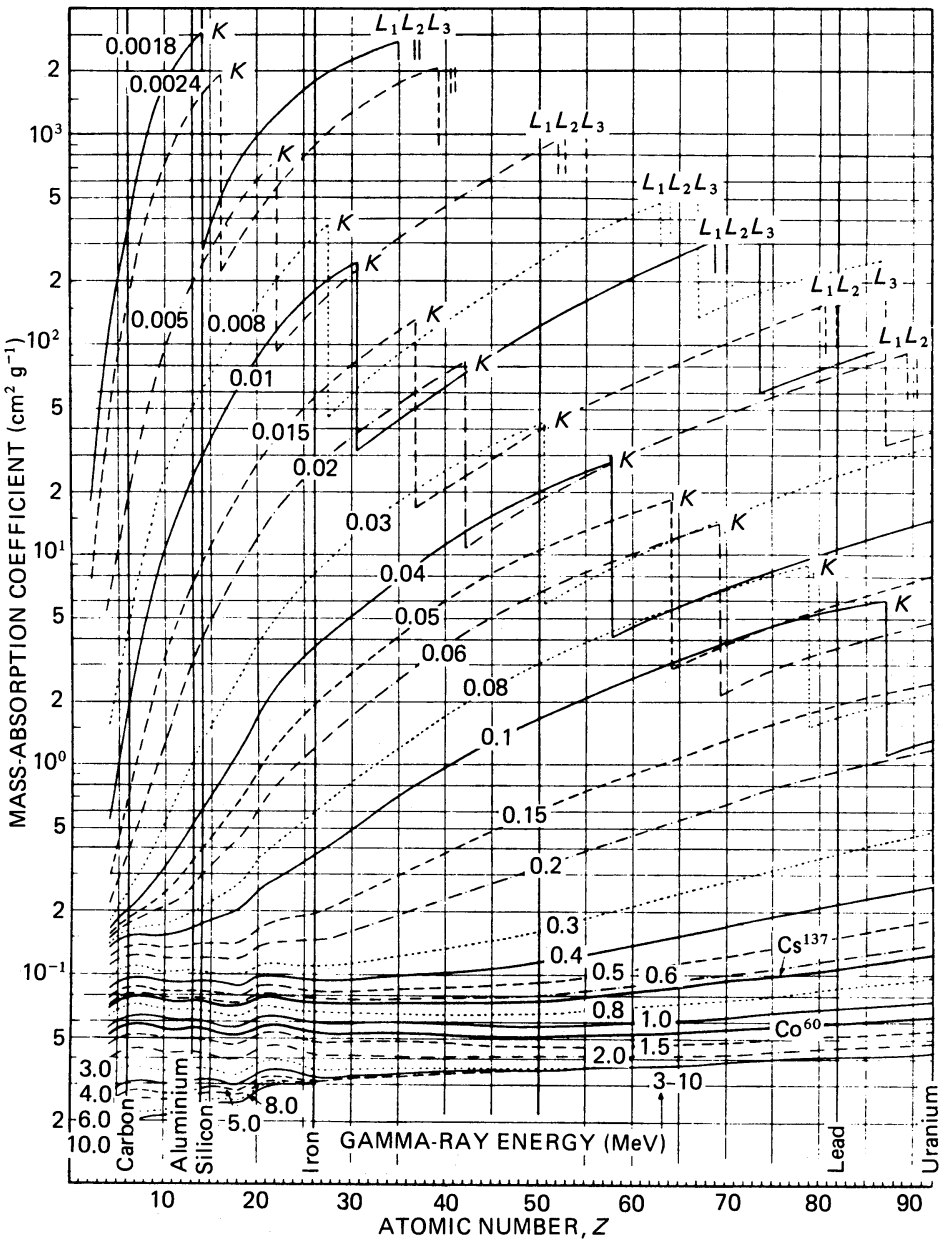

© Cambridge University Press • Provided by the NASA Astrophysics Data System

© Cambridge University Press • Provided by the NASA Astrophysics Data System

Mass attenuation coefficients (*cont.*)

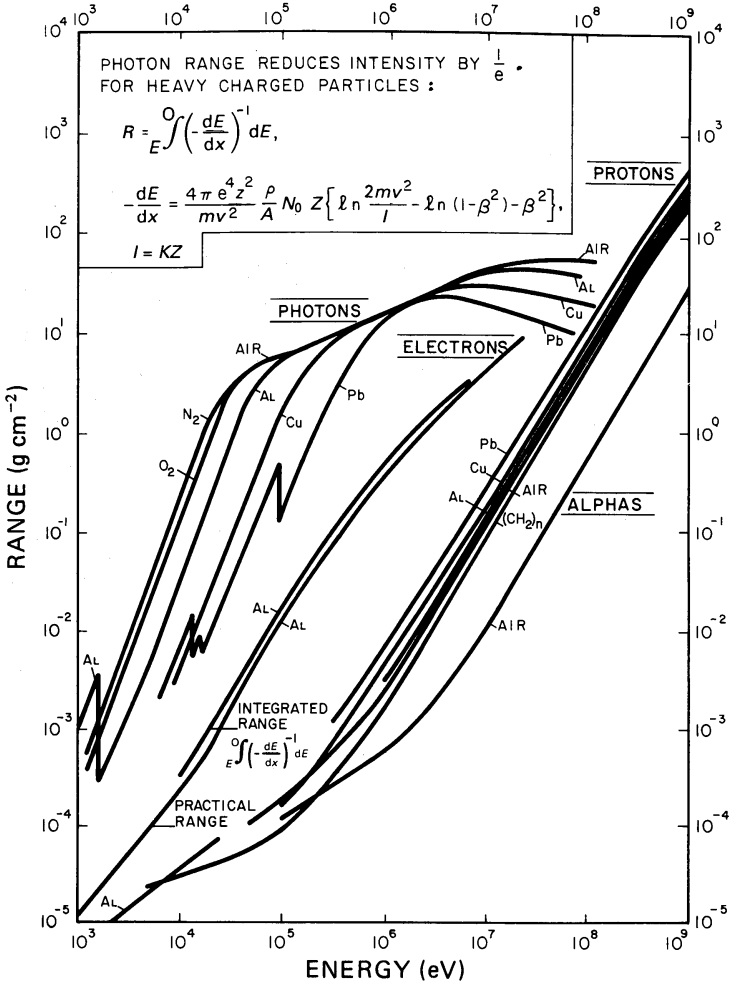

RANGE-ENERGY CURVES FOR PENETRATING RADIATION

(Adapted from Filius, R., *Satellite Instruments Using Solid State Detectors*, Ph.D. thesis, State University of Iowa, Iowa City, 1963.)

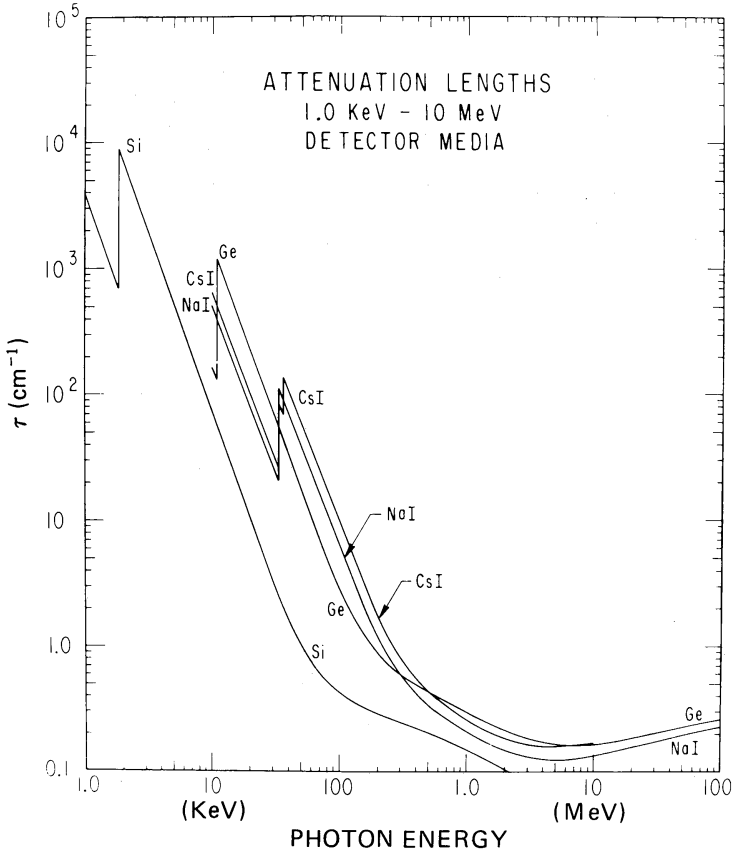

(Adapted from Peterson, L. in *Annual Review of Astronomy and Astrophysics*, Annual Review Inc., Palo Alto, California, 1975.)

Mass attenuation coefficients *(cont.)*

Photoelectric mass absorption coefficients for various window or filter materials.

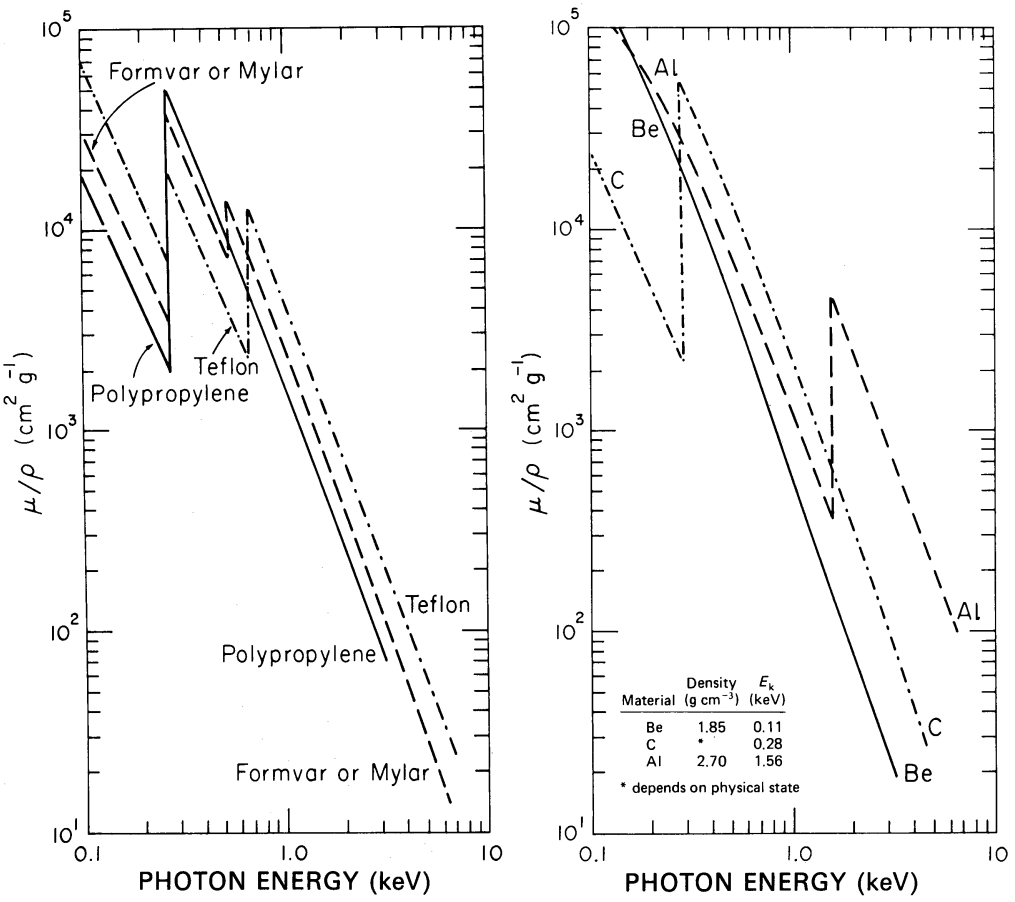

© Cambridge University Press • Provided by the NASA Astrophysics Data System

Mass attenuation coefficients (*cont.*)

Photoelectric mass absorption coefficients for various gases.

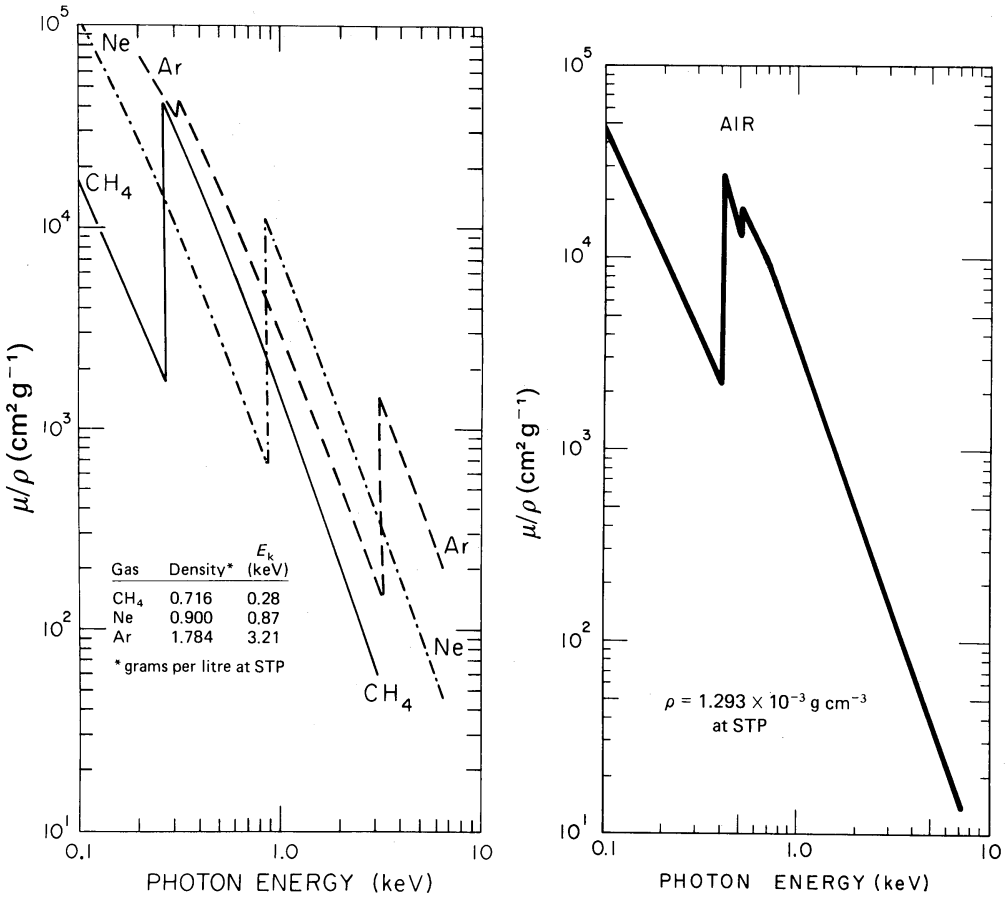

© Cambridge University Press • Provided by the NASA Astrophysics Data System

Mass attenuation coefficients (*cont.*)

Photoelectric cross-section of xenon and argon as a function of photon energy. (Adapted from Anderson, F. D., *A High Resolution Large Area Gas Scintillation Proportional Counter for Use in X-ray Astronomy*, Ph.D. thesis, Columbia University, 1978.)

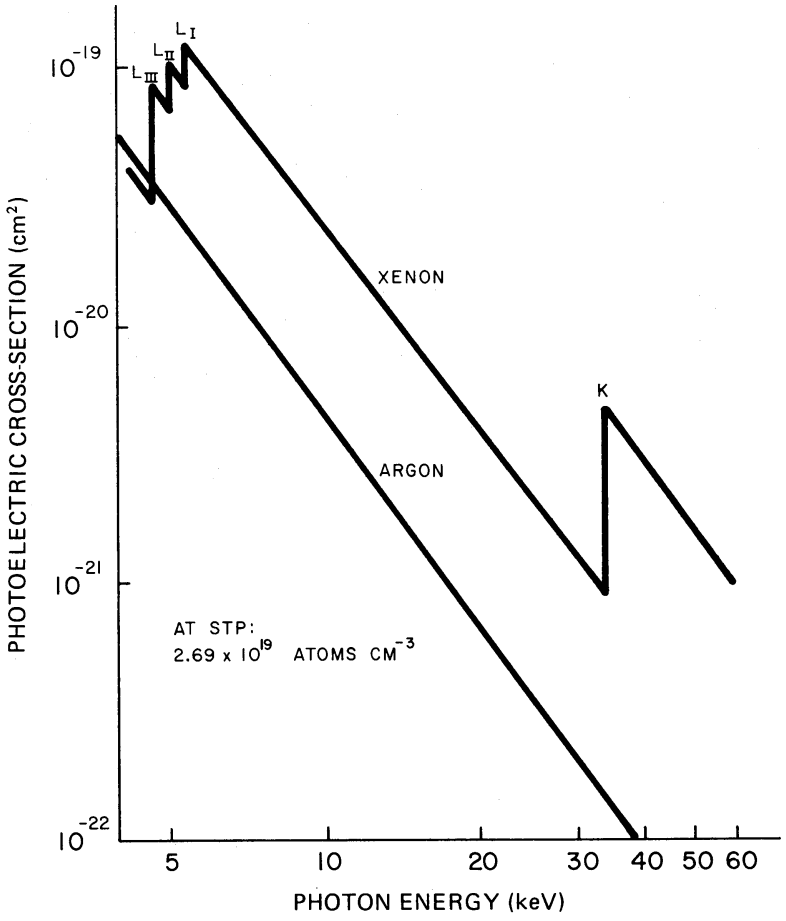

Photon mean free path versus energy for various gases at STP.

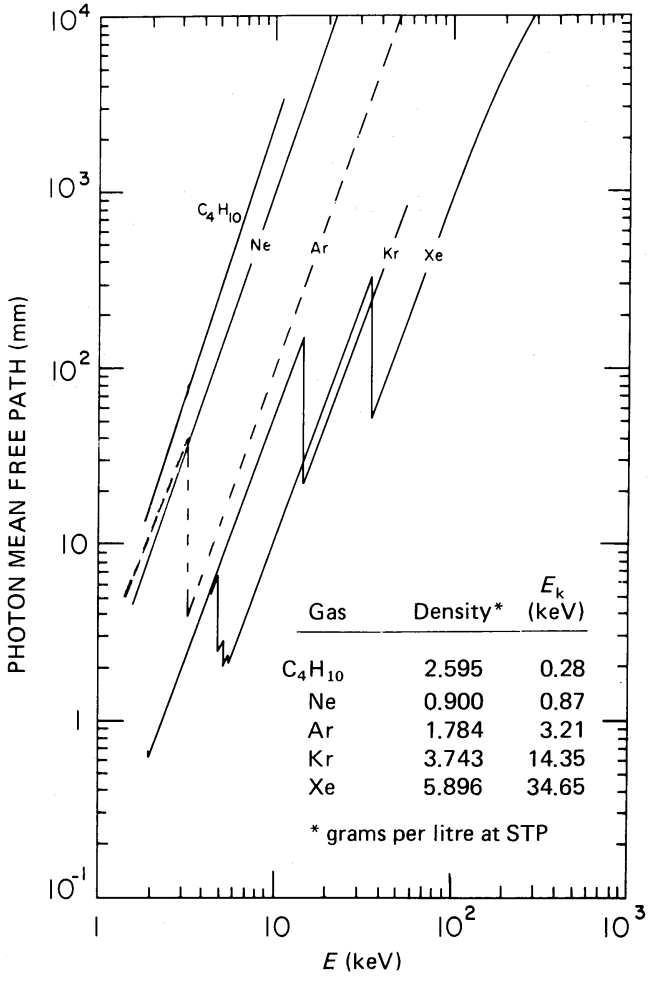

© Cambridge University Press • Provided by the NASA Astrophysics Data System

© Cambridge University Press • Provided by the NASA Astrophysics Data System

Mass attenuation coefficients for photons in air. The curve marked 'total absorption' is $(\mu_a/\rho) = (\sigma_a/\rho) + (\tau/\rho) + (\kappa/\rho)$, where σ_a, τ, and κ are the corresponding linear coefficients for Compton absorption, photoelectric absorption, and pair production. When the Compton scattering coefficient σ_s is added to μ_a, we obtain the curve marked 'total attenuation' which is $(\mu_0/\rho) = (\mu_a/\rho) + (\sigma_s/\rho)$. The total Rayleigh scattering cross-section (σ_r/ρ) is shown separately. Because the Rayleigh scattering is elastic and is confined to small angles, it has not been included in μ_0/ρ. In computing these curves, the composition of 'air' was taken as 78.04 volume per cent nitrogen, 21.02 volume per cent oxygen, and 0.94 volume per cent argon. At 0°C and 760 mm Hg pressure, the density of air is $\rho = 0.001\,293\ \mathrm{g\ cm^{-3}}$. (Adapted from Evans, R. D., *The Atomic Nucleus*, McGraw-Hill, 1955, with permission.)

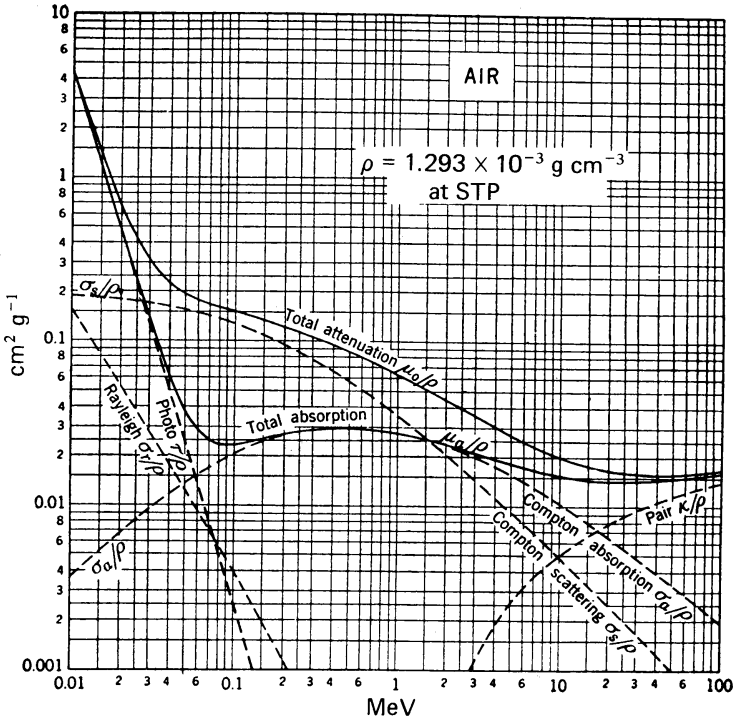

Mass attenuation coefficients for photons in water. (From Evans, R. D., op. cit.)

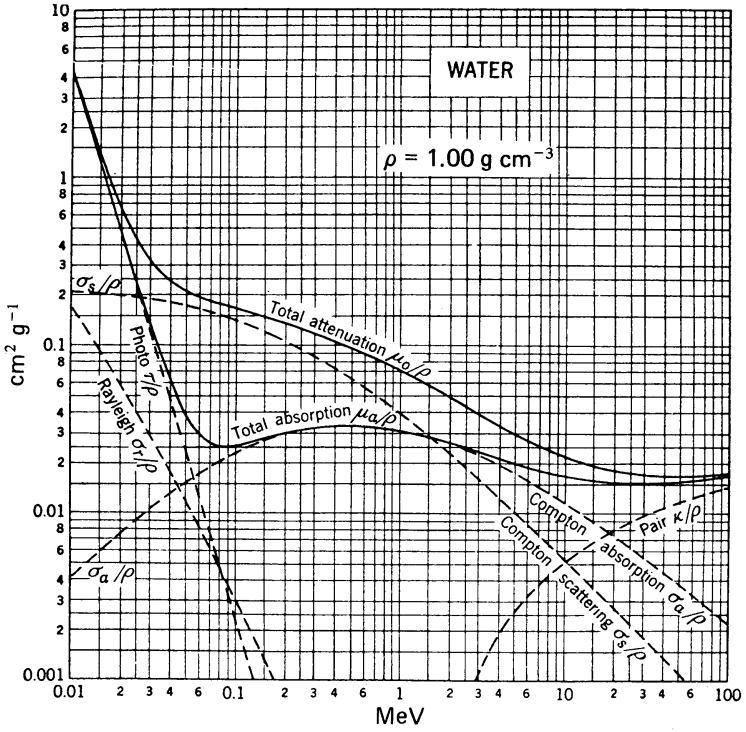

Mass attenuation coefficients (*cont.*)

Mass attenuation coefficients for photons in lead.
(From Evans, R. D., *op. cit.*)

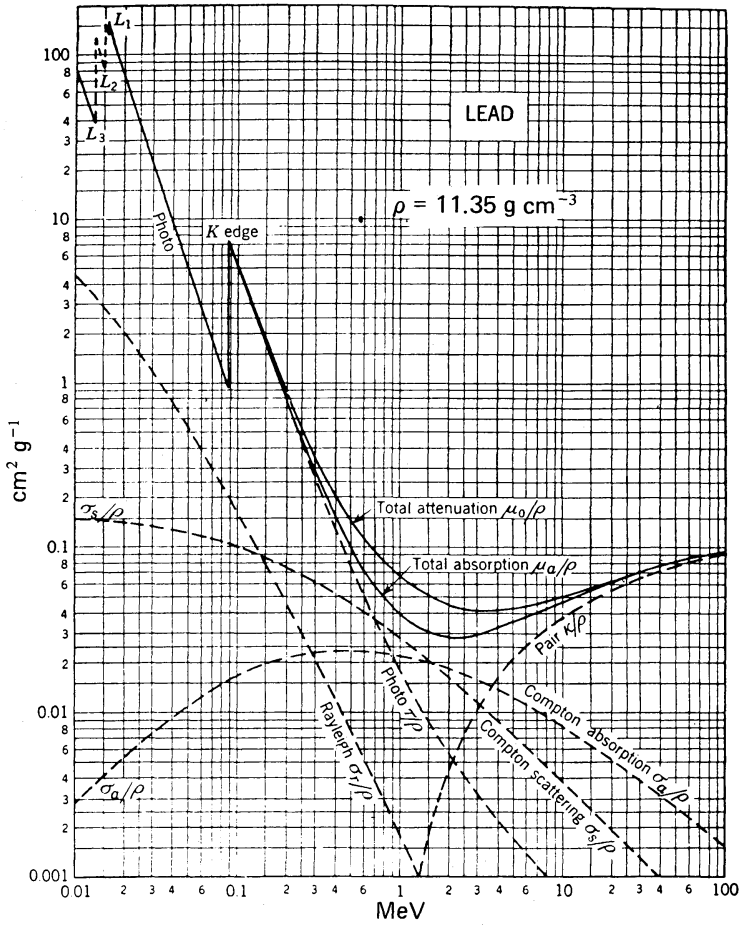

Mass attenuation coefficients for photons in aluminum.
(From Evans, R. D., *op. cit.*)

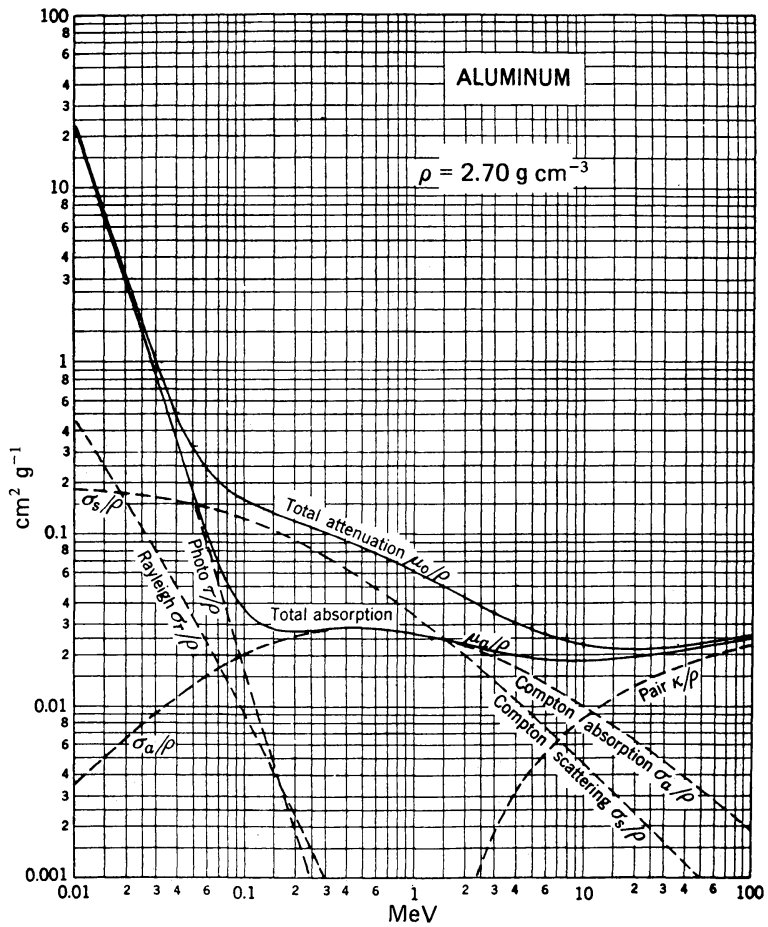

© Cambridge University Press • Provided by the NASA Astrophysics Data System

Mass attenuation coefficients for sodium iodide. The 'Compton total' attenuation coefficient $\sigma/\rho = \sigma_a/\rho + \sigma_s/\rho$ is shown explicitly. (From Evans, R. D., *op. cit.*)

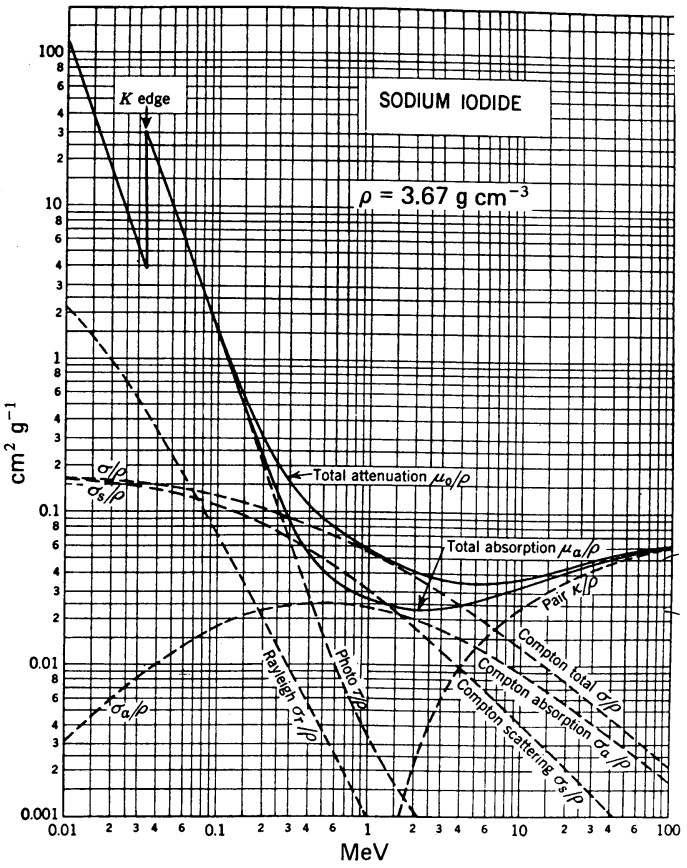

Mass attenuation coefficient for photons in xenon. (Adapted from Chupp, E. L., *Gamma-Ray Astronomy*, D. Reidel Publishing Co., Dordrecht, 1976, with permission.)

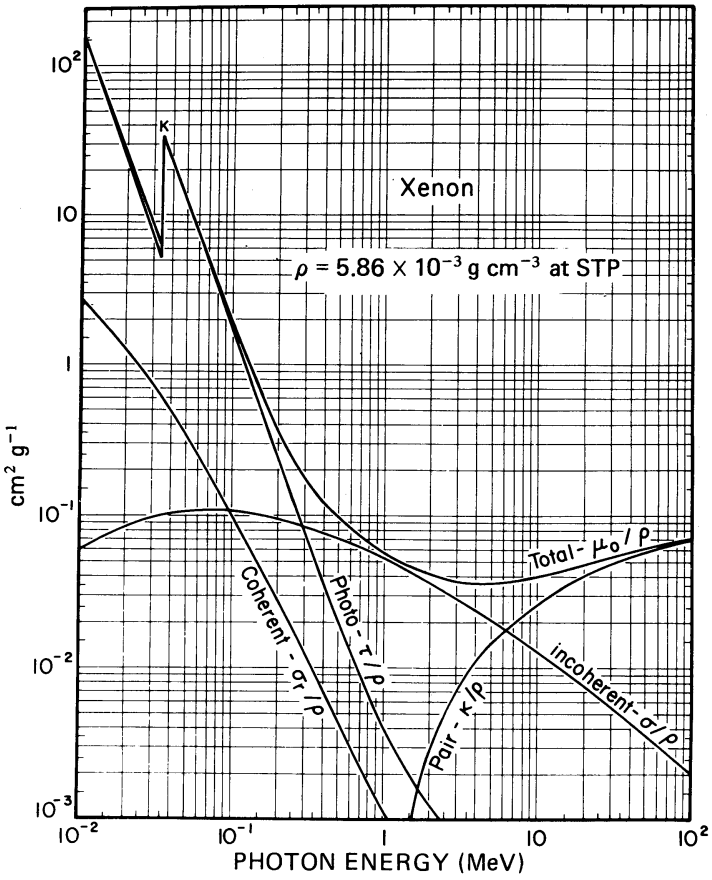

© Cambridge University Press • Provided by the NASA Astrophysics Data System

Mass attenuation coefficients (*cont.*)

Mass attenuation coefficient for photons in hydrogen. (From Chupp, E. L., *op. cit.*)

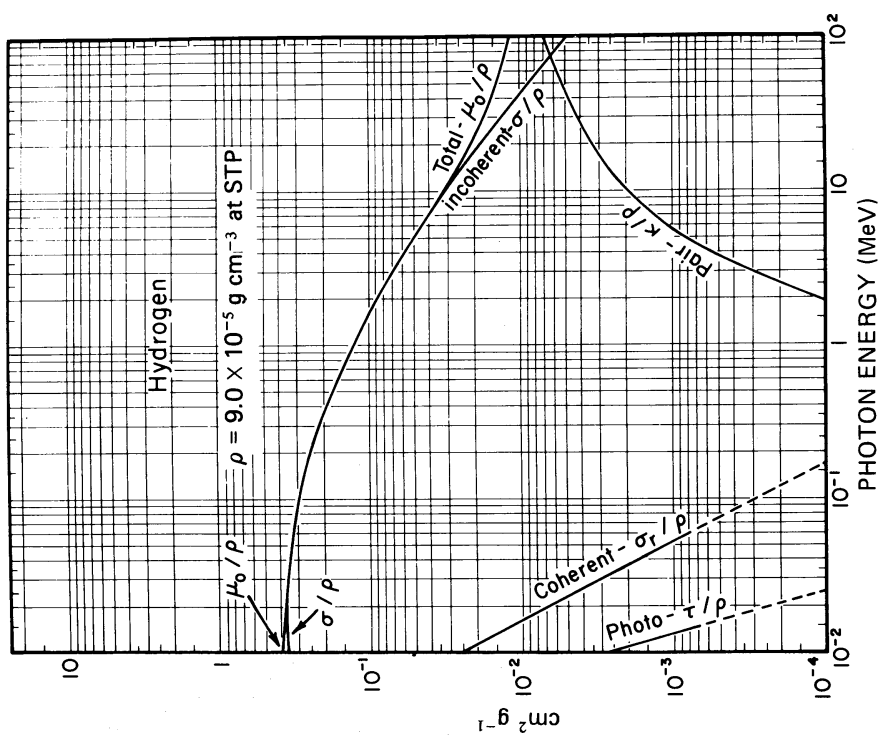

Mass attenuation coefficient for photons in polystyrene. (From Chupp, E. L., *op. cit.*)

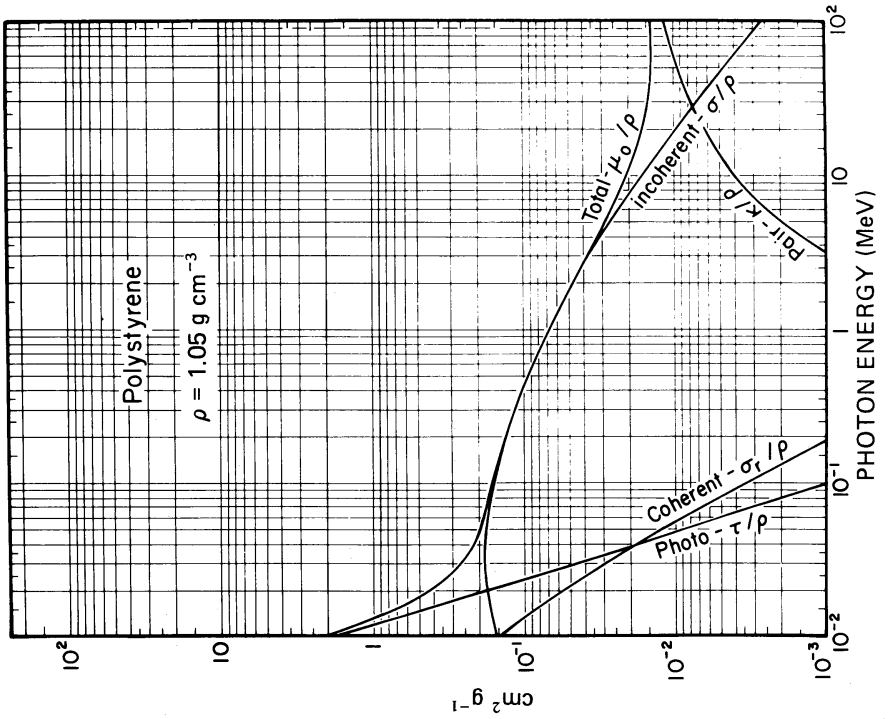

© Cambridge University Press • Provided by the NASA Astrophysics Data System

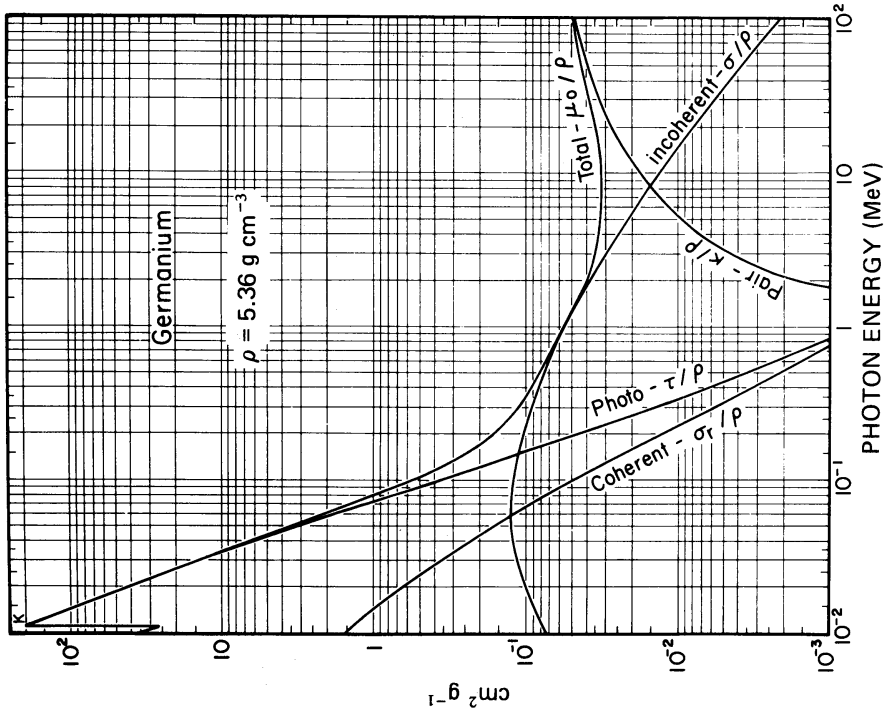

Mass attenuation coefficient for photons in germanium. (From Chupp, E. L., *op. cit.*)

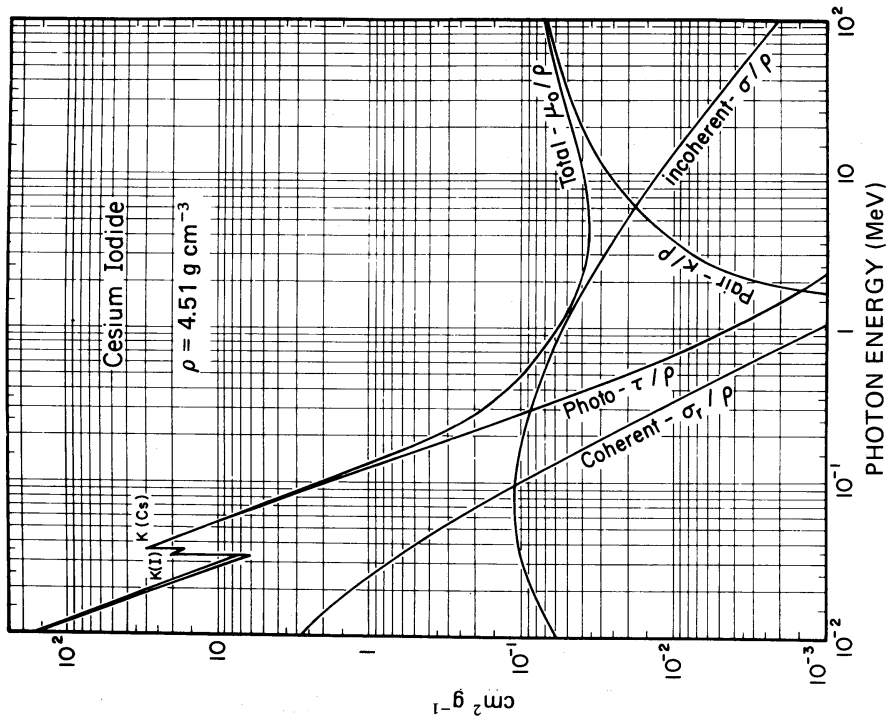

Mass attenuation coefficient for photons in cesium iodide. (From Chupp, E. L., *op. cit.*)

© Cambridge University Press • Provided by the NASA Astrophysics Data System

Fluorescence yields

Fluorescence yields for K and L shells for $5 \leqslant Z \leqslant 110$. The plotted curve for the L shell represents an average of L_1, L_2 and L_3 effective yields. (From Kortright, J. B. in *X-ray Data Booklet*, Lawrence Berkeley Laboratory, University of California, 1986. Data from Krause, M. O., *J. Phys. Chem. Ref. Data*, **8**, 307, 1979.)

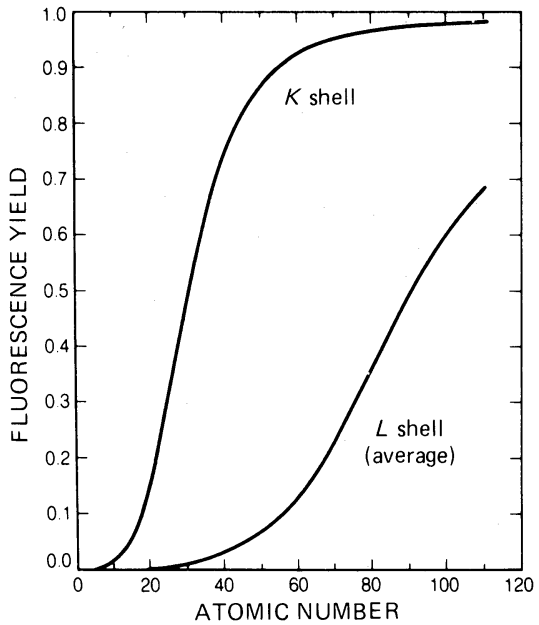

Passage of charged particles through matter

Total ionization loss by electrons or positrons (valid for all cases except extremely relativistic electrons)

$$-\left(\frac{dT}{ds}\right)_{ion} = \frac{2\pi e^4}{m_0 v^2} NZ\left\{\ln\left[\frac{m_0 v^2 T}{I^2(1-\beta^2)}\right] - \beta^2\right\} \quad \text{erg cm}^{-1}$$

(all quantities in cgs units).

For numerical calculations:

$$-\left(\frac{dT}{ds}\right)_{ion} = 4\pi r_0^2 \frac{m_0 c^2}{\beta^2} NZ\left[\ln\left[\beta\left(\frac{T+m_0c^2}{I}\right)\left(\frac{T}{m_0c^2}\right)^{1/2}\right] - \tfrac{1}{2}\beta^2\right] \quad \text{MeV cm}^{-1},$$

where

$\beta^2 = (v/c)^2 = 1 - [(T/m_0c^2) + 1]^{-2}$,

v = velocity of particle,

$m_0c^2 = 0.51\,\text{MeV}$,

$4\pi r_0^2 = 1.00 \times 10^{-24}\,\text{cm}^2$,

$r_0 = e^2/m_0c^2$ = classical electron radius,

NZ = electrons cm^{-3},

© Cambridge University Press • Provided by the NASA Astrophysics Data System

Z = atomic number,
I = mean excitation potential (MeV),
$I \simeq (13 \times 10^{-6})Z$ (MeV),
T = kinetic energy (MeV),
N = atoms cm^{-3}
(e.g., 0.1 MeV electron: 4.7 keV per cm of air).

	Mean excitation potential I		
	Z	I (eV)	I/Z
H_2	1	19	19
He	2	44	22
Be	4	64	16
Air	7.2	94	13.1
Al	13	166	12.7
Ar	18	230	12.8
Cu	29	371	12.8
Ag	47	586	12.5
Xe	54	660	12.2
Au	79	1017	12.8
Pb	82	1070	13.1

(List from Sternheimer, R. M., *Methods of Experimental Physics*, L. Marton, ed., Vol. 5, part A, Academic Press, New York, 1961.)

For $I << T << m_0c^2$:

$$-\left(\frac{dT}{ds}\right)_{ion} = \frac{2\pi e^4}{T} NZ \ln\left(\frac{T\sqrt{2}}{I}\right) \quad \text{erg cm}^{-1}.$$

In the range 0–10 MeV:

$$-\left(\frac{dT}{ds}\right)_{ion} \approx \frac{45}{\beta^2} \quad \text{ion pairs (air-cm)}^{-1}.$$

Radiative loss for non-relativistic electrons

$$-\left(\frac{dT}{ds}\right)_{rad} = 3.09 \times 10^{-27} NZ^2(T + m_0c^2) \quad \text{MeV cm}^{-1},$$

where

$T + m_0c^2$ = total energy of electron in MeV,
N = atoms $cm^{-3} = (\rho/A) \times 6.022 \times 10^{23}$,
Z = atomic number of absorber.
A = atomic weight of absorber,
ρ = density of absorber.

© Cambridge University Press • Provided by the NASA Astrophysics Data System

Ionization and radiative loss for highly relativistic electrons $(T >> m_0c^2)$

$$-\left(\frac{dT}{ds}\right)_{ion} = \frac{2\pi e^4 NZ}{m_0 v^2}\left[\ln\frac{m_0 v^2 T}{2I^2(1-\beta^2)} - (2\sqrt{(1-\beta^2)} - 1 + \beta^2)\ln 2 + 1 - \beta^2 + \tfrac{1}{8}(1-\sqrt{(1-\beta^2)})^2\right] \text{ erg cm}^{-1}.$$

(Bethe, H. A., *Handbuch der Physik*, Vol. 24, p. 273, Julius Springer, Berlin, 1933.)

$$-\left(\frac{dE}{ds}\right)_{rad} = N\frac{Z^2}{137}r_0^2 E\left[4\log\left(\frac{2E}{mc^2}\right) - \tfrac{4}{3}\right] \text{ erg cm}^{-1}$$

(for $mc^2 \ll E \ll 137mc^2Z^{-1/3}$).

$$-\left(\frac{dE}{ds}\right)_{rad} = N\frac{Z^2 r_0^2}{137}E[4\log(183Z^{-1/3}) + \tfrac{2}{9}] \text{ erg cm}^{-1}$$

(for $E >> 137mc^2Z^{-1/3}$).

$$E = T + m_0c^2$$

(Bethe, H. A. & Heitler, W., *Proc. Roy. Soc.* (*London*), **A146**, 83, 1934.)

$$-\left(\frac{dT}{d\xi}\right)_{rad} = \frac{T}{X_0}, \quad T = T_0 e^{-\xi/X_0},$$

where

ξ is the distance travelled measured in g cm^{-2}, T_0, the initial energy,

X_0, the radiation length $= \dfrac{716M_A}{Z(Z+1.3)[\ln(183Z^{-1/3}) + \frac{1}{8}]}$ g cm^{-2}

(M_A = atomic weight).

Radiation lengths X_0 and critical energy T_c for various substances

Absorber	Z	M_A	X_0 (gm cm^{-2})	T_c (MeV)
Hydrogen	1	1	58	340
Helium	2	4	85	220
Carbon	6	12	42.5	103
Nitrogen	7	14	38	87
Oxygen	8	16	34.2	77
Aluminium	13	27	23.9	47
Argon	18	39.9	19.4	34.5
Iron	26	55.8	13.8	24
Copper	29	63.6	12.8	21.5
Lead	82	207.2	5.8	6.9
Air			36.5	83
Water			35.9	93

(List from Bethe, H. A. & Ashkin, J., *Experimental Nuclear Physics*, E. Segrè, ed., Vol. I, John Wiley and Sons, New York, 1953.)

© Cambridge University Press • Provided by the NASA Astrophysics Data System

$T_c \simeq \dfrac{1600 m_0 c^2}{Z}$, the energy at which ionization losses equal radiation losses.

$$\frac{(dT/dx)_{rad}}{(dT/dx)_{ion}} \simeq \frac{TZ}{1600mc^2}.$$

Total ionization loss by heavy charged particles (kinetic energy $\lesssim$ rest mass)

$$-\left(\frac{dT}{ds}\right)_{ion} = \frac{4\pi z^2 e^4}{m_0 V^2} NZ\left[\ln\frac{2m_0V^2}{I} - \ln(1-\beta^2) - \beta^2\right] \quad \text{erg cm}^{-1}$$

(all quantities in cgs units).

For numerical calculations:

$$-\left(\frac{dT}{ds}\right)_{ion} = 4.58 \times 10^{-4}\frac{z^2NZ}{V^2}\left[\ln\left(\frac{1.14 \times 10^{-15}V^2}{I}\right) - \ln(1-\beta^2) - \beta^2\right] \quad \text{MeV cm}^{-1},$$

where

z = particle charge,
Z = absorber atomic number,
V = velocity of particle in cm s^{-1} = $3 \times 10^{10}\beta$,
N = absorber atomic density = $\rho/A \times 6.022 \times 10^{23}$,
I = mean excitation potential (in eV),
$I \approx 13Z$ (eV),
$(1-\beta^2) = (1 + T/M)^{-2}$,
T = kinetic energy in MeV,
M = mass of particle in MeV
(e.g., 2 MeV α particle in Si: 0.27 MeV μm^{-1}).

Approximate range–energy relationships

Range–energy for monoenergetic electrons

20 eV $\leqslant E \leqslant$ 10 keV:

$$\ln((Z/A)R_{ex}) = -4.5467 + 0.311\,04\ln E + 0.077\,73(\ln E)^2$$

where

R_{ex} = extrapolated range in μg cm^{-2} (25% precision),
Z/A = charge to mass ratio for absorbing medium,
E = energy in eV.

(Iskef, H. *et al.*, *Phys. Med. Biol.*, **28**, 535, 1983.)

© Cambridge University Press • Provided by the NASA Astrophysics Data System

Approximate range–energy relationships *(cont.)*

$10\,\text{keV} \lesssim E \lesssim 3\,\text{MeV}$:

$$R_{ex}\ (\text{mg cm}^{-2}) = 412E\ (\text{MeV})^n, \text{ where}$$

$$n = 1.265 - 0.0954 \ln E\ (\text{MeV}).$$

$1\,\text{MeV} \lesssim E \lesssim 20\,\text{MeV}$:

$$R_{ex}\ (\text{mg cm}^{-2}) = 530E\ (\text{MeV}) - 106.$$

Continuous β-ray spectra

β-ray spectra are exponentially attenuated with a mass-absorption coefficient nearly independent of the absorbing material:

$$\mu/\rho\ (\text{cm}^2\,\text{gm}^{-1}) = 17E_m^{-1.14},$$

where E_m (in MeV) is the maximum energy of the β-ray spectrum.
The thickness of absorber required to reduce the β-ray intensity to one-half its original value:

$$t_{1/2}\ (\text{mg cm}^{-2}) = 0.693/(\mu/\rho) = 41E_m^{1.14}.$$

Range–energy relationships for heavy particles

Alpha particles in air at 15 °C, 760 mm, 4–15 MeV,

$$R\ (\text{cm}) = (0.005E\ (\text{MeV}) + 0.285)E\ (\text{MeV})^{1.5}.$$

Protons in air at 15 °C, 760 mm, 10–200 MeV,

$$R\ (\text{cm}) = 100\left(\frac{E(\text{MeV})}{9.3}\right)^{1.8}.$$

Range of heavy particles in other materials

Bragg–Kleeman rule:

$$\frac{R_1}{R_0} = \frac{\rho_0}{\rho_1}\sqrt{\left(\frac{A_1}{A_0}\right)} \quad (\pm 15\%),$$

where

ρ = density
A = atomic weight.

For mixtures:

$$\sqrt{A} = \sum_i n_i \sqrt{A_i},$$

where n_i = atomic fraction of element i.

For air, $\sqrt{A_0} = 3.81$, $\rho_0 = 1.226 \times 10^{-3}\,\text{gm cm}^{-3}$ at 15 °C, 760 mm, and therefore:

$$R_1 = 3.2 \times 10^{-4} \frac{\sqrt{A_1}}{\rho_1} R_{air}.$$

© Cambridge University Press • Provided by the NASA Astrophysics Data System

Charged particles in silicon

Range–energy curves for charged particles in silicon. Channeling of ions between crystal planes can result in significant variations from the data shown here. (Adapted from *ORTEC Manual on Surface Barrier Detectors.*)

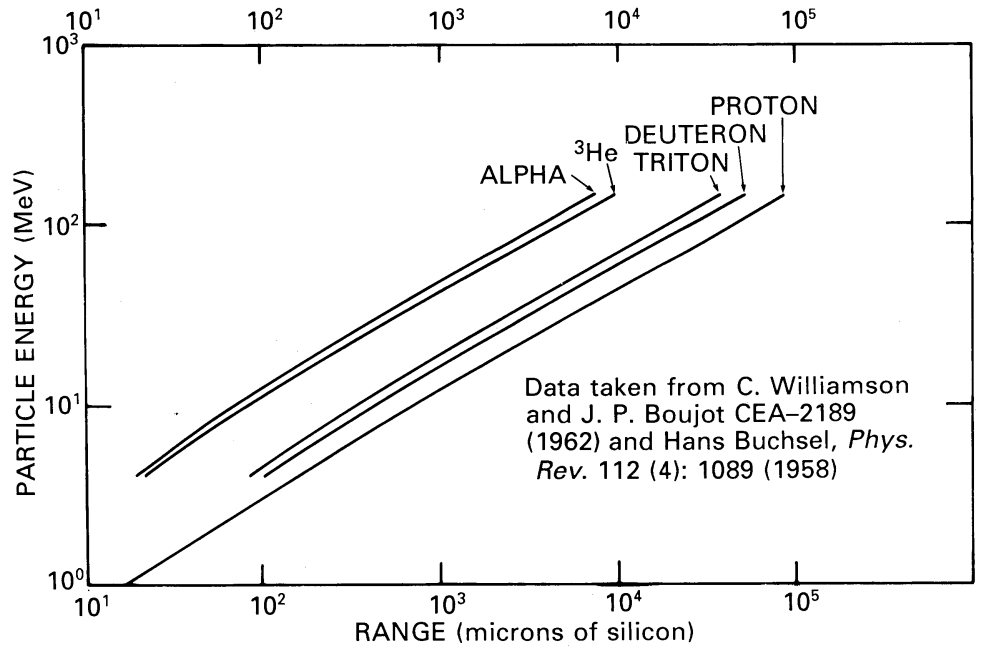

Specific energy loss for charged particles in silicon. Channeling of ions between crystal planes can result in significant variations from the data shown here. (Adapted from *ORTEC Manual on Surface Barrier Detectors.*)

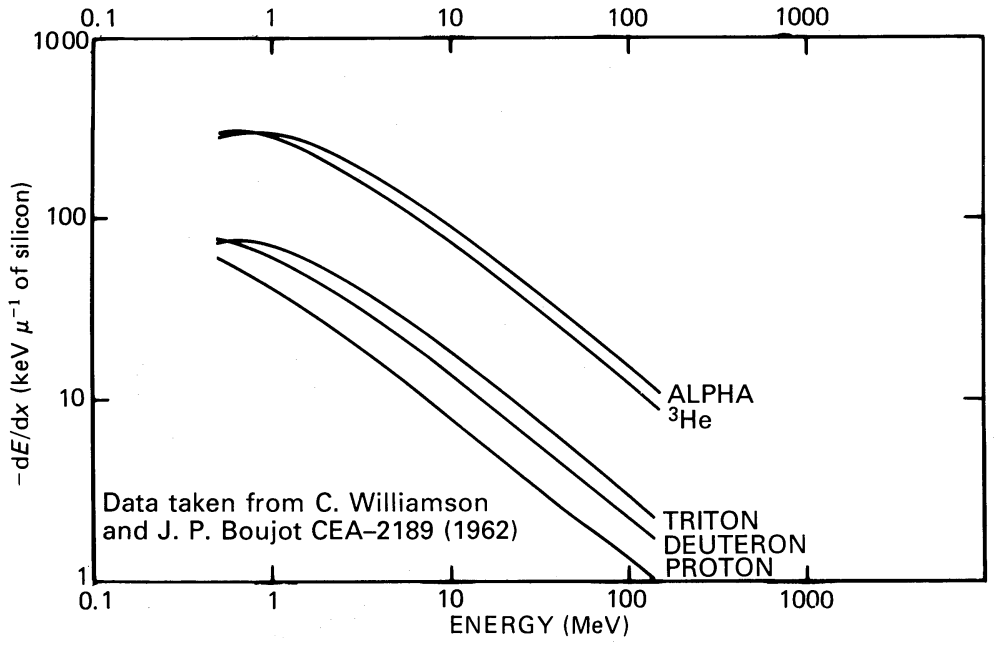

© Cambridge University Press • Provided by the NASA Astrophysics Data System

Charged particles in silicon *(cont.)*

Specific energy loss for electrons in silicon. Channeling of ions between crystal planes can result in significant variations from the data shown here. (Adapted from *ORTEC Manual on Surface Barrier Detectors.*)

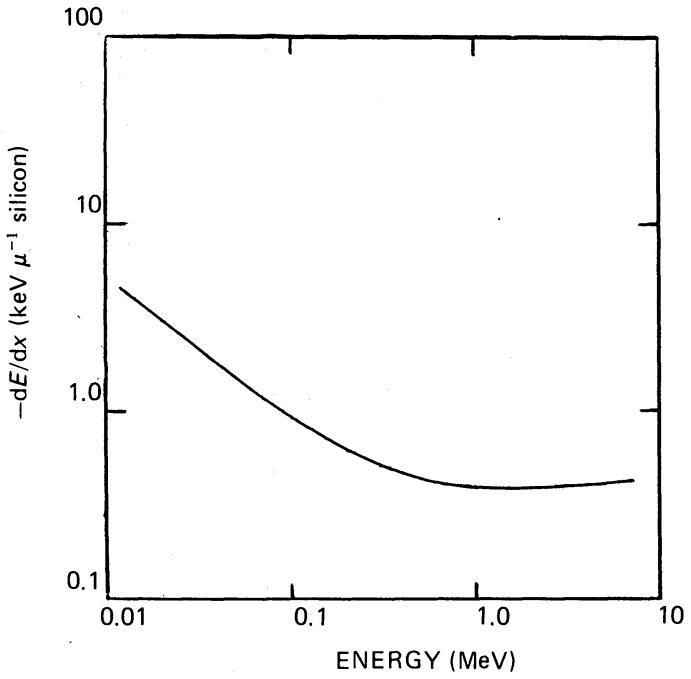

Specific energy loss for protons in silicon. Channeling of ions between crystal planes can result in significant variations from the data shown here. (Adapted from *ORTEC Manual on Surface Barrier Detectors.*)

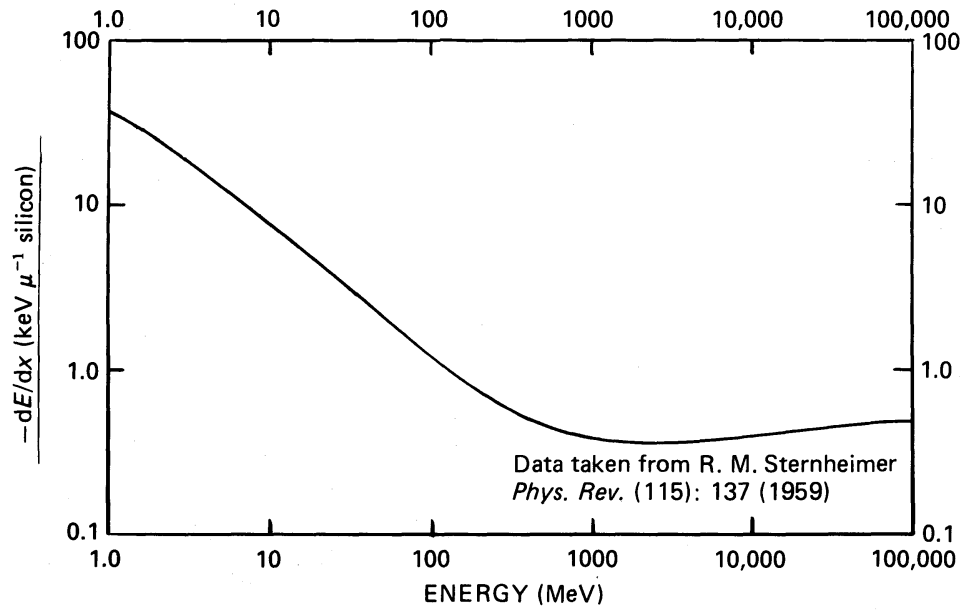

© Cambridge University Press • Provided by the NASA Astrophysics Data System

Charged particles in silicon *(cont.)*

Beta-ray range energy curve in silicon. Channeling of ions between crystal planes can result in significant variations from the data shown here. (Adapted from *ORTEC Manual on Surface Barrier Detectors.*)

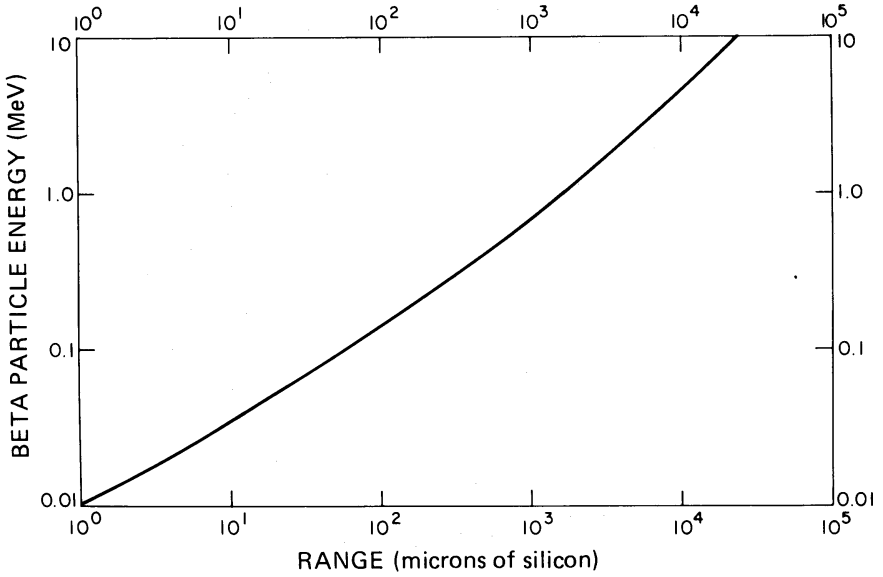

Radioactive sources (Adapted from Lederer, C. M. *et al.*, *Table of Isotopes*, John Wiley & Sons, 1968.)

X-ray sources

Source	X-ray energy (keV)	Half-life
^{49}V	Ti X-rays: 4.5, 4.9	330 d
^{55}Fe	Mn X-rays: 5.9, 6.5	2.6 yr
^{59}Ni	Co X-rays: 6.9, 7.7	8×10^4 yr
^{109}Cd	Ag X-rays: 22, 25	453 d
^{207}Bi	Pb X-rays: 73, 75, 85, 87	30 yr

© Cambridge University Press • Provided by the NASA Astrophysics Data System

Alpha sources

Source	Alpha energies (MeV)	Half-life
^{241}Am	5.443, 5.486	458 yr
^{252}Cf	6.117	2.65 yr
^{242}Cm	6.017, 6.115	163 d
^{244}Cm	5.81, 5.77	17.6 yr
^{148}Gd	3.18	84 yr
^{237}Np	4.78, 4.65	2.14×10^6 yr
^{208}Po	5.11	2.93 yr
^{210}Po	5.305	138 d
^{239}Pu	5.105, 5.143, 5.156	2.4×10^4 yr
^{226}Ra	4.782, 5.490, 6.002, 7.687	1600 yr
^{228}Th	5.427 through 8.785	1.91 yr
^{230}Th	4.617, 4.684	8×10^4 yr
^{235}U	4.336 through 4.597	7.1×10^8 yr
^{238}U	4.200	4.5×10^9 yr

Gamma-ray energy standards

Source	γ-ray energy (keV)	Half-life	Source	γ-ray energy (keV)	Half-life
^{57}Co	14.359	268 d	^{54}Mn	834.861	314 d
^{241}Am	26.350	458 yr	^{46}Sc	899.25	84.2 d
^{241}Am	59.554	458 yr	^{88}Y	898.033	108 d
^{203}Hg	70.830	47 d	^{207}Bi	1063.578	30 yr
^{203}Hg	72.871	47 d	^{65}Zn	1115.522	246 d
^{131}I	80.164	8.05 d	^{46}Sc	1120.50	84.2 d
^{203}Hg	82.572	47 d	^{60}Co	1173.231	5.26 yr
^{203}Hg	84.916	47 d	^{22}Na	1274.552	2.58 yr
^{57}Co	121.969	268 d	^{41}Ar	1293.641	1.85 hr
^{57}Co	136.328	268 d	^{60}Co	1332.518	5.26 yr
^{141}Ce	145.433	32.5 d	^{24}Na	1368.526	15.0 hr
^{139}Ce	165.85	140 d	^{52}V	1434.19	3.77 min
^{203}Hg	279.150	47 d	^{124}Sb	1691.24	60.9 d
^{131}I	284.307	8.05 d	^{28}Al	1778.77	2.31 min
^{51}Cr	320.102	27.8 d	^{88}Y	1836.111	108 d
^{131}I	364.493	8.05 d	Th C″	2614.47	1.91 yr
^{198}Au	411.795	2.70 d	^{24}Na	2753.92	15.0 hr
^{7}Be	477.556	53 d	^{12}B(β^-)^{12}C	4438.41	—
m_0c^2	511.003	—	^{14}C(d, p, β^+)^{15}N	5298.53	—
^{85}Sr	513.95	64 d	^{16}O(^{3}He, α)^{15}O	5240.03	—
^{207}Bi	569.62	30 yr	^{14}N(d, p)^{15}N	5270.10	—
Th C′	583.139	1.91 yr	^{16}O*	6127.8	—
^{137}Cs	661.632	30 yr	^{13}C(p, γ)^{14}N	9169.0	—
^{95}Nb	765.83	35 d	—	—	—

© Cambridge University Press • Provided by the NASA Astrophysics Data System

Electron energy standards

Source	Conversion-electron energy (keV)	Half-life
Cd^{109}	62.19	453 d
Cd^{109}	84.2	453 d
Ce^{141}	103.44	33 d
Ce^{139}	126.91	140 d
Ce^{141}	138.63	33 d
Ce^{139}	159.61	140 d
Hg^{203}	193.64	46.9 d
Hg^{203}	264.49	46.9 d
Au^{198}	328.69	2.698 d
Sn^{113}	363.8	115 d
Sn^{113}	387.6	115 d
Au^{198}	397.68	2.698 d
Bi^{207}	481.61	30 yr
Bi^{207}	554.37	30 yr
Cs^{137}	624.15	30.0 yr
Cs^{137}	655.88	30.0 yr
Co^{58}	803.35	71.3 d
Co^{58}	809.62	71.3 d
Mn^{54}	828.86	303 d
Mn^{54}	834.17	303 d
Y^{88}	881.86	108 d
Y^{88}	895.76	108 d
Bi^{207}	975.57	30 yr
Bi^{207}	1048.1	30 yr
Zn^{65}	1106.46	345 d
Zn^{65}	1114.35	245 d

© Cambridge University Press • Provided by the NASA Astrophysics Data System

Characteristics of synchrotron radiation

The angular and spectral distribution of radiation emitted by a relativistic electron in instantaneously circular motion is, according to Schwinger (*Phys. Rev.*, **75**, 1912, 1949), given by (cgs units):

$$\frac{\partial^2 P}{\partial\lambda\,\partial\psi} = \frac{27}{32\pi^3}\frac{e^2 c}{R^3}\left(\frac{\lambda_c}{\lambda}\right)^4 \gamma^8 (1+(\gamma\psi)^2)^2\left[K_{2/3}^2(\xi) + \frac{(\gamma\psi)^2}{1+(\gamma\psi)^2}K_{1/3}^2(\xi)\right]$$

$$\text{erg s}^{-1}\,\text{rad}^{-1}\,\text{cm}^{-1},$$

where

e = electron charge,
c = velocity of light,
R = radius of curvature,
λ = wavelength,
$\lambda_c = \frac{4}{3}\pi R\gamma^{-3}$, the 'critical wavelength',
$\gamma = E/m_0c^2$, where E = electron energy and m_0 = electron mass,
ψ = vertical angle measured from the plane of the orbit,
$K_{1/2}(\xi)$, $K_{2/3}(\xi)$ are modified Bessel functions of the second kind, where $\xi \equiv (\lambda_c/2\lambda)(1+(\gamma\psi)^2)^{3/2}$.

The first term within the brackets corresponds to radiation polarized in the plane of the orbit, the second to radiation polarized perpendicular to the orbital plane.

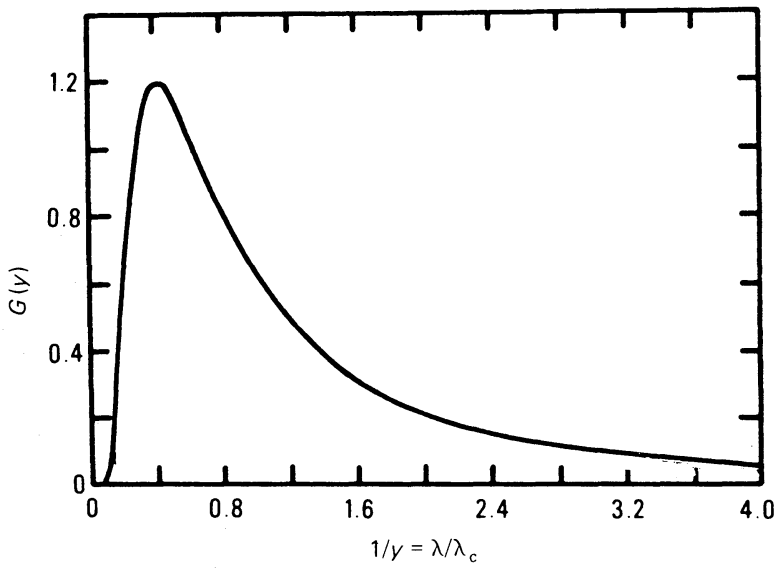

The universal synchrotron radiation function $G(y)$ for monoenergetic electrons as a function of $1/y$.

© Cambridge University Press • Provided by the NASA Astrophysics Data System

The spectral distribution of power is obtained by integrating the above equation over the angle ψ:

$$\frac{dP}{d\lambda} = \frac{3^{5/2}}{16\pi^2}\frac{e^2c}{R^3}\left(\frac{E}{mc^2}\right)^7 G(y),$$

where

$$G(y) = y^3\int_y^\infty K_{5/3}(\eta)\,d\eta, \quad y = \lambda_c/\lambda.$$

The total power radiated,

$$P = \int\frac{dP}{d\lambda}d\lambda = \frac{2}{3}\frac{e^2c}{R^2}\left(\frac{E}{mc^2}\right)^4.$$

The photon flux distribution is obtained by dividing the power distribution function by the photon energy:

$$\frac{\partial^3 N}{\partial\lambda\,\partial\psi\,\partial t} = \frac{\lambda}{hc}\frac{\partial^2 P}{\partial\lambda\,\partial\psi} \quad \text{photons s}^{-1}\,\text{rad}^{-1}\,\text{cm}^{-1}.$$

The radiation emitted by the electron in the plane of its orbit is 100% polarized. Above and below this plane, the radiation is elliptically polarized.

Polarization:

$$(I_\parallel - I_\perp)/(I_\parallel + I_\perp) = \frac{K_{2/3}^2(\xi) - [(\gamma\psi)^2/(1+(\gamma\psi)^2)]K_{1/3}^2(\xi)}{K_{2/3}^2(\xi) + [(\gamma\psi)^2/(1+(\gamma\psi)^2)]K_{1/3}^2(\xi)}.$$

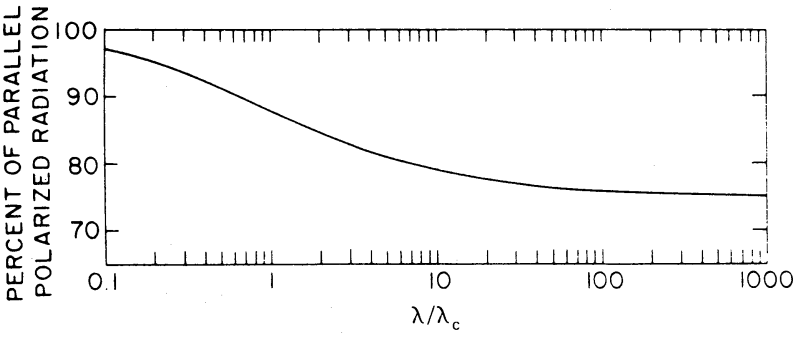

Fraction of radiation, integrated over vertical angle ψ, that is parallel polarized (From Krinsky, S. *et al.* in *Handbook of Synchrotron Radiation*, E. Koch, ed., North-Holland Publishing Co., 1983, with permission.)

© Cambridge University Press • Provided by the NASA Astrophysics Data System

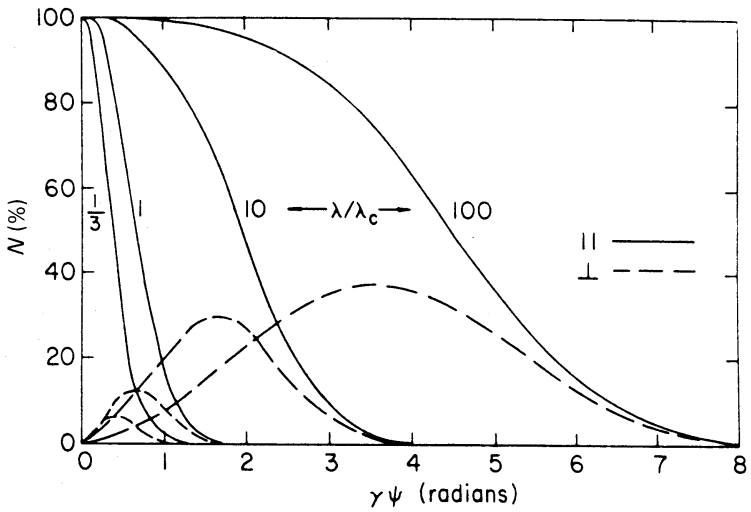

Dependence on the vertical angle ψ of the intensities of the parallel (solid line) and perpendicular (dashed line) polarization components of the photon flux. The individual curves, plotted for $\lambda/\lambda_c = \frac{1}{3}$, 1, 10, and 100, are individually normalized to the intensity in the orbital plane ($\psi = 0$) at the respective λ/λ_c value. Note that the abscissa, ψ multiplied by the electron energy γ, makes these curves universal. (From Krinsky, S. *et al.* in *Handbook of Synchrotron Radiation*, E. Koch, ed., North-Holland Publishing Co., 1983, with permission.)

Practical formulae for electron storage rings

E: electron energy R: radius of ring J: electron current.

Energy loss per turn, per electron:

$$\delta E\,(\text{keV}) = 88.5\frac{E^4(\text{GeV})}{R(\text{m})}.$$

Critical wavelength:

$$\lambda_c\,(\text{Å}) = 5.59\frac{R(\text{m})}{E^3(\text{GeV})}.$$

Characteristic energy:

$$\varepsilon_c\,(\text{eV}) = 2218\frac{E^3(\text{GeV})}{R(\text{m})} = 2.96\times 10^{-7}\frac{\gamma^3}{R(\text{m})}.$$

Emission angle:

$$\approx \frac{1}{\gamma} = \frac{m_0c^2}{E},$$

with

$$\gamma = \frac{E}{m_0c^2} = 1957E(\text{GeV}).$$

© Cambridge University Press • Provided by the NASA Astrophysics Data System

Energy of a photon:

$$\varepsilon(\text{KeV}) = \frac{12.40}{\lambda(\text{Å})}.$$

Photon flux angular distribution:

$$\frac{\partial^4 N}{\partial\lambda\,\partial\psi\,\partial\theta\,\partial t} = 8.267 \times 10^{-5}\left(\frac{\lambda_c}{\lambda}\right)\frac{3\gamma^5}{R}F\left(\frac{\lambda_c}{\lambda}, \gamma\psi\right)J$$

$$\text{photons s}^{-1}\,\text{mrad}^{-1}\,\text{mrad}^{-1}\,\text{Å}^{-1},$$

where

$$F\left(\frac{\lambda_c}{\lambda}, \gamma\psi\right) = (1+\gamma^2\psi^2)^2\left[K_{2/3}^2(\xi) + \frac{\gamma^2\psi^2}{1+\gamma^2\psi^2}K_{1/3}^2(\xi)\right],$$

$$\xi = \frac{1}{2}\frac{\lambda_c}{\lambda}(1+\gamma^2\psi^2)^{3/2},$$

where

θ = horizontal angle,
ψ = vertical angle,
J = current (mA),
R = radius of ring (m).

Photon flux integrated over all vertical angles

$$\frac{\partial^3 N}{\partial\lambda\,\partial\theta\,\partial t} = 7.9 \times 10^{11} G(y) J(\text{mA})\frac{[E(\text{GeV})]^7}{[R(\text{m})]^2}\lambda\,(\text{Å})$$

$$\text{photons s}^{-1}\,\text{mrad}^{-1}\,\text{Å}^{-1},$$

$$\frac{\partial^3 N}{\partial\varepsilon\,\partial\theta\,\partial t} = 5.56 \times 10^{7} G(y) J(\text{mA})\frac{[E(\text{GeV})]^7}{[R(\text{m})]^2}\lambda^3\,(\text{Å})$$

$$\text{photons s}^{-1}\,\text{mrad}^{-1}\,\text{eV}^{-1},$$

for $\lambda >> \lambda_c$

$$\frac{\partial^3 N}{\partial\lambda\,\partial\theta\,\partial t} = 9.35 \times 10^{13} J(\text{mA})\frac{[R(\text{m})]^{1/3}}{[\lambda(\text{Å})]^{4/3}}\ \text{photons s}^{-1}\,\text{mrad}^{-1}\,\text{Å}^{-1}.$$

V. Kostroun (*Nuc. Inst. Meth.*, **172**, 371, 1980) provides series expressions for the modified Bessel functions of fractional order which are suitable for evaluation with programmable calculators or desktop computers.

© Cambridge University Press • Provided by the NASA Astrophysics Data System

Crystal spectroscopy

Collimated single crystal Bragg spectrometer. Bragg condition: $n\lambda = 2d \sin\theta$, where d is the effective spacing of the crystal planes that participate in the reflection. (Adapted from Burek, A., *Space Sci. Inst.*, **2**, 53, 1976.)

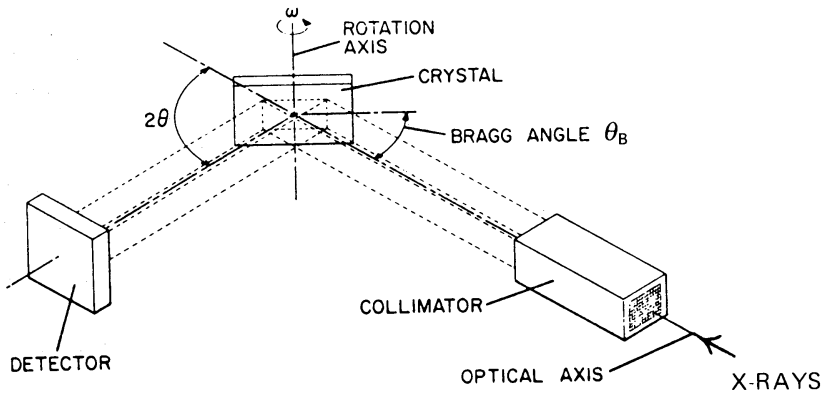

Single crystal rocking curve C_λ. $\theta_B + \Delta = \sin^{-1}(n\lambda/2d_\infty)$, where Δ = refraction correction, d_∞ = physical spacing of reflecting planes, and θ_B = Bragg angle ignoring refraction. (Adapted from Burek, A., *Space Sci. Inst.*, **2**, 53, 1976.)

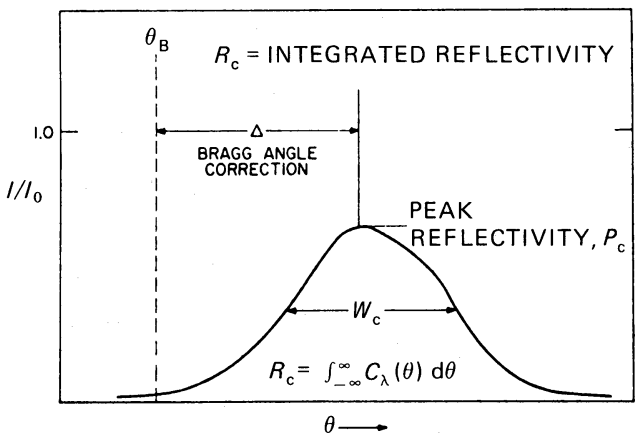

© Cambridge University Press • Provided by the NASA Astrophysics Data System

Crystal properties

Crystal	Density ($g\ cm^{-3}$)	Plane	$2d$ (Å)	Integrated reflectivity ($\theta = 60°$)
Quartz	2.66	$10\bar{1}0$	8.350	6.25×10^{-5} (D)
		$10\bar{1}\bar{1}$	6.592	1.23×10^{-4} (D)
		$20\bar{2}\bar{3}$	2.750	$\approx 1.5 \times 10^{-5}$ (D)
		$22\bar{4}\bar{3}$	2.028	$\approx 6 \times 10^{-6}$ (D)
Topaz	3.49–3.57	303	2.712	(40°) 6×10^{-5} (D)
		040	4.40	
		400	2.3246	(43°) 1×10^{-5} (D)
		200	4.64	
Calcite	2.710	211	6.083	1.62×10^{-4} (D)
Silicon	2.33	111	6.284	1.2×10^{-4} (D)
		220	3.840	8×10^{-5} (D)
		200	5.441 69	
Germanium	5.33	111	6.545	
		220	4.000	2.3×10^{-4} (D)
		200	5.668 97	
Beryl (golden)	2.66	$10\bar{1}0$	15.9549	$\approx 6 \times 10^{-5}$ (D)
Sylvite	1.99	200	6.292	
Halite	2.164	200	5.641	
KBr	2.756	200	6.584	
Fluorite	3.18	111	6.306	
		200	5.4744	
Aluminum	2.699	200	4.057	
		111	4.676	
LiF	2.64	420	1.80	
		200	4.027	10^{-4}–3×10^{-4} (D)
		220	2.848	
Graphite	2.21	002	6.708	1.52×10^{-3} (S)
Mica	2.77–2.88	002	19.84	$\approx 2 \times 10^{-5}$ (S)
Clinochlore	2.6–3.3	001	28.392	
ADP	1.803	101	10.648	9.0×10^{-5} (S)
		220	5.305	1.4×10^{-5} (S)
		200	7.50	
EDDT	1.538	020	8.808	1.15×10^{-4} (S)
PET	1.39	002	8.742	2.2×10^{-4} (S)
SHA	1.3	110	13.98	
KAP	1.636	001	26.5790	5×10^{-5} (S)
RAP	1.94	001	26.121	1.5×10^{-4} (S)
TlAP	2.7	001	25.7567	7.0×10^{-4} (S)
CsAP	2.178	001	25.68	
NH_4AP	1.415	002	26.14	1.5×10^{-4} (S)
NaAP	1.504	002	26.42	

D = double crystal; S = single crystal.
(Adapted from Burek, A., *Space Sci. Inst.*, **2**, 53, 1976.)

© Cambridge University Press • Provided by the NASA Astrophysics Data System

Useful characteristic lines for X-ray spectroscopy

Wavelength (Å)	Energy (keV)	Element	Designation
1.54	8.04	Cu	$K\alpha_{1,2}$
1.66	7.47	Ni	$K\alpha_{1,2}$
1.94	6.40	Fe	$K\alpha_{1,2}$
2.29	5.41	Cr	$K\alpha_{1,2}$
2.75	4.51	Ti	$K\alpha_{1,2}$
3.60	3.44	Sn	$L\alpha_{1,2}$
4.15	2.98	Ag	$L\alpha_{1,2}$
5.41	2.29	Mo	$L\alpha_{1,2}$
6.86	1.80	Sr	$L\alpha_{1,2}$
7.13	1.74	Si	$K\alpha_{1,2}$
8.34	1.49	Al	$K\alpha_{1,2}$
8.99	1.38	Se	$L\alpha_{1,2}$
9.89	1.25	Mg	$K\alpha_{1,2}$
10.44	1.19	Ge	$L\alpha_{1,2}$
12.25	1.01	Zn	$L\alpha_{1,2}$
13.34	0.930	Cu	$L\alpha_{1,2}$
14.56	0.852	Ni	$L\alpha_{1,2}$
15.97	0.776	Co	$L\alpha_{1,2}$
17.59	0.705	Fe	$L\alpha_{1,2}$
18.32	0.677	F	$K\alpha$
19.45	0.637	Mn	$L\alpha_{1,2}$
21.64	0.573	Cr	$L\alpha_{1,2}$
23.62	0.525	O	$K\alpha$
27.42	0.452	Ti	$L\alpha_{1,2}$
31.36	0.395	Ti	Ll
31.60	0.392	N	$K\alpha$
44.7	0.277	C	$K\alpha$
58.4	0.212	W	$N_{\mathrm{V}}N_{\mathrm{VII}}$
64.38	0.193	Mo	$M\zeta$
67.6	0.183	B	$K\alpha$
82.1	0.151	Zr	$M\zeta$
114	0.109	Be	$K\alpha$

Grating spectroscopy

Concave grating equation:

$$\pm m\lambda = d(\sin\alpha + \sin\beta),$$

where m is the spectral order, d is the groove separation, α is the angle of incidence, and β is the angle of diffraction. The negative sign applies when the spectrum lies between the central image ($\alpha = \beta$) and the tangent to the grating (sometimes referred to as the 'outside order'). When the spectrum lies between the incident beam and the central image, the positive sign must be used, and the spectrum is referred to as the 'inside order'. The signs of α and β are opposite when they lie on different sides of the grating normal.

© Cambridge University Press • Provided by the NASA Astrophysics Data System

Angular dispersion (α fixed):

$$\frac{d\beta}{d\lambda} = \frac{m}{d\cos\beta}.$$

Plate factor:

$$\frac{d\lambda}{dl} = \frac{d\cos\beta}{mR}, \quad \frac{d\lambda}{dl} = \frac{\cos\beta}{mR(1/d)} \times 10^4 \quad \text{Å mm}^{-1},$$

where R is in meters, $1/d$ is the number of lines mm^{-1}, and l is the distance along the Rowland circle.

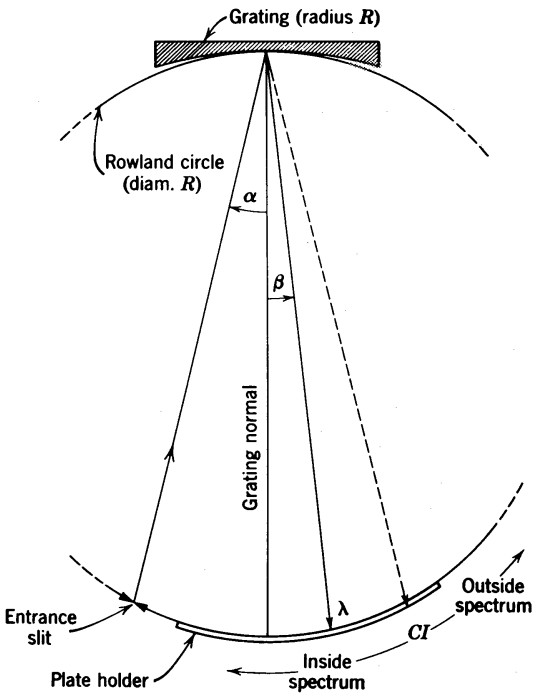

Optical layout of basic spectograph.

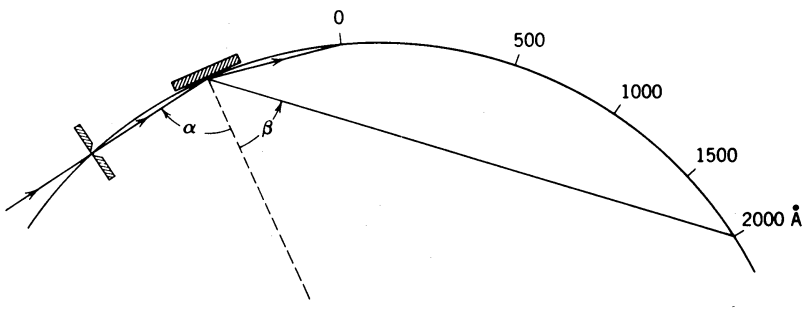

Grazing incidence spectrograph.

(Adapted from Samson, J., *Techniques of Vacuum Ultraviolet Spectroscopy*, John Wiley and Sons, 1967.)

© Cambridge University Press • Provided by the NASA Astrophysics Data System

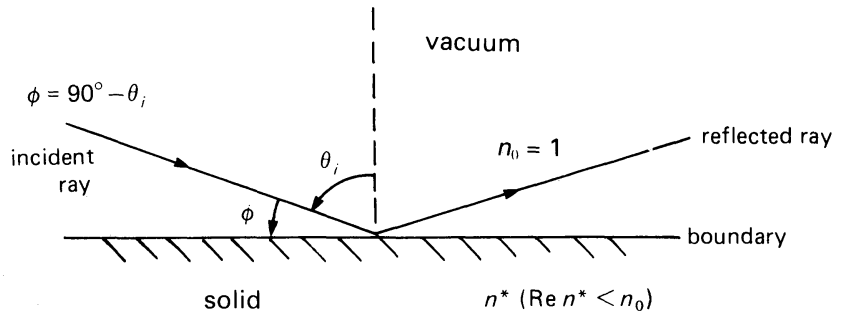

In the X-ray band the complex refractive index n^* is usually expressed as:

$$n^* = (1 - \delta) - i\beta,$$

with

$$\delta = \frac{1}{2\pi}\left(\frac{e^2}{m_e c^2}\right)\left(\frac{N_0 \rho}{A}\right) f_1 \lambda^2$$

and

$$\beta = \frac{1}{2\pi}\left(\frac{e^2}{m_e c^2}\right)\left(\frac{N_0 \rho}{A}\right) f_2 \lambda^2,$$

where

$$\frac{e^2}{m_e c^2} = r_e = \text{the classical electron radius},$$

N_0 = Avogadro's number,
ρ = density,
A = atomic weight,
λ = wavelength of the incident radiation,
f_1 = real part of the atomic scattering factor, and
f_2 = imaginary part of the atomic scattering factor.

$$f_1 = (\pi r_e hc)^{-1} \int_0^\infty \frac{E'^2 \mu_a(E')\, dE'}{E^2 - E'^2} + Z,$$

$$f_2 = \frac{\pi}{2}(\pi r_e hc)^{-1} E \mu_a,$$

where

Z = atomic number,
h = Planck's constant,
c = velocity of light,
E = incident photon energy, and
μ_a = atomic photoabsorption cross-section.

© Cambridge University Press • Provided by the NASA Astrophysics Data System

The atomic photoabsorption cross-section μ_a is related to the mass absorption coefficient (μ/ρ) or to the linear absorption coefficient μ by:

$$\mu_a = \left(\frac{A}{N_0}\right)\left(\frac{\mu}{\rho}\right) = \left(\frac{A}{N_0\rho}\right)\mu.$$

Numerically,

$$\delta = 2.701 \times 10^{-6} \frac{\rho(\mathrm{g\,cm^{-3}})}{A} \lambda^2(\text{Å}) f_1,$$

$$\beta = 2.701 \times 10^{-6} \frac{\rho(\mathrm{g\,cm^{-3}})}{A} \lambda^2(\text{Å}) f_2$$

The reflection of X-rays by a perfectly smooth surface for an angle of incidence θ_i is given by the Fresnel equations:

$$R_s = \frac{a^2 + b^2 - 2a\cos\theta_i + \cos^2\theta_i}{a^2 + b^2 + 2a\cos\theta_i + \cos^2\theta_i}$$

for perpendicular polarization, and

$$R_p = R_s \frac{a^2 + b^2 - 2a\sin\theta_i\tan\theta_i + \sin^2\theta_i\tan^2\theta_i}{a^2 + b^2 + 2a\sin\theta_i\tan\theta_i + \sin^2\theta_i\tan^2\theta_i}$$

for parallel polarization, where

$$2a^2 = [(n^2 - \beta^2 - \sin^2\theta_i)^2 + 4n^2\beta^2]^{1/2} + (n^2 - \beta^2 - \sin^2\theta_i),$$

and

$$2b^2 = [(n^2 - \beta^2 - \sin^2\theta_i)^2 + 4n^2\beta^2]^{1/2} - (n^2 - \beta^2 - \sin^2\theta_i),$$

with $n = 1 - \delta$.

Since the real part of the index of refraction is less than 1, near total external reflection occurs at a grazing angle ϕ_c given by Snell's law:

$$\cos\phi_c = 1 - \delta,$$
$$\phi_c \approx \sqrt{(2\delta)} \quad \text{for } \delta << 1.$$

Since $\beta \neq 0$, reflection is not total for $\phi < \phi_c$ but is less than 1.
Away from an absorption edge,

$$\delta \approx 2.70 \times 10^{-6} \left(\frac{Z_e}{A}\right) \rho\ (\mathrm{g\,cm^{-3}})\ \lambda^2(\text{Å})$$

where Z_e is the number of electrons associated with wavelengths greater than λ. $Z_e = Z$ for $\lambda < \lambda_k$ (K edge).

© Cambridge University Press • Provided by the NASA Astrophysics Data System

Calculated specular reflectivity of an ideal surface as a function of normalized grazing angle ϕ/ϕ_c for various values of β/δ. (After Hendrick, *JOSA*, **47**, 165, 1957.)

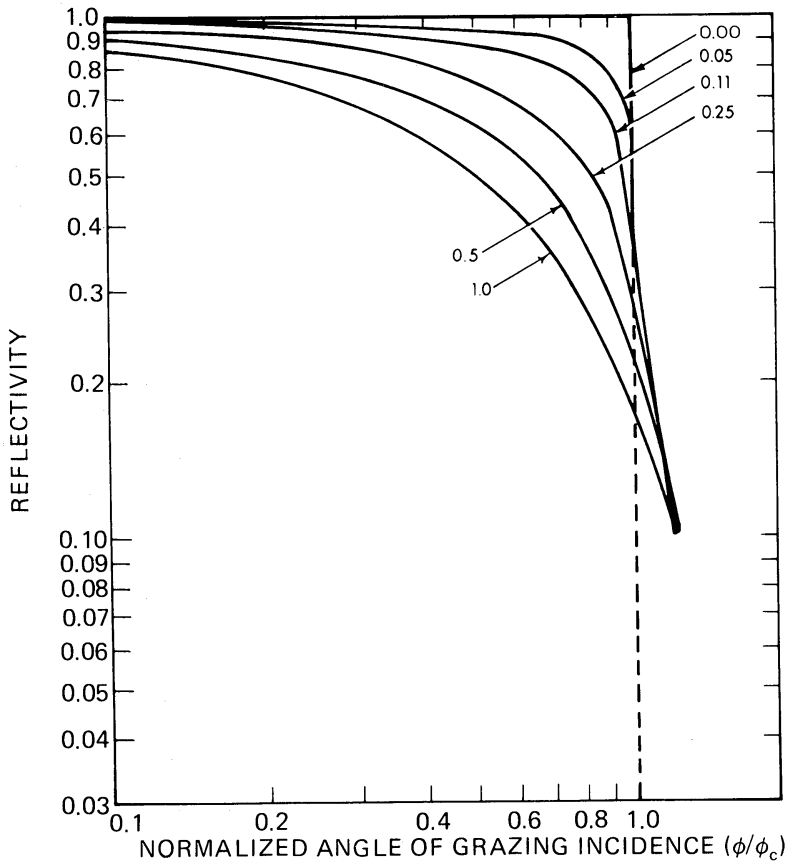

P, R̄

© Cambridge University Press • Provided by the NASA Astrophysics Data System

Optical constants at soft X-ray wavelengths

λ (Å)	$\delta \times 10^4$	$\beta \times 10^4$
NICKEL		
1.25†	0.17	0.02
2.0†	0.42	0.01
5.0†	2.85	0.4
8.34	5.91 ± 0.17	1.9 ± 0.2
9.89	8.00 ± 0.20	3.2 ± 0.3
10.44	8.70 ± 0.20	4.4 ± 0.4
12.25	8.85 ± 0.21	5.3 ± 0.5
13.34	10.20 ± 0.22	7.2 ± 0.7
14.56	1.37 ± 0.08	9.6 ± 1.0
15.97	12.30 ± 0.20	2.1 ± 0.2
17.59	17.50 ± 0.30	2.8 ± 0.3
19.4	21.70 ± 0.30	3.7 ± 0.4
21.64	30.50 ± 0.40	6.1 ± 0.6
23.62	33.30 ± 0.40	7.3 ± 0.7
24.78	39.40 ± 0.44	9.1 ± 0.9
27.42	47.30 ± 0.48	10.0 ± 1.0
31.36	60.00 ± 0.50	15.0 ± 1.5
41.3†	120.0	51.3
47.7†	148.6	76.5
GOLD		
1.25†	0.28	0.02
2.0†	0.77	0.1
5.0†	2.94	2.4
8.34	9.15 ± 0.21	3.1 ± 0.3
9.89	11.50 ± 0.24	4.4 ± 0.4
12.254	18.00 ± 0.30	9.4 ± 0.9
13.34	21.20 ± 0.30	12.3 ± 1.2
14.56	24.10 ± 0.30	15.7 ± 1.6
15.97	26.60 ± 0.40	18.6 ± 1.9
17.59	29.20 ± 0.40	23.4 ± 2.3
19.45	33.50 ± 0.40	26.8 ± 2.7
21.64	34.80 ± 0.40	28.5 ± 2.9
23.62	37.60 ± 0.40	37.6 ± 3.8
24.78	40.00 ± 0.40	56.0 ± 5.6
27.42	40.80 ± 0.50	61.0 ± 6.0
31.36	47.50 ± 0.50	61.5 ± 6.2
44.7	58.00 ± 0.30	58.0 ± 5.9
67.6	136.00 ± 1.0	102.0 ± 10.5

† δ and β are calculated for these wavelengths.
$n^* = (1 - \delta) - i\beta$, complex refractive index.
(Adapted from Ershov, O. A., *Optical Spectroscopy*, **22**, 66, 1967; Lukirskii, A. P. *et al.*, *Optical Spectroscopy*, **16**, 168, 1964.)

© Cambridge University Press • Provided by the NASA Astrophysics Data System

Reflectivity vs. wavelength (energy) for various grazing angles and materials

(Courtesy of M. Hettrick, Lawrence Berkeley Laboratory, Berkeley, CA.) Whenever possible, direct measurements should be made of grazing incidence reflectivity in the X-ray region because of uncertainties in the optical constants.

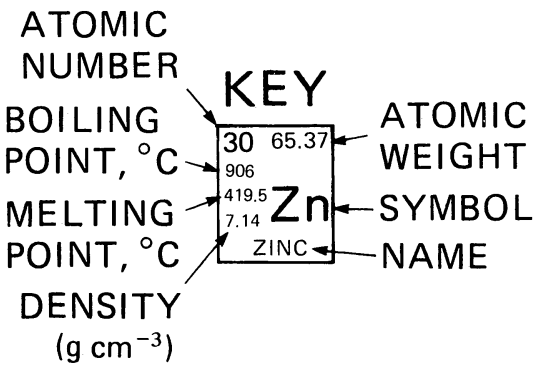

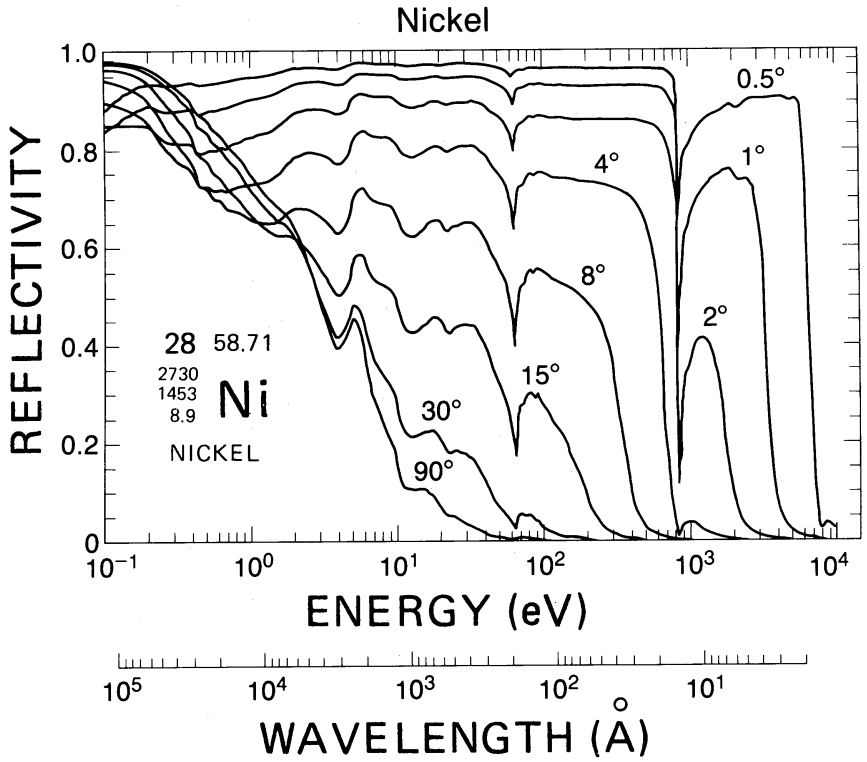

© Cambridge University Press • Provided by the NASA Astrophysics Data System

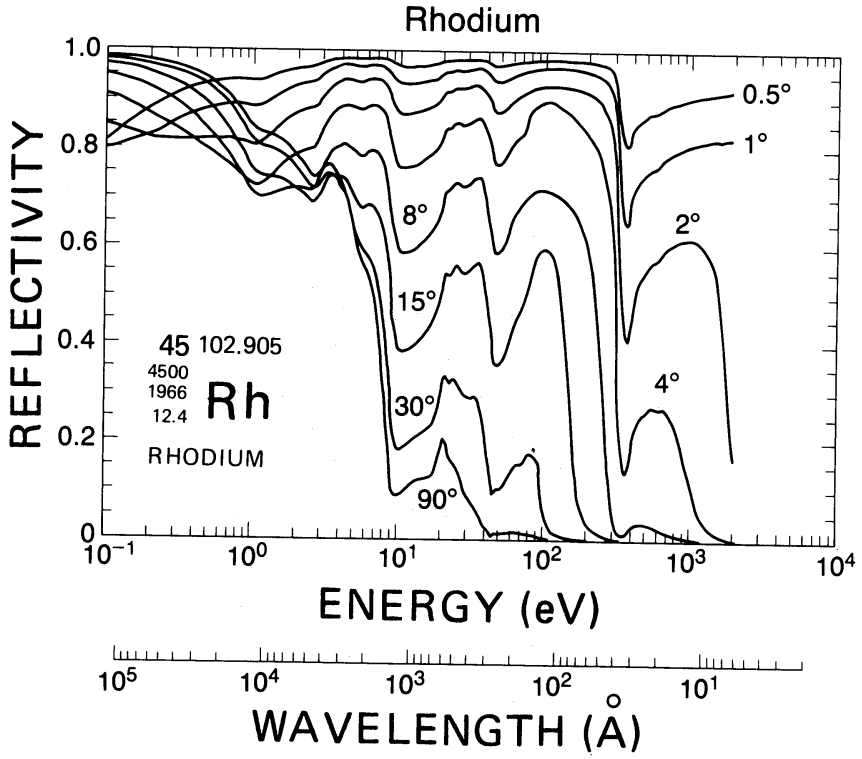

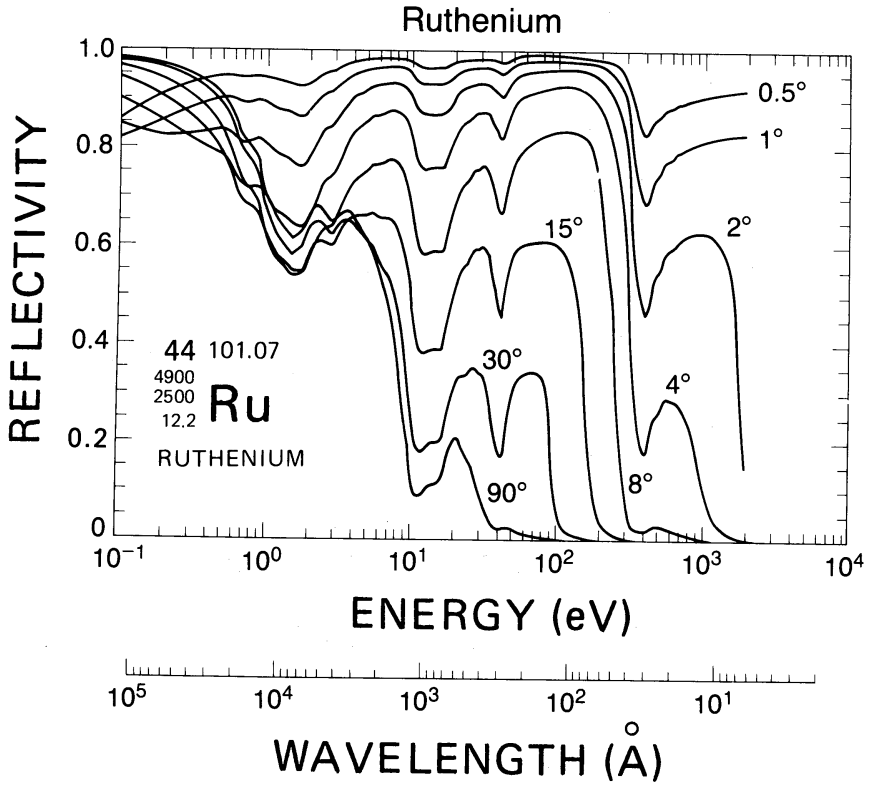

© Cambridge University Press • Provided by the NASA Astrophysics Data System

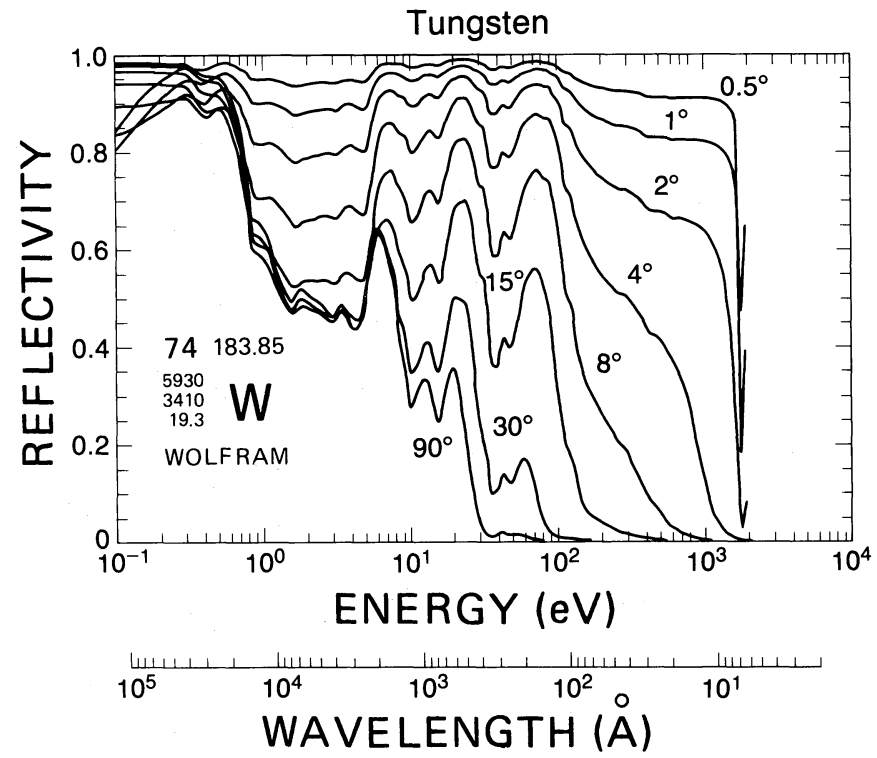

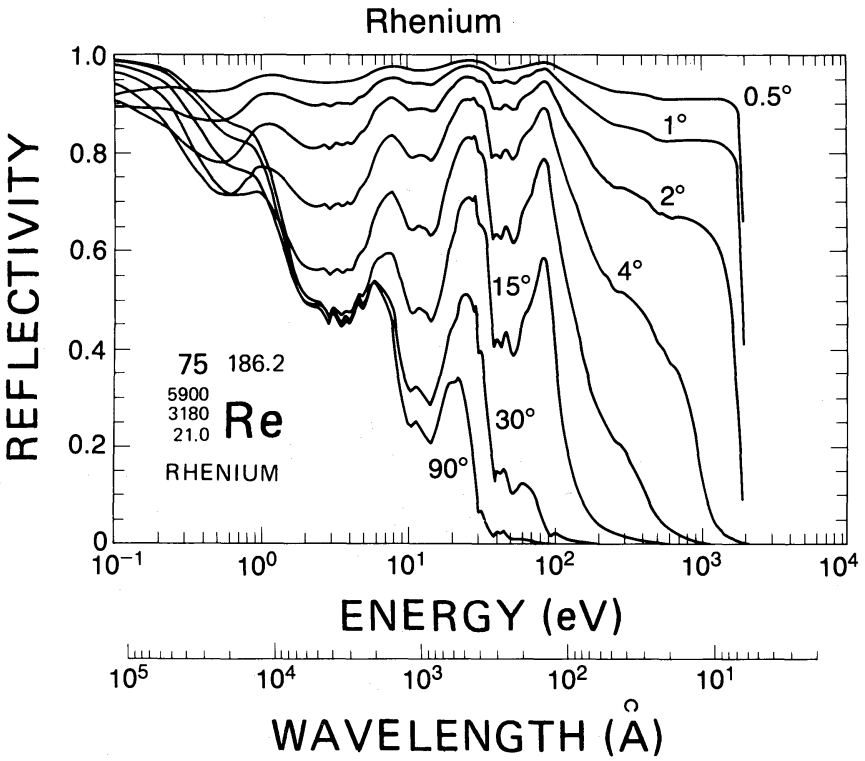

© Cambridge University Press • Provided by the NASA Astrophysics Data System

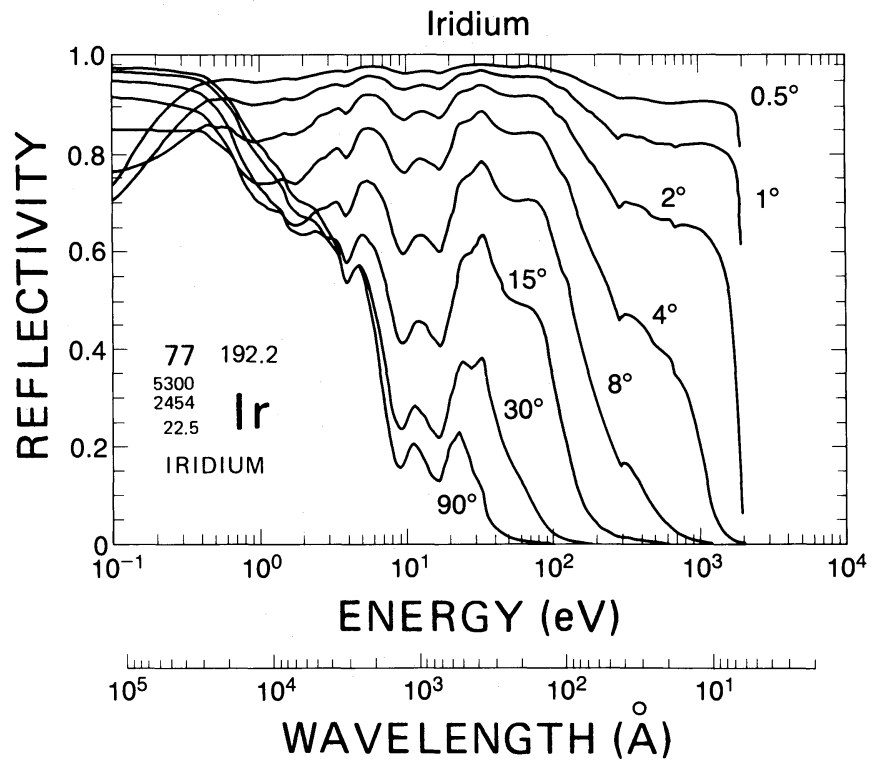

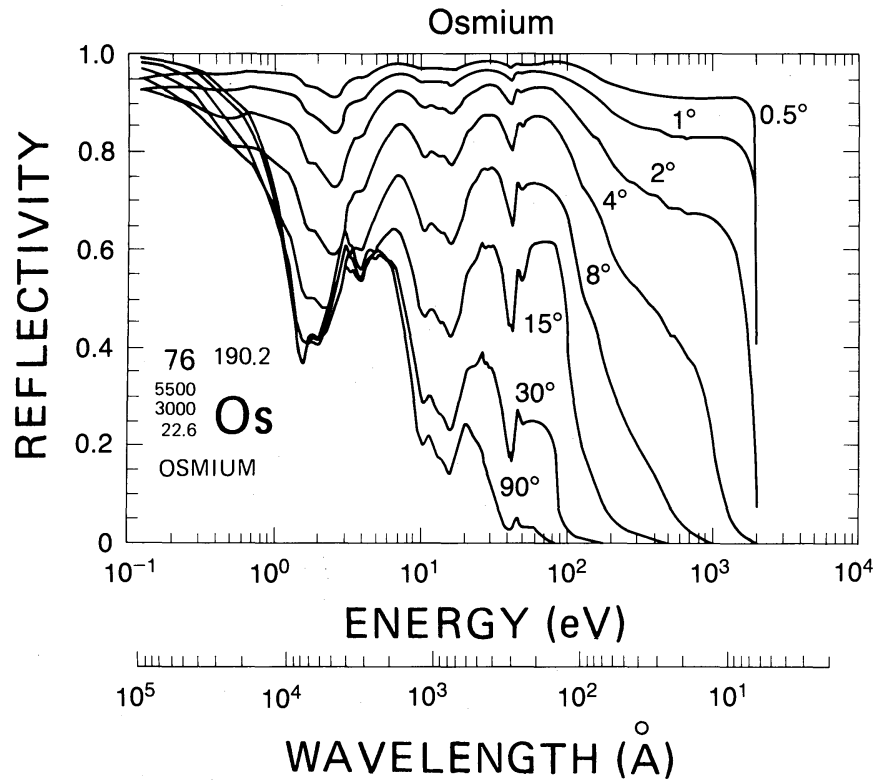

© Cambridge University Press • Provided by the NASA Astrophysics Data System

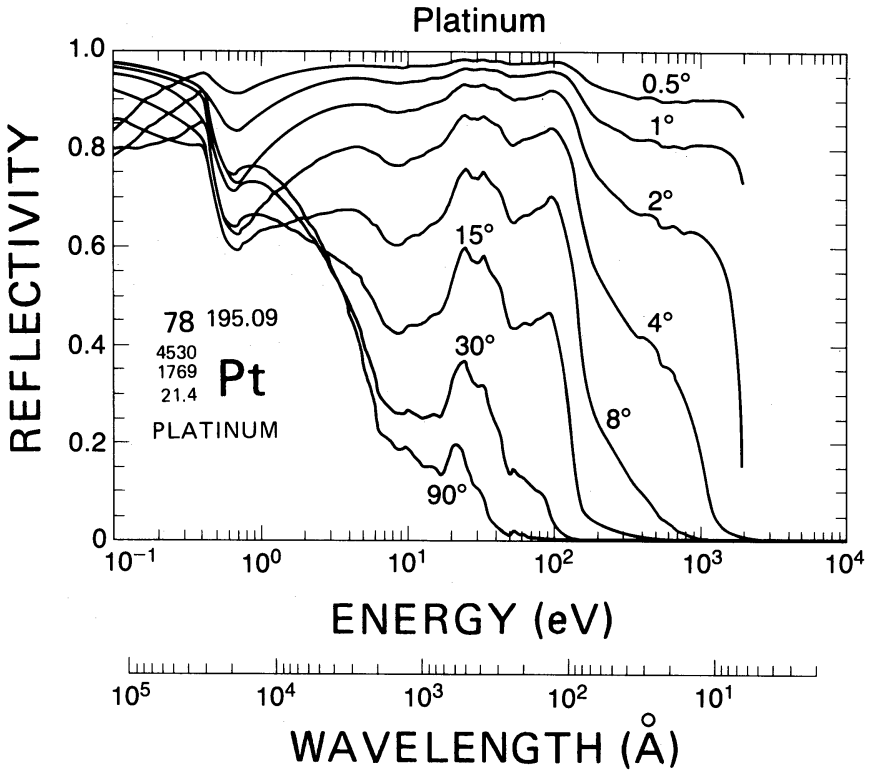

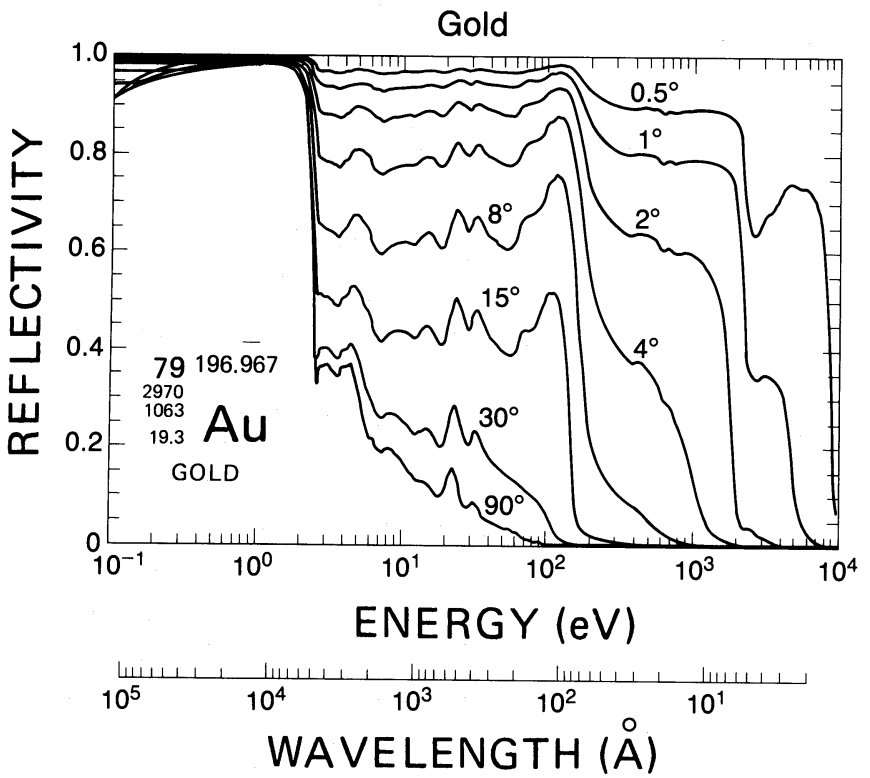

© Cambridge University Press • Provided by the NASA Astrophysics Data System

Reflectivity versus wavelength for various materials and grazing angles. (Adapted from Giacconi, R. *et al.*, *Space Science Review*, **9**, 3, 1969.)

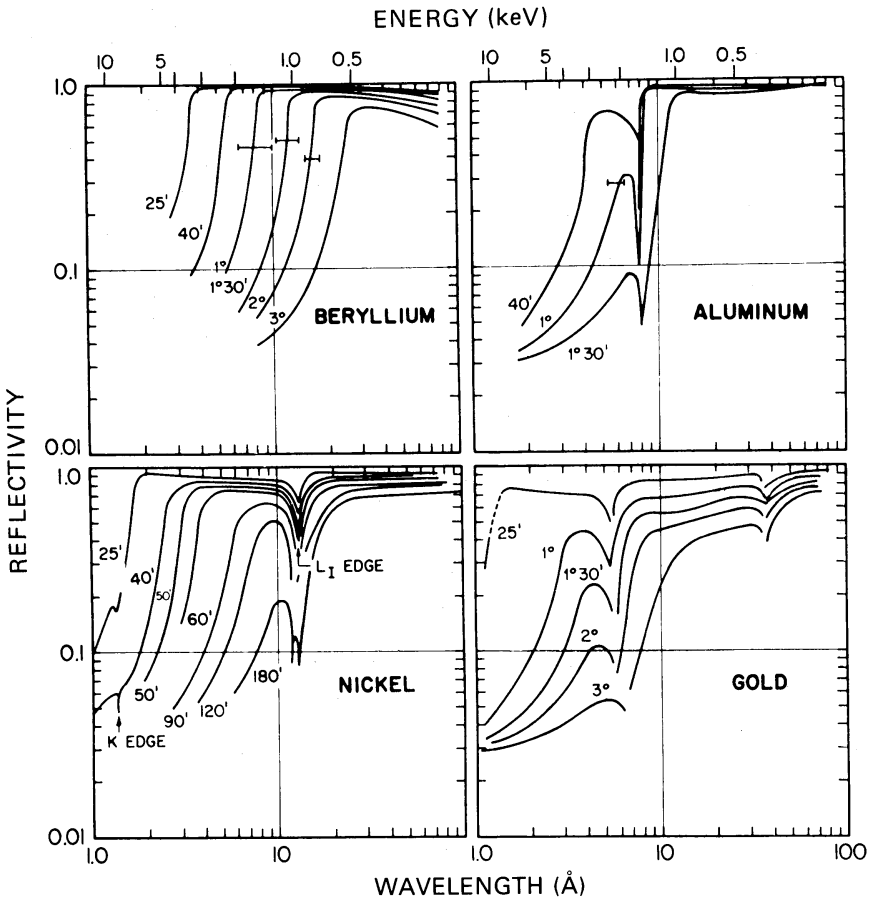

© Cambridge University Press • Provided by the NASA Astrophysics Data System

Wolter type I mirror system

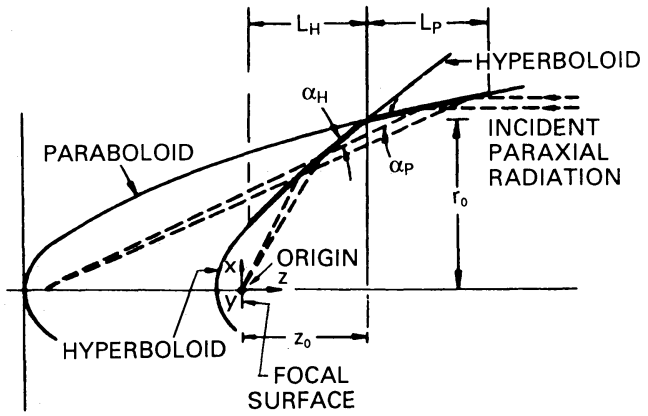

The equations for a paraboloid and hyperboloid which are concentric and confocal can be written as:

$$r_p^2 = P^2 + 2PZ + [4e^2Pd/(e^2 - 1)] \quad \text{(paraboloid)},$$

$$r_h^2 = e^2(d + Z)^2 - Z^2 \quad \text{(hyperboloid)}.$$

The origin is at the focus for axial rays, Z is the coordinate along the axis of symmetry, and r is the radius of the surface at Z.

RMS blur circle radius:

$$\sigma = \frac{(\xi + 1)}{10} \frac{\tan^2 \theta}{\tan \alpha} \left(\frac{L_p}{Z_0}\right) + 4 \tan \theta \tan^2 \alpha \quad \text{radians}$$

and

$$\xi = \alpha_p^*/\alpha_h^*$$

(α_p^* and α_h^* are the grazing angles between the two surfaces and the path of an axial ray that strikes at an infinitesimal distance from the intersection).

For most telescope designs: $\xi = 1$.

$$\alpha = \tfrac{1}{4} \tan^{-1}(r_0/Z_0) = \tfrac{1}{2}(\alpha_p^* + \alpha_h^*),$$

θ = angle between incident rays and optical axis.

Geometrical collecting area:

$$A \approx 2\pi r_0 L_p \tan \alpha.$$

Effective collecting area:

$$A_e(\alpha, E) \approx AR^2(\alpha, E) \approx 8\pi Z_0 L_p R^2(\alpha, E)\alpha^2,$$

where R is the Fresnel reflectivity at energy E and mean grazing angle α.

(Adapted from Van Speybroeck, L. & Chase, R., *Ap. Opt.* **11**, 440, 1972.)

© Cambridge University Press • Provided by the NASA Astrophysics Data System

Vacuum nomograph. (Adapted from Roth, A., *Vacuum Technology*, North-Holland Pub. Co., 1976.)

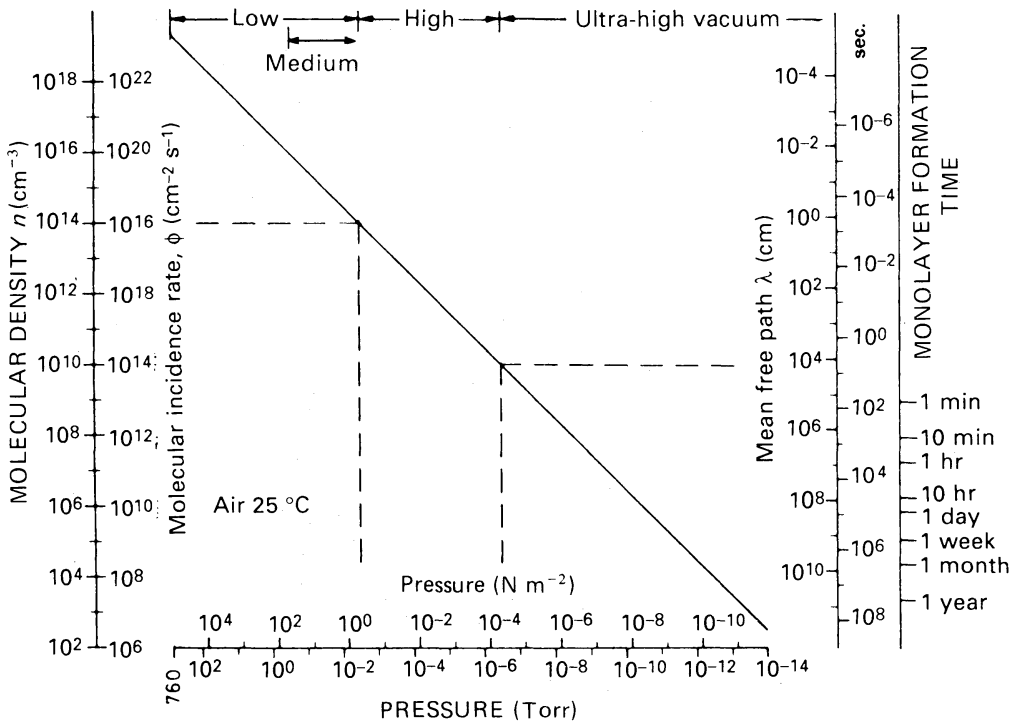

Pumping speed of an aperture of area A:

$$\frac{dV}{dt} = A(\text{cm}^2)\sqrt{[1.32 \times 10^7 T(\text{K})/\text{mol. wt.}]}\ \text{cm}^3\ \text{s}^{-1}.$$

Kinetic theory of gases

Mean free path, $\lambda = 1/\sqrt{2}\pi n\sigma^2$

viscosity, $\eta = \rho\bar{v}\lambda/3$

heat conductivity, $K = \eta c_v \varepsilon$,

mean speed, $\bar{v} = \sqrt{[2.1 \times 10^8 T\,(\text{K})/\text{mol. wt.}]}\ \ \text{cm s}^{-1}$,

where

n = number of molecules cm^{-3},

ρ = gas density in g cm^{-3},

σ = mol. diameter,

c_v = specific heat capacity at constant volume,

$\varepsilon = 2.5$ and 1.9 for monatomic and diatomic gas, respectively.

© Cambridge University Press • Provided by the NASA Astrophysics Data System

Equivalents for various cryogenic fluids

Fluid	Boiling point at 1 atm	Weight in pounds	Ft^3 at 70°F and 1 atm	Liquid liters at b.p.	Liquid gallons at b.p.	Heat of vapor. (Btu)
Nitrogen	−320.4 F	1	13.81	0.5618	0.1484	85.2
	−195.8 C	0.0724	1	0.0407	0.0108	6.168
	77.3 K	1.780	24.58	1	0.2642	151.7
		6.738	92.94	3.785	1	574.1
Helium	−452.1 F	1	96.8	3.628	0.9585	8.8
	−268.9 C	0.0103	1	0.375	0.0099	0.0906
	4.2 K	0.2756	26.68	1	0.2642	2.425
		1.043	101.0	3.785	1	9.178
Oxygen	−297.4 F	1	12.09	0.3973	0.1050	91.7
	−183.0 C	0.827	1	0.0329	0.0087	7.584
	90.1 K	2.517	30.43	1	0.2642	230.8
		9.527	115.2	3.785	1	873.6
Hydrogen	−423.2 F	1	192.3	6.481	1.712	193
	−252.9 C	0.0052	1	0.0337	0.0089	1.004
	20.2 K	0.1543	29.67	1	0.2642	29.78
		0.5841	112.3	3.785	1	112.7
Argon	−302.6 F	1	9.680	0.3235	0.0855	70.2
	−185.9 C	0.1033	1	0.0334	0.0088	7.251
	87.2 K	3.091	29.92	1	0.2642	217.0
		11.70	113.3	3.785	1	821.3

Optical point spread function

The irradiance distribution of the monochromatic image of a point object, $h_\lambda(x, y; \alpha, \beta)$, is called the point spread function (PSF) of an optical system. x and y are the coordinates of the image points and α and β are the coordinates of the ideal image of the object (a point). If $f_\lambda(x, y)$ is the ideal image of an extended monochromatic object, the image produced by the optical system is given by:

$$g_\lambda(x, y) = \iint_{-\infty}^{\infty} h_\lambda(x, y; \alpha, \beta) f_\lambda(\alpha, \beta)\, d\alpha\, d\beta.$$

In some cases, the optical system is *shift-invariant* (at least, over a restricted field):

$$h_\lambda(x, y; \alpha, \beta) = K_\lambda(x - \alpha, y - \beta),$$

© Cambridge University Press • Provided by the NASA Astrophysics Data System

and the above integral can be written as a convolution:

$$g_\lambda(x, y) = \iint_{-\infty}^{\infty} K_\lambda(x_\lambda - \alpha, y - \beta) f_\lambda(\alpha, \beta)\, d\alpha\, d\beta.$$

In general, for optical systems, the PSF is wavelength dependent, *shift-varying*, and asymmetric. Over a restricted field, say within a few arc minutes of the optical axis, it is approximately shift-invariant and symmetric and it is possible to simplify the deconvolution of an image and use Fourier transforms.

In the following discussion we will consider the PSF to be shift invariant and symmetric and will drop the λ subscript.

The PSF is the function that completely characterizes the imaging properties of an optical system. Several useful functions and quantities can be derived from it:

The line spread function

$$A(x) = \int_{-\infty}^{\infty} K(x, y)\, dy \quad (K(x, y) \text{ is the PSF})$$

represents the intensity distribution for a line object.

The edge trace

$$I(x_0) = \int_{-\infty}^{x_0} A(x)\, dx$$

represents the intensity distribution for a knife edge object.

The modulation transfer function (MTF)

This represents the response of an optical system to an object with a sinusoidally varying radiance G of spatial frequency v:

$$\mathrm{MTF}(v) = \frac{M_i(v)}{M_o(v)},$$

where M_i and M_o are the modulation of the image and object, respectively. The modulation is given by:

$$M_{i \text{ or } o}(v) = \left(\frac{\max - \min}{\max + \min}\right) \quad \text{image or object.}$$

Since the radiance of the object (image) varies sinusoidally, we can write:

$$G_o(x) = a_o + b_o \sin 2\pi v x,$$

$$G_i(x) = a_i + b_i \sin 2\pi v x.$$

Then

$$M_o = \frac{(a_o + b_o) - (a_o - b_o)}{(a_o + b_o) + (a_o - b_o)} = \frac{b_o}{a_o},$$

© Cambridge University Press • Provided by the NASA Astrophysics Data System

$$M_i = \frac{(a_i + b_i) - (a_i - b_i)}{(a_i + b_i) + (a_i - b_i)} = \frac{b_i}{a_i},$$

and the modulation transfer function,

$$\text{MTF} = \frac{(b_i/a_i)}{(b_o/a_o)}.$$

The MTF is also given by the absolute value of the Fourier transform of the line spread function:

$$\text{MTF}(v) = \int_{-\infty}^{\infty} A(x) e^{-2\pi i v x} \, dx.$$

The full-width-half-maximum (FWHM) of a rotationally symmetric PSF is the width of the function at half its peak value. If $K(x, y) = K(r)$, where r is the radial coordinate in the image plane, and the radius r_0 is such that:

$$K(r_0) = \tfrac{1}{2}K(0) \quad \text{(half the peak value of the PSF)},$$

then

$$\text{FWHM} = 2r_0; \quad r_0 = \textit{half-width},$$

or half-width-half-maximum (HWHM).

The root mean square (rms) radius $\langle r \rangle$ is defined by:

$$\langle r \rangle^2 = \frac{\int_0^\infty r^2 K(r) r \, dr}{\int_0^\infty K(r) r \, dr},$$

The encircled energy function *E(r)*, the fraction of the total imaged photons that are within a circle of radius r, is given by:

$$E(r) = \frac{\int_0^r K(r) r \, dr}{\int_0^\infty K(r) r \, dr}.$$

The radius of the circle which contains 50% of the imaged photons, *the* **half-power radius**, $r_{1/2}$ is defined by:

$$E(r_{1/2}) \equiv 0.50 = \frac{\int_0^{r_{1/2}} K(r) r \, dr}{\int_0^\infty K(r) r \, dr}.$$

In order to complete the discussion of the point spread function, we give here the various functions and parameters derived from a Gaussian point spread since this can be a useful description of the inner core of the PSF.

© Cambridge University Press • Provided by the NASA Astrophysics Data System

The form of the radial symmetric Gaussian is given as:

$$\text{PSF} = Ce^{-r^2/2\sigma^2},$$

where C and σ are arbitrary constants. We have derived the following functions and quantities:

the line spread function,

$$A(x) = C\sigma\sqrt{(2\pi)}e^{-x^2/2\sigma^2},$$

the edge trace,

$$I(x_0) = C\sigma\frac{\sqrt{(2\pi)}}{2}(1 + \text{erf}(x_0/\sigma\sqrt{2}))$$

where erf(z) is the error function,

the modulation transfer function,

$$M(v) = Ce^{-2(\pi v\sigma)^2}, \text{ and}$$

the encircled energy,

$$E(r) = 1 - e^{-r^2/2\sigma^2}.$$

The table below gives the relations between the FWHM, the rms radius, and the half-power radius for the Gaussian spread function.

PARAMETERS FOR THE GAUSSIAN SPREAD FUNCTION

Spread function	rms radius $\langle r \rangle$	Full width half maximum (FWHM)	Half power radius $r_{1/2}$
$Ce^{-r^2/2\sigma^2}$	$\sigma\sqrt{2}$	$2.36\,\sigma$	$1.18\,\sigma$

Point spread function for a circular aperture (diffraction by a circular aperture)

If the transmission of the system is uniform over the (circular) aperture and the system is aberration-free, the illuminance distribution in the image becomes:

$$P(y, z) = \pi\left(\frac{\text{NA}}{\lambda}\right)^2 P_t\left[\frac{2J_1(m)}{m}\right]^2,$$

where NA is the numerical aperture of the system, J_1 is the first-order Bessel function:

$$J_1(x) = \frac{x}{2} - \frac{(x/2)^3}{1^2 2} + \frac{(x/2)^5}{1^2 2^2 3} - \cdots,$$

P_t is the total power in the point image, and m is the normalized radial

© Cambridge University Press • Provided by the NASA Astrophysics Data System

Point spread function for a circular aperture (diffraction by a circular aperture) (*cont.*)

coordinate:

$$m = \frac{2\pi}{\lambda} \mathrm{NA}(y^2 + z^2)^{1/2} = \frac{2\pi}{\lambda} \mathrm{NA} \cdot s.$$

The fraction of the total power falling within a radial distance s_0 of the center of the pattern is given by $1 - J_0^2(m_0) - J_1^2(m_0)$, where J_0 is the zero-order Bessel function:

$$J_0(x) = 1 - \left(\frac{x}{2}\right)^2 + \frac{(x/2)^4}{1^2 2^2} - \frac{(x/2)^6}{1^2 2^2 3^2} + \cdots.$$

Fraunhofer diffraction at a rectangular aperture (*a*) and at a circular aperture (*b*). (Adapted from Born, M. & Wolf, E., *Principles of Optics*, Pergamon Press, 1984.)

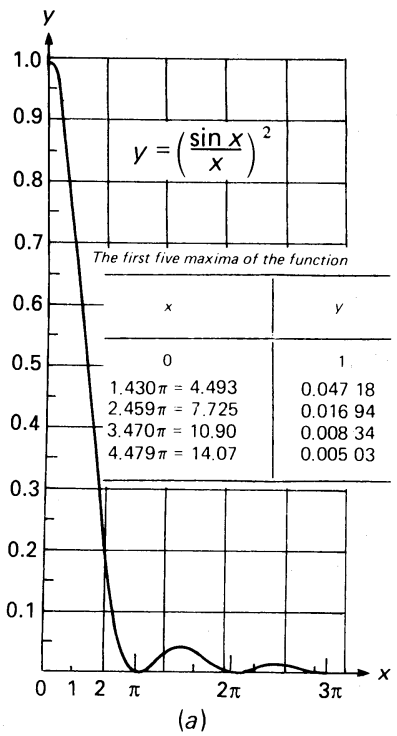

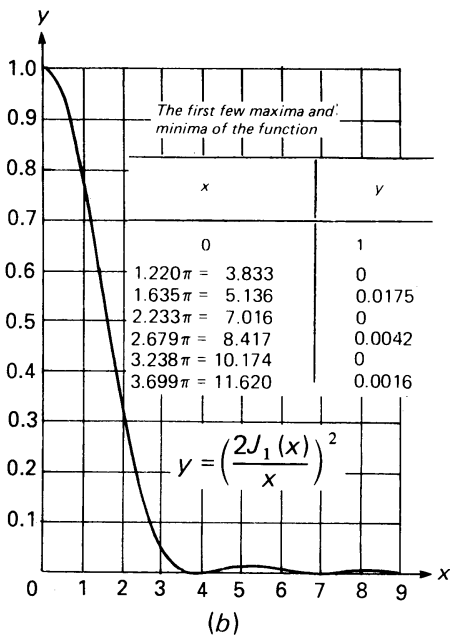

© Cambridge University Press • Provided by the NASA Astrophysics Data System

Configurations of optical telescopes. (Adapted from Sinnott, R. W., *Sky and Telescope*, July 1980.)

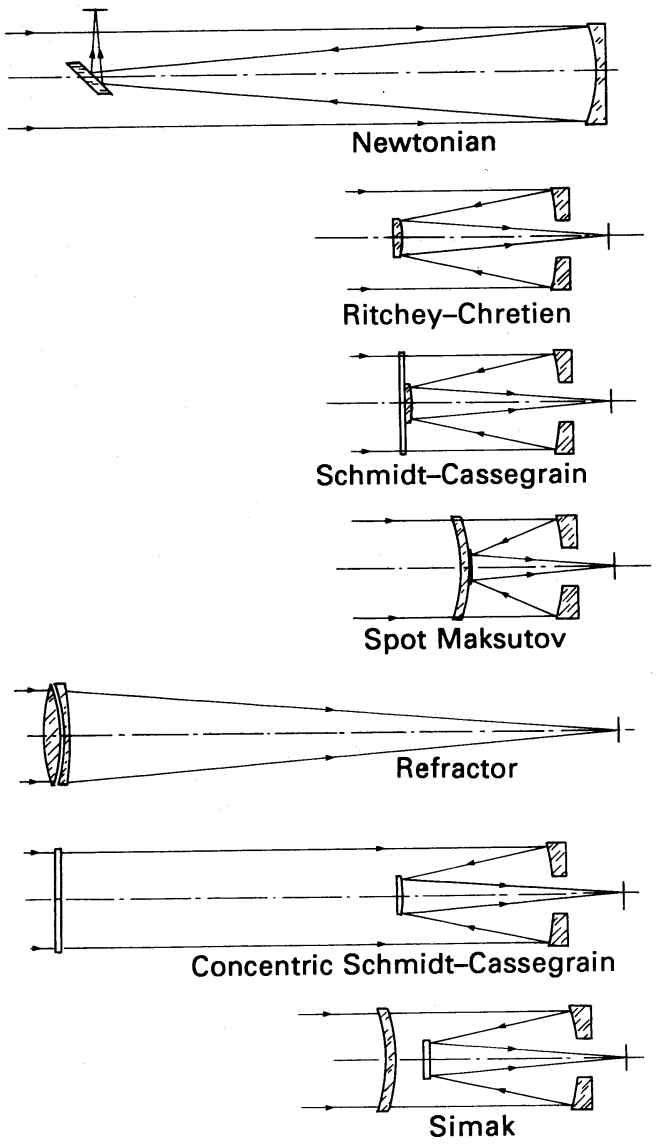

© Cambridge University Press • Provided by the NASA Astrophysics Data System

Optical telescopes (*cont.*)

Focus configurations for optical telescopes. (Adapted from *Survey of Catadioptric Optical Systems*, J. B. Galligan, ed., Itek Corporation, 1966.)

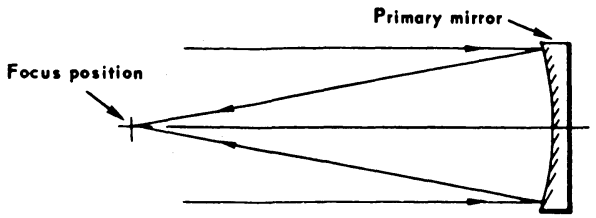

Prime Focus

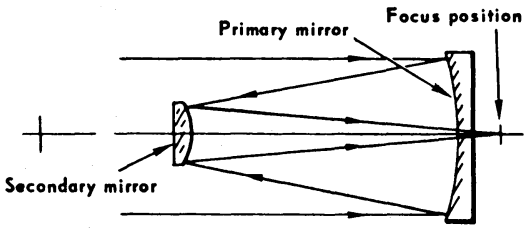

Cassegrain Focus

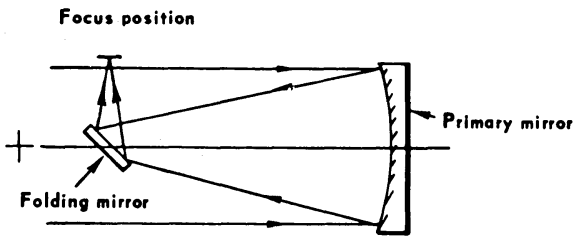

Newtonian Focus

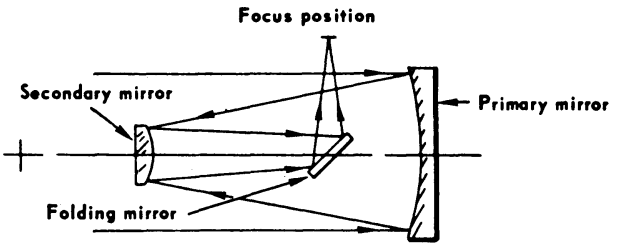

Coudé Focus

© Cambridge University Press • Provided by the NASA Astrophysics Data System

Spectral luminous efficiency. Relative luminosity values for photopic and scotopic vision

Wavelength (nm)	Photopic $V(\lambda)$ ($B > 3\,\mathrm{cd\,m^{-2}}$)	Scotopic $V(\lambda)$ ($B < 3 \times 10^{-5}\,\mathrm{cd\,m^{-2}}$)
350	—	0.0003
360	—	0.0008
370	—	0.0022
380	0.000 04	0.0055
390	0.000 12	0.0127
400	0.0004	0.0270
410	0.0012	0.0530
420	0.0040	0.0950
430	0.0116	0.157
440	0.023	0.239
450	0.038	0.339
460	0.060	0.456
470	0.091	0.576
480	0.139	0.713
490	0.208	0.842
500	0.323	0.948
510	0.503	0.999
520	0.710	0.953
530	0.862	0.849
540	0.954	0.697
550	0.995	0.531
560	0.995	0.365
570	0.952	0.243
580	0.870	0.155
590	0.757	0.0942
600	0.631	0.0561
610	0.503	0.0324
620	0.381	0.0188
630	0.265	0.0105
640	0.175	0.0058
650	0.107	0.0032
660	0.061	0.0017
670	0.032	0.0009
680	0.017	0.0005
690	0.0082	0.0002
700	0.0041	0.0001
710	0.0021	—
720	0.001 05	—
730	0.000 52	—
740	0.000 25	—
750	0.000 12	—
760	0.000 06	—
770	0.000 03	

© Cambridge University Press • Provided by the NASA Astrophysics Data System

$K(\lambda)$, spectral luminous efficacy for scotopic and photopic vision.
Scotopic:
max $K = K(511\,\text{nm}) = 1746$ lm W^{-1}.
Photopic:
max $K = K(555\,\text{nm}) = 680\,\text{ln}\,\text{W}^{-1}$

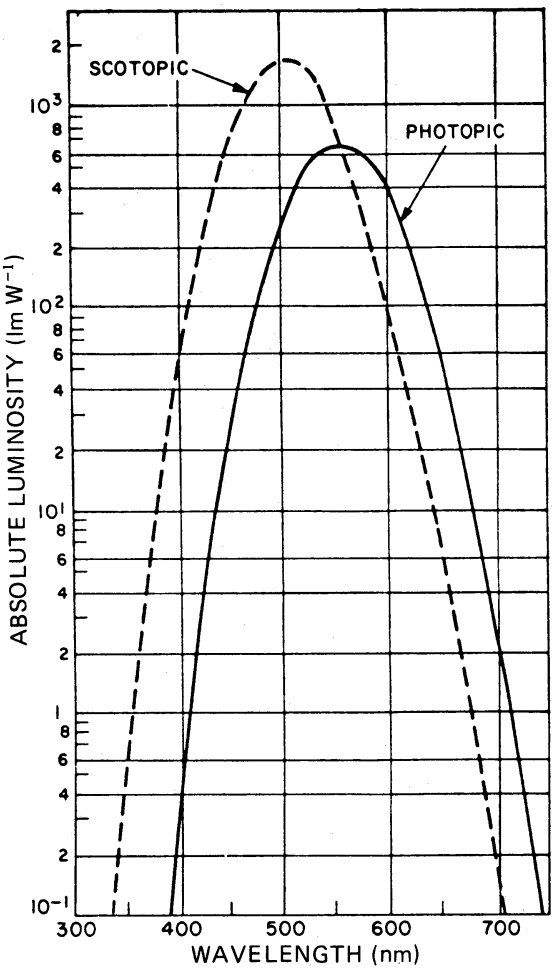

© Cambridge University Press • Provided by the NASA Astrophysics Data System

Summary of typical sources/parameters for the most commonly used radiant energy sources

Lamp type	DC input power (watts)	Arc dimensions (mm)	Luminous flux (lm)†	Luminous efficiency (lm W^{-1})	Average luminance (cd mm^{-2})
Mercury short arc (high pressure)	200	2.5 × 1.8	9500	47.5	250
Xenon short arc	150	1.3 × 1.0	3200	21	300
Xenon short arc	20 000	12.5 × 6	1 150 000	57	3000 (in 3 mm × 6 mm)
Zirconium arc	100	1.5 (diam.)	250	2.5	100
Vortex-stabilized argon arc	24 800	3 × 10	422 000	17	1400
Tungsten light bulbs	10	—	79	7.9	10 to 25
	100	—	1630	16.3	
	1000	—	21 500	21.5	
Fluorescent lamp standard warm white	40	—	2560	64	—
Carbon arc, non-rotating	2000	≈ 5 × 5	36 800	18.4	175 to 800
rotating	15 800	≈ 8 × 8	350 000	22.2	
Deuterium lamp	40	1.0 (diam.)	(Nominal irradiance at 250 nm at 30 cm = 0.2 μW cm^{-2} nm^{-1})		

† Luminous flux Φ in lumens from a source of total radiant power $W(\lambda)$ watts per unit wavelength:

$$\Phi = 680 \int_0^\infty W(\lambda)\, V(\lambda)\, d\lambda,$$

where $V(\lambda)$ represents the spectral luminous efficiency.

Conversion table for various photometric units

Luminous intensity (I)

1 candela (cd) = 1 lumen/steradian (lm sr^{-1})

Luminous flux (Φ) [lumen (lm)]

4π lumens = total flux from uniform point source of 1 candela

Illuminance (E)

1 footcandle (fc) = 1 lumen $foot^{-2}$

1 lux (lx) = 1 lumen m^{-2} = 0.0929 footcandle

© Cambridge University Press • Provided by the NASA Astrophysics Data System

Luminance (L)
1 footlambert (fL) = $1/\pi$ candela foot^{-2}.
1 nit (nt) = 1 candela m^{-2} = 0.2919 footlambert

Luminance values for various sources

Source	Luminance (fL)	Luminance (cd m^{-2})
Sun, as observed from Earth's surface at meridian	4.7×10^8	1.6×10^9
Moon, bright spot, as observed from Earth's surface	730	2500
Clear blue sky	2300	7900
Lightning flash	2×10^{10}	7×10^{10}
Atomic fission bomb, 0.1 ms after firing, 90-ft diameter ball	6×10^{11}	2×10^{12}
Tungsten filament lamp, gas-filled, 16 lm W^{-1}	2.6×10^6	9×10^6
Plain carbon arc, positive crater	4.7×10^6	1.6×10^7
Fluorescent lamp, T-12 bulb, cool white, 430 mA, medium loading	2000	7000
Color television screen, average brightness	50	170

Typical values of natural scene illuminance

Sky condition	Approximate levels of illuminance (lux)
Direct sunlight	$1–1.3 \times 10^5$
Full daylight (not direct sunlight)	$1–2 \times 10^4$
Overcast day	10^3
Very dark day	10^2
Twilight	10
Deep twilight	1
Full moon	10^{-1}
Quarter moon	10^{-2}
Moonless, clear night sky	10^{-3}
Moonless, overcast night sky	10^{-4}

© Cambridge University Press • Provided by the NASA Astrophysics Data System

Natural illuminance on the Earth for the hours immediately before and after sunset with a clear sky and no moon

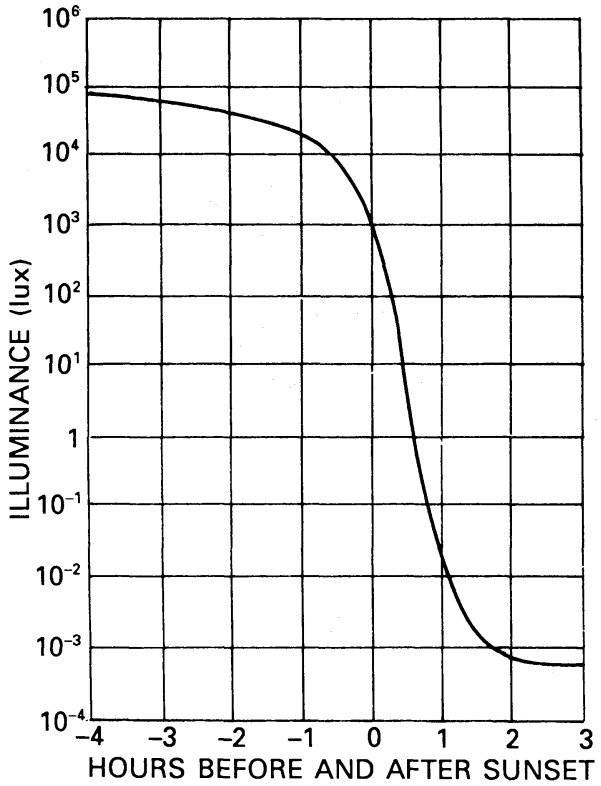

Radiant responsivity

Calculation of radiant responsivity from luminous responsivity for photocathodes:

The response of a photocathode (in amperes) to the total radiation $W(\lambda)$ watts per unit wavelength is:

$$\int \sigma R(\lambda) W(\lambda)\, \mathrm{d}\lambda,$$

where the relative spectral response of the photocathode is $R(\lambda)$ ($R_{\max} = 1$) and σ is the absolute radiant response at the peak of the response curve (amperes per watt). The light flux (in lumens) is given by:

$$680 \int V(\lambda) W(\lambda)\, \mathrm{d}\lambda,$$

where $V(\lambda)$ is the spectral luminous efficiency. The luminous responsivity of the photocathode in amperes per lumen is then given by:

$$S = \frac{\sigma \int R(\lambda) W(\lambda)\, \mathrm{d}\lambda}{680 \int V(\lambda) W(\lambda)\, \mathrm{d}\lambda}$$

and, therefore,

$$\sigma = \frac{680 S \int V(\lambda) W(\lambda)\, \mathrm{d}\lambda}{\int R(\lambda) W(\lambda)\, \mathrm{d}\lambda}.$$

(The material in the preceding sections was adapted from Engstrom, R. W., *Photomultiplier Handbook*, RCA Corporation, 1980.)

© Cambridge University Press • Provided by the NASA Astrophysics Data System

Standard units, symbols, and defining equations for fundamental photometric and radiometric quantities

Quantity[a]	Symbol[a]	Defining equation[b]	Commonly used units[c]	Symbol
RADIOMETRIC				
Radiant energy	Q (Q_e)	—	erg	
			†joule	J
			kilowatt-hour	kWh
Radiant density	w (w_e)	$w = dQ/dV$	†joule per cubic meter	$J\,m^{-3}$
			erg per cubic centimeter	$erg\,cm^{-3}$
Radiant flux	Φ (Φ_e)	$\Phi = dQ/dt$	erg per second	$erg\,s^{-1}$
			†watt	W
Radiant flux density at a surface				
Radiant exitance (radiant emittance)[d]	M (M_e)	$M = d\Phi/dA$	watt per square centimeter	$W\,cm^{-2}$
Irradiance	E (E_e)	$E = d\Phi/dA$	†watt per square meter, etc.	$W\,m^{-2}$
Radiant intensity	I (I_e)	$I = d\Phi/d\omega$[i]	†watt per steradian	$W\,sr^{-1}$
Radiance	L (L_e)	$L = d^2\Phi/d\omega(dA\cos\theta) = dI/(dA\cos\theta)$[e]	watt per steradian and square centimeter	$W\,sr^{-1}\,cm^{-2}$
			†watt per steradian and square meter	$W\,sr^{-1}\,m^{-2}$
Emissivity	ε	$\varepsilon = M/M_{\text{blackbody}}$[f]	one (numeric)	—
PHOTOMETRIC				
Absorptance	α (α_v, α_e)	$\alpha = \Phi_a/\Phi_i$[g]	one (numeric)	—
Reflectance	ρ (ρ_v, ρ_e)	$\rho = \Phi_r/\Phi_i$[g]	one (numeric)	—
Transmittance	τ (τ_v, τ_e)	$\tau = \Phi_t/\Phi_i$[g]	one (numeric)	—
Luminous energy (quantity of light)	Q (Q_v)	$Q_v = \int_{380}^{760} K(\lambda) Q_e \lambda\, d\lambda$	lumen-hour	lm-h
			†lumen-second (talbot)	lm-s
Luminous density	w (w_v)	$w = dQ/dV$	†lumen-second per cubic meter	$lm\text{-}s\,m^{-3}$
Luminous flux	Φ (Φ_v)	$\Phi = dQ/dt$	†lumen	lm

© Cambridge University Press • Provided by the NASA Astrophysics Data System

© Cambridge University Press • Provided by the NASA Astrophysics Data System

Standard units, symbols, and defining equations for fundamental photometric and radiometric quantities (*cont.*)

Quantity[a]	Symbol[a]	Defining equation[b]	Commonly used units[c]	Symbol
Luminous flux density at a surface				
Luminous exitance (luminous emittance)[d]	M (M_v)	$M = d\Phi/dA$	lumen per square foot	$lm\ ft^{-2}$
Illumination (illuminance)	E (E_v)	$E = d\Phi/dA$	footcandle (lumen per square foot)	fc
			†lux ($lm\ m^{-2}$)	lx
			phot ($lm\ cm^{-2}$)	ph
Luminous intensity (candlepower)	I (I_v)	$I = d\Phi/d\omega$[i]	†candela (lumen per steradian)	cd
Luminance (photometric brightness)	L (L_v)	$L = d^2\Phi/d\omega(dA\cos\theta)$	candela per unit area	$cd\ in^{-2}$, etc.
		$= dI/(dA\cos\theta)$[e]	stilb ($cd\ cm^{-2}$)	sb
			nit (†$cd\ m^{-2}$)	nt
			footlambert (cd per πft^2)	fL
			lambert (cd per πcm^2)	L
			apostilb (cd per πm^2)	asb
Luminous efficacy	K	$K = \Phi_v/\Phi_e$	†lumen $watt^{-1}$	$lm\ W^{-1}$
Luminous efficiency	V	$V = K/K_{max}$[h]	one (numeric)	—

[a] The symbols for photometric quantities are the same as those for the corresponding radiometric quantities. When it is necessary to differentiate them, the subscripts v and e, respectively, should be used, e.g., Q_v and Q_e. Quantities may be restricted to a narrow wavelength band by adding the word spectral and indicating the wavelength. The corresponding symbols are changed by adding a subscript λ, e.g., Q_λ for a spectral concentration or a λ in parentheses, e.g., $K(\lambda)$, for a function of wavelength.

[b] The equations in this column are given merely for identification.

[c] International System (SI) unit indicated by dagger (†).

[d] To be deprecated.

[e] θ is the angle between line of sight and normal to surface considered.

[f] M and $M_{blackbody}$ are, respectively, radiant exitance of a measured specimen and of a blackbody at the same temperature as the specimen.

[g] Φ_i is incident flux, Φ_a is absorbed flux, Φ_r is reflected flux, Φ_t is transmitted flux.

[h] K_{max} is the maximum value of the $K(\lambda)$ function.

[i] ω is the solid angle through which flux from point source is radiated.

(*Photoelectronic Imaging Devices*, Vol. 1, L. M. Biberman & S. Nudelman, eds., Plenum Press, 1971, with permission.)

Visible and ultraviolet light detectors

Photodiode

Schematics of photodiodes (*a*) sealed with semi-transparent photocathode, (*b*) open (or sealed) with opaque photocathode. (From Timothy, J. G. & Madden, R. P. in *Handbook on Synchrotron Radiation*, E. Koch, ed., North-Holland Publishing Co., 1983, with permission.)

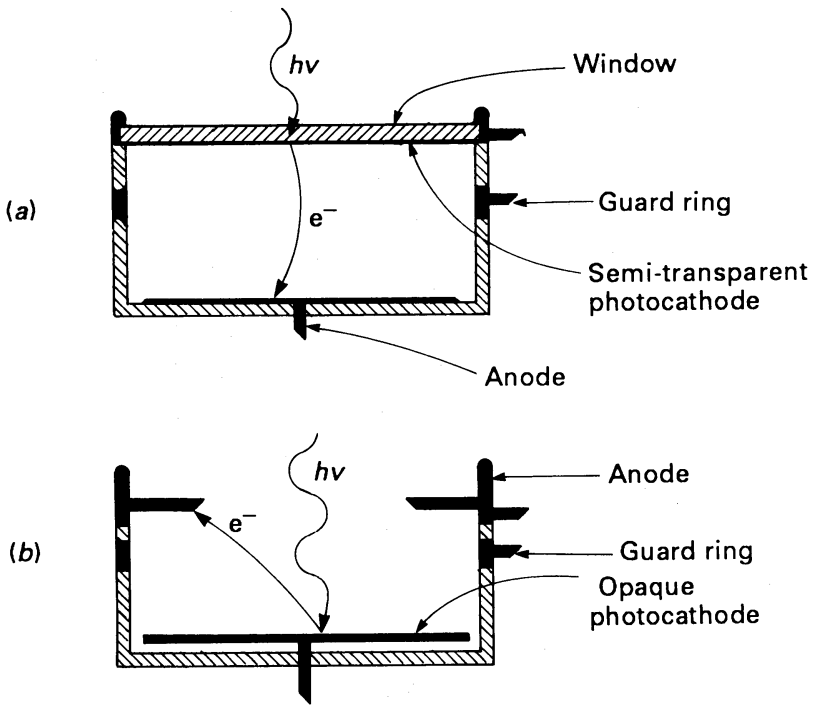

© Cambridge University Press • Provided by the NASA Astrophysics Data System

Quantum efficiencies of opaque Cs_2Te and CsI photocathodes. (From Timothy, J. G. & Madden, R. P., *op. cit.*)

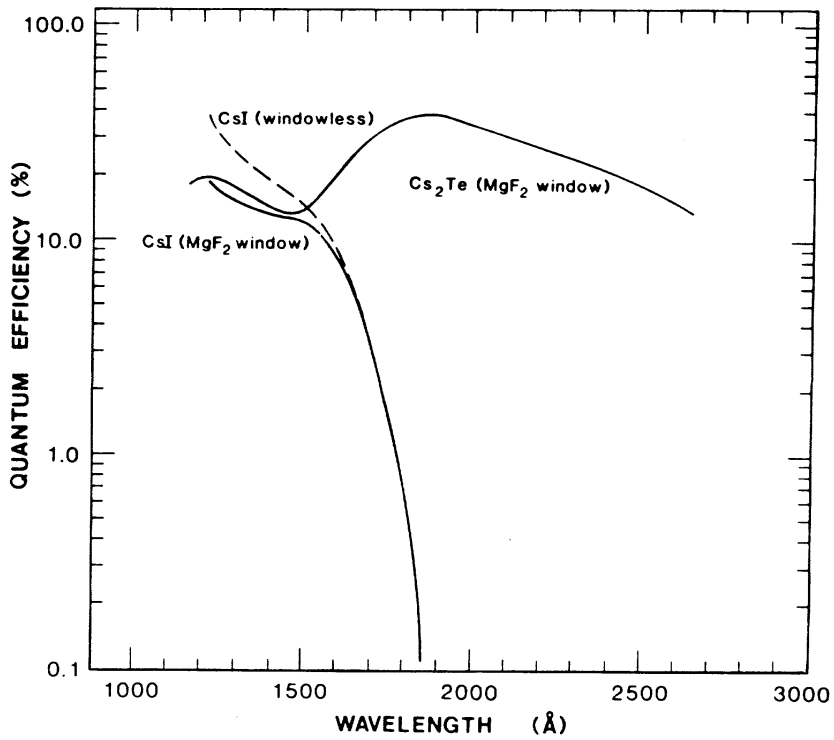

Quantum efficiencies of transfer standard detectors available from NBS. (From Timothy, J. G. & Madden, R. P., *op. cit.*)

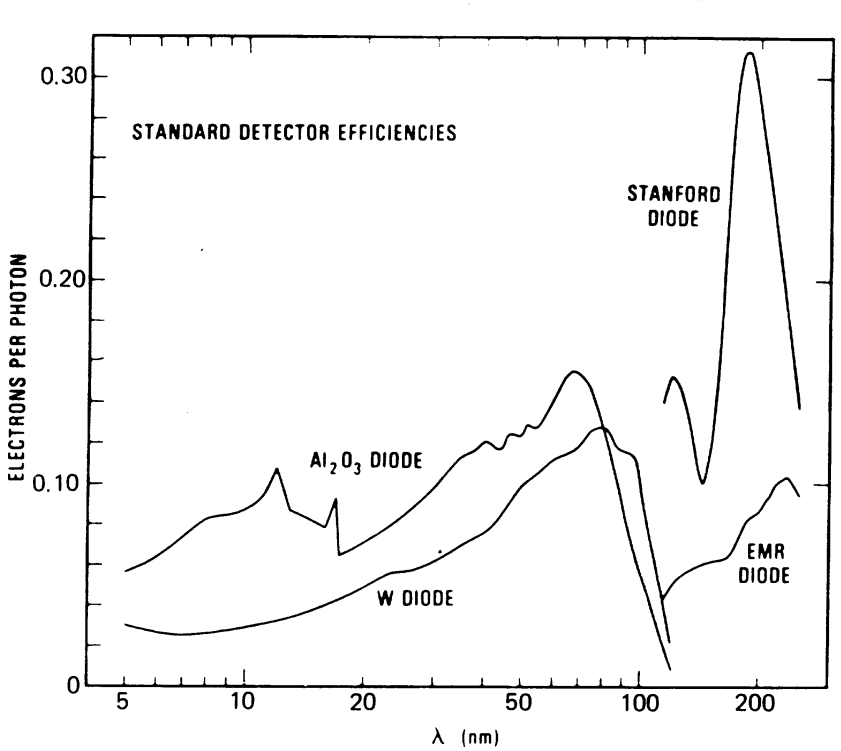

© Cambridge University Press • Provided by the NASA Astrophysics Data System

Image intensifiers

Generation I electrostatically focused image intensifier. (Reproduced with permission of the publisher, Howard W. Sams & Co., Indianapolis, *Image Tubes*, by Illes P. Csorba, © 1985.)

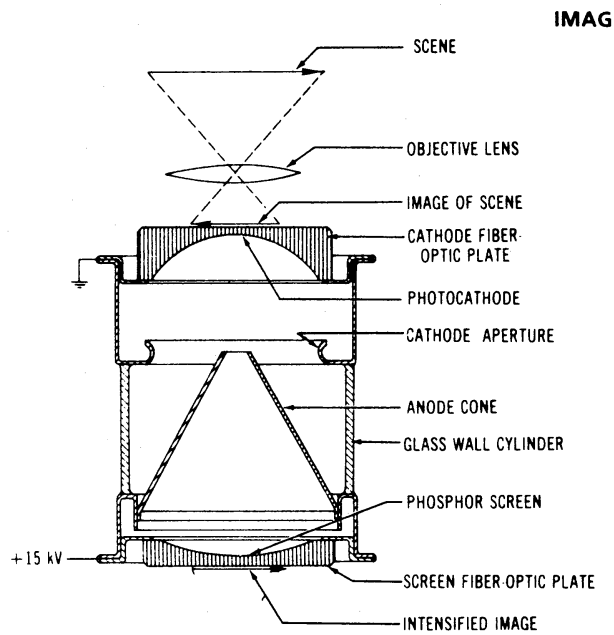

The electrostatic image-inverting generation II image intensifier employs a microchannel plate (MCP). (From Csorba, I. P., *op. cit.*)

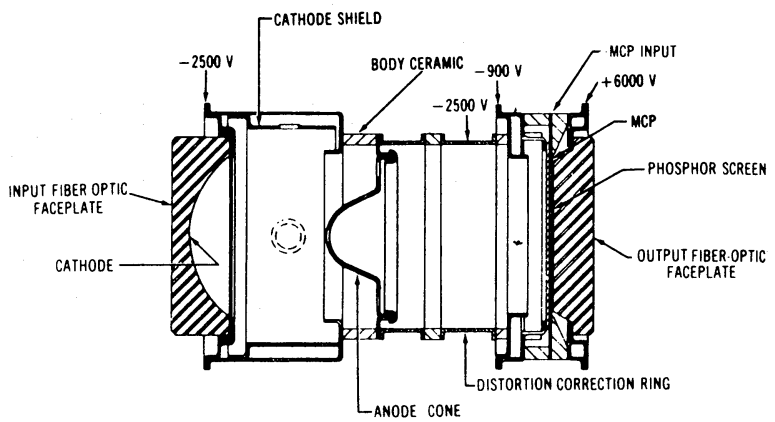

© Cambridge University Press • Provided by the NASA Astrophysics Data System

© Cambridge University Press • Provided by the NASA Astrophysics Data System

Photomultipliers

Schematic of typical photomultiplier showing some electron trajectories (RCA).

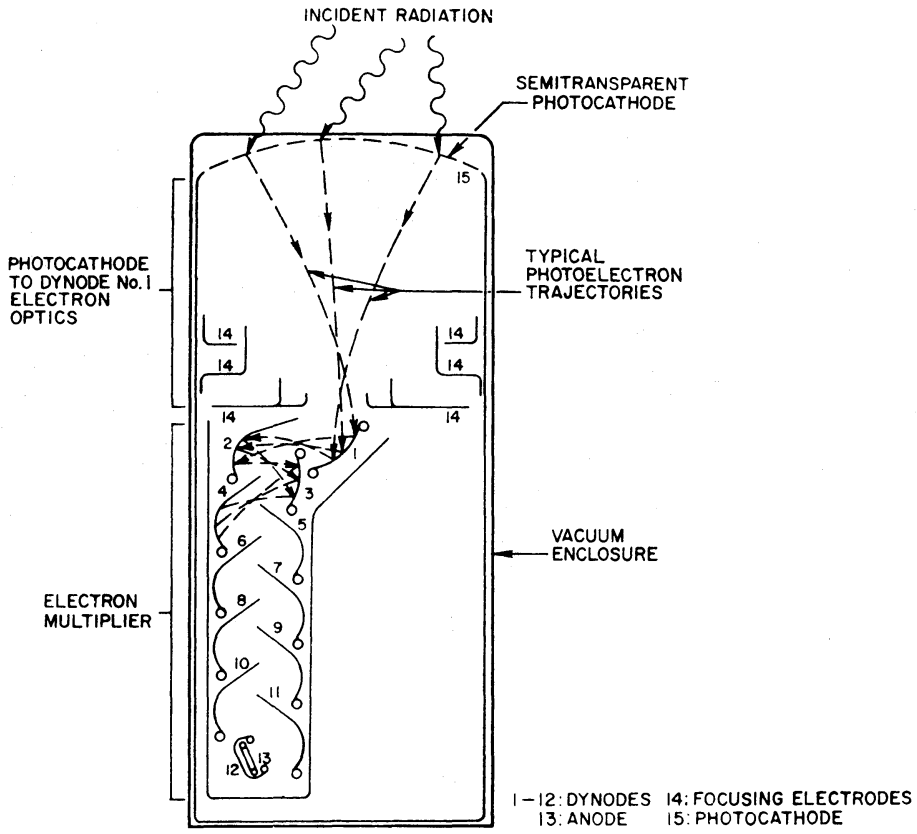

Typical anode sensitivity and amplification characteristics of a 9-dynode photomultiplier tube as a function of applied voltage (RCA).

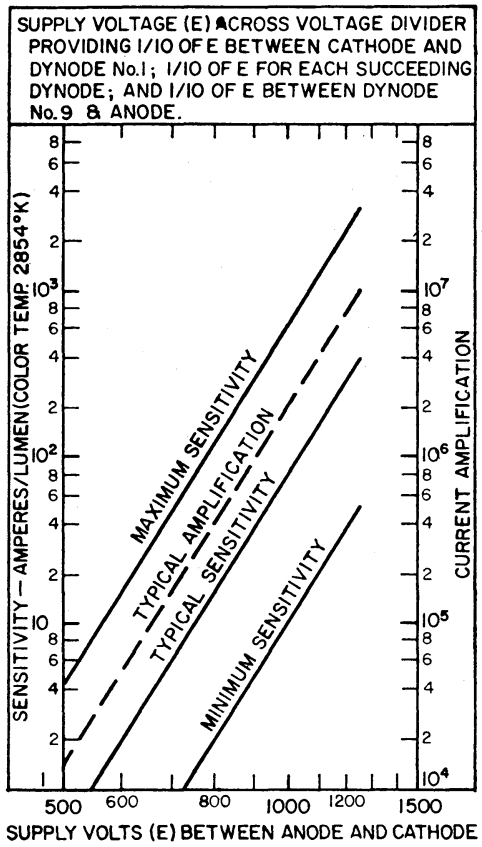

Typical voltage-divider arrangement for fast pulse response and high peak current systems.

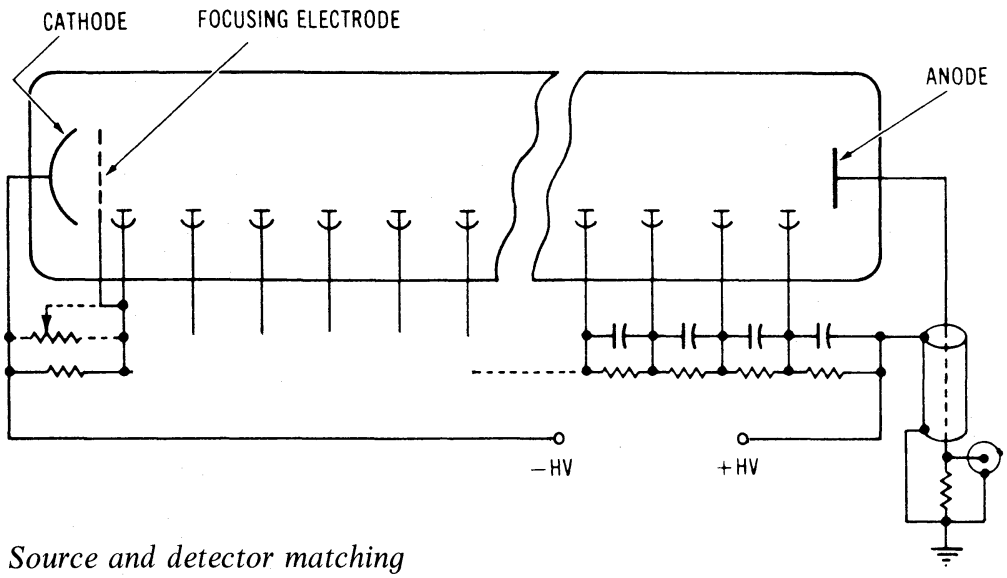

Source and detector matching

The average power radiating from a light source is given by:

$$P = P_0 \int_0^\infty W(\lambda)\,\mathrm{d}\lambda,$$

where P_0 is the incident power in watts per unit wavelength at the peak of the relative spectral radiation characteristic, $W(\lambda)$, which is normalized to unity.

The resulting photocathode current I, when the light is incident on the detector, is given by:

$$I_k = \sigma P_0 \int_0^\infty W(\lambda)R(\lambda)\,\mathrm{d}\lambda,$$

where σ is the radiant sensitivity of the photocathode in amperes per watt at the peak of the relative curve, and $R(\lambda)$ represents the relative photocathode spectral response as a function of wavelength normalized to unity at the peak.

$$I_\mathrm{k} = \sigma P \frac{\int_0^\infty W(\lambda)R(\lambda)\,\mathrm{d}\lambda}{\int_0^\infty W(\lambda)\,\mathrm{d}\lambda}.$$

The ratio of the dimensionless integrals can be defined as the *matching factor*, M.

$$M = \frac{\int_0^\infty W(\lambda)R(\lambda)\,\mathrm{d}\lambda}{\int_0^\infty W(\lambda)\,\mathrm{d}\lambda}.$$

© Cambridge University Press • Provided by the NASA Astrophysics Data System

© Cambridge University Press • Provided by the NASA Astrophysics Data System

Spectral matching factors

Source	Photocathodes							Photopic eye	Scotopic eye
	S1	S4	S10	S11	S17	S20	S25		
PHOSPHORS									
P1	0.278	0.498	0.807	0.687	0.892	0.700	0.853	0.768	0.743
P4	0.310	0.549	0.767	0.661	0.734	0.724	0.861	0.402	0.452
P7	0.312	0.611	0.805	0.709	0.773	0.771	0.882	0.411	0.388
P11	0.217	0.816	0.949	0.914	0.954	0.877	0.953	0.201	0.601
P15	0.385	0.701	0.855	0.787	0.871	0.802	0.904	0.376	0.495
P16	0.830	0.970	0.853	0.880	0.855	0.902	0.922	0.003	0.042
P20	0.395	0.284	0.612	0.427	0.563	0.583	0.782	0.707	0.354
P22B	0.217	0.893	0.974	0.960	0.948	0.927	0.979	0.808	0.477
P22G	0.278	0.495	0.807	0.686	0.896	0.699	0.855	0.784	0.747
P22R	0.632	0.036	0.264	0.055	0.077	0.368	0.623	0.225	0.008
P24	0.279	0.545	0.806	0.696	0.827	0.725	0.869	0.540	0.621
P31	0.276	0.533	0.811	0.698	0.853	0.722	0.868	0.626	0.651
NaI	0.534	0.923	0.885	0.889	0.889	0.900	0.933	0.046	0.224

Spectral matching factors (cont'd)

Source	Photocathodes							Photopic eye	Scotopic eye
	S1	S4	S10	S11	S17	S20	S25		
LAMPS									
2870/2856 std	0.516†	0.046†	0.095†	0.060†	0.072†	0.112†	0.227†	0.071†	0.040†
Fluorescent	0.395	0.390	0.650	0.496	0.575	0.635	0.805	0.502	0.314
SUN									
In space	0.535†	0.308†	0.388†	0.328†	0.380†	0.406†	0.547†	0.179†	0.172†
+2 air masses	0.536†	0.236†	0.348†	0.277†	0.315†	0.360†	0.513†	0.197†	0.175†
Day sky	0.537†	0.520†	0.556†	0.508†	0.589†	0.581†	0.700†	0.170†	0.218†
BLACKBODIES									
6000 K	0.533†	0.308†	0.376†	0.320†	0.375†	0.397†	0.521†	0.167†	0.159†
3000 K	0.512†	0.053†	0.102†	0.067†	0.080†	0.120†	0.232†	0.075†	0.044†
2870 K	0.504†	0.044†	0.090†	0.057†	0.069†	0.106†	0.216†	0.067†	0.038†
2856 K	0.500†	0.042†	0.088†	0.055†	0.068†	0.103†	0.211†	0.065†	0.037†
2810 K	0.493†	0.039†	0.081†	0.051†	0.062†	0.097†	0.150†	0.061†	0.034†
2042 K	0.401†	0.008†	0.023†	0.011†	0.014†	0.033†	0.090†	0.018†	0.007†

† Entry valid only for 300–1200 nm wavelength interval.

© Cambridge University Press • Provided by the NASA Astrophysics Data System

Nominal composition and characteristics of various photocathodes

Nominal composition	JETEC response designation	Conversion factor[a] (lumen watt^{-1} at λ_{max})	Luminous responsivity (μA lumen^{-1})	Wavelength of maximum response, λ_{max} (nm)	Responsivity at λ_{max} (mA watt^{-1})	Quantum efficiency at λ_{max} (%)	Dark emission at 25 °C (fA cm^{-2})
Ag–O–Cs	S-1	92.7	25	800	2.3	0.36	900
Ag–O–Rb	S-3	285	6.5	420	1.8	0.55	—
Cs_3Sb	S-19	1603	40	330	64	24	0.3
Cs_3Sb	S-4	1044	40	400	42	13	0.2
Cs_3Sb	S-5	1262	40	340	50	18	0.3
Cs_3Bi	S-8	757	3	365	2.3	0.77	0.13
Ag–Bi–O–Cs	S-10	509	40	450	20	5.6	70
Cs_3Sb	S-13	799	60	440	48	14	4
Cs_3Sb	S-9	683	30	480	20	5.3	—
Cs_3Sb	S-11	808	60	440	48	14	3
Cs_3Sb	S-21	783	30	440	23	6.7	—
Cs_3Sb	S-17	667	125	490	83	21	1.2
Na_2KSb	S-24	758	85	420	64	19	0.0003

© Cambridge University Press • Provided by the NASA Astrophysics Data System

Nominal composition and characteristics of various photocathodes (cont'd)

Nominal composition	JETEC response designation	Conversion factor[a] (lumen watt^{-1} at λ_{max})	Luminous responsivity (μA lumen^{-1})	Wavelength of maximum response, λ_{max} (nm)	Responsivity at λ_{max} (mA watt^{-1})	Quantum efficiency at λ_{max} (%)	Dark emission at 25 °C (fA cm^{-2})
K_2CsSb	—	1117	85	400	95	29	0.02
Rb–Cs–Sb	—	767	120	450	92	25	1
Na_2KSb:Cs	—	429	150	420	64	19	0.4
Na_2KSb:Cs	S-20	428	150	420	64	19	0.3
Na_2KSb:Cs	S-25	276	160	420	44	13	—
Na_2KSb:Cs	ERMA II	220	200	530	44	10.3	2.1
Na_2KSb:Cs	ERMA III	160	230	575	37	8	0.2
GaAs:Cs–O	—	116	1025	850	119	17	92
GaAsP:Cs–O	—	310	200	450	61	17	0.01
$In_{0.06}Ga_{0.94}As$:Cs–O	—	200	250	400	50	15.5	220
$In_{0.12}Ga_{0.88}As$:Cs–O	—	255	270	400	69	21	40
$In_{0.18}Ga_{0.82}As$:Cs–O	—	280	150	400	42	13	75
Cs_2Te	—			250	25	12.4	0.0006
Cs I	—			120	24	20	Very low
Cu I	—			150	13	10.7	Very low
K–Cs–Rb–Sb	—	672	125	440	84	24	Very low

[a] These conversion factors are the ratio of the radiant responsivity at the peak of the spectral response characteristic in amperes per watt to the luminous responsivity in amperes per lumen for a tungsten lamp operated at a color temperature of 2856 K.

© Cambridge University Press • Provided by the NASA Astrophysics Data System

Typical photocathode spectral response characteristics (from RCA Corp.)

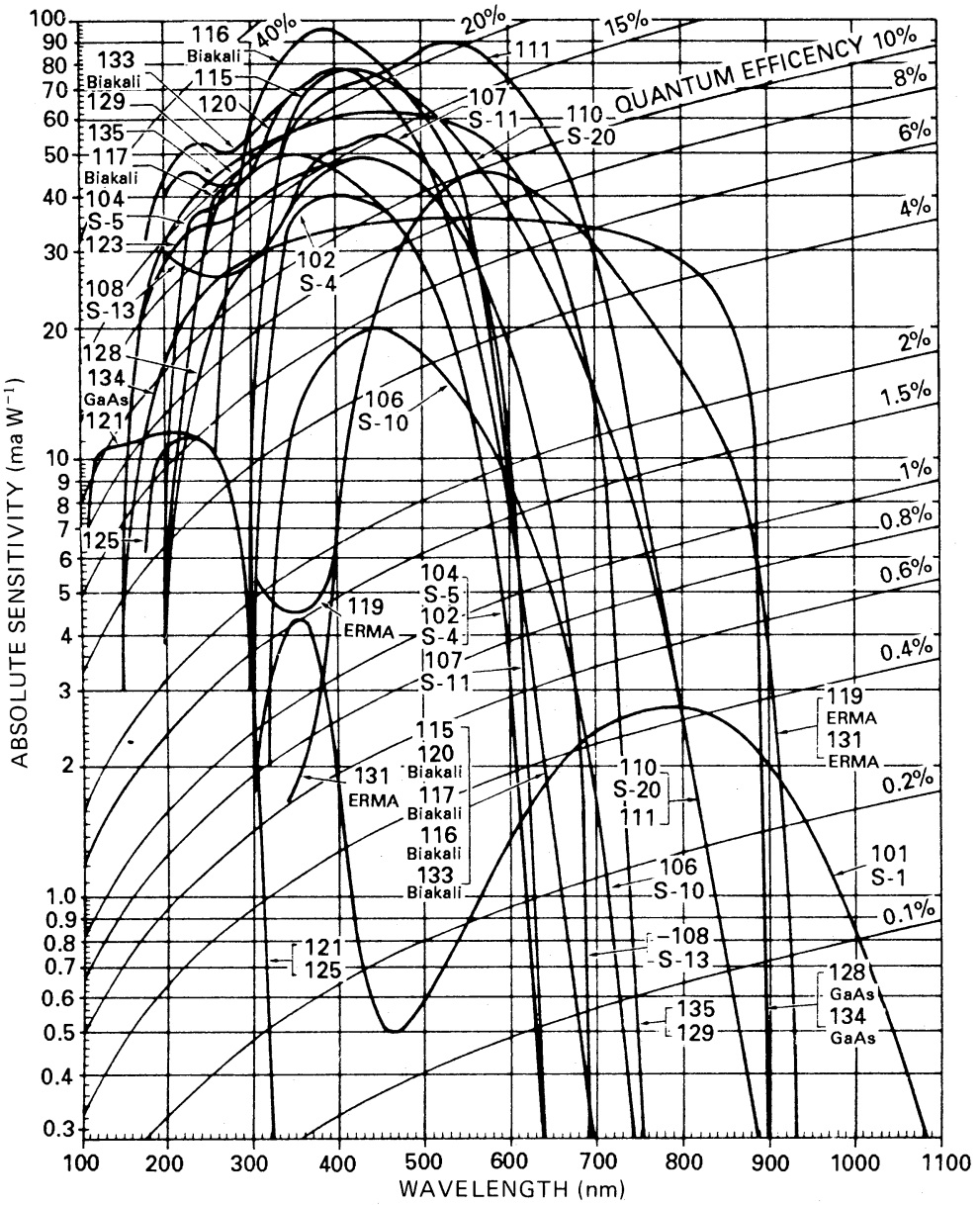

Short wavelength transmission limits of some UV window materials

Material	Approximate limit (10%, 2 mm thick)
LiF	1040 Å
MgF_2	1120
CaF_2	1220
SrF_2	1280
BaF_2	1340
Al_2O_3 (sapphire)	1410
SiO_2 (fused quartz)	1600

© Cambridge University Press • Provided by the NASA Astrophysics Data System

UV fluorescent converters (wavelength shifters)

Sodium salicylate	Diphenylstilbene
Tetraphenyl butadiene	*p*-Terphenyl
Coronene	Dimethyl POPOP
p-Quaterphenyl	POPOP

X-ray and gamma-ray detectors

Detection principles – quantum efficiency

In general, the quantum efficiency, $\varepsilon(E)$, for an incident photon of energy E is determined by the transmission of the detector window or any 'dead layer' and by the absorption of the detector medium:

$$\varepsilon(E) = e^{-(\mu/\rho)_w \rho_w t_w}(1 - e^{-(\mu/\rho)_d \rho_d t_d}),$$

where $(\mu/\rho)_w$ and $(\mu/\rho)_d$ are the mass absorption coefficients of the detector window (or 'dead layer') and detector medium, respectively, ρ_w and ρ_d are the densities of the detector window (or 'dead layer') and detector medium, respectively, and t_w and t_d are the thicknesses of the detector window (or 'dead layer') and detector medium, respectively.

Detection principles – point source detection with X-ray telescopes

The fluctuation δN_S in the number of counts from a point source of flux density F photons $cm^{-2}\ s^{-1}\ keV^{-1}$ is given by:

$$\delta N_S = (A_{eff}\Delta E F t + f^2 \omega B_i \Delta E t + A_{eff}\omega j_D \Delta E t)^{1/2},$$

where

A_{eff} = effective area (cm^2) of telescope including detector,
ΔE = energy interval (keV),
t = observing time (s),
f = focal length (cm) of telescope,
ω = solid angle (sr) of picture element,
B_i = internal background ($ct\ cm^{-2}\ s^{-1}\ keV^{-1}$) of detector,
j_D = diffuse X-ray background (photons $cm^{-2}\ s^{-1}\ keV^{-1}\ sr^{-1}$).

The background, both internal and from diffuse X-rays, is assumed to be steady and well known. For a strong source, the signal-to-noise ratio $N_S/\delta N_S = (A_{eff}\Delta E F t)^{1/2}$ is given by the fluctuations in the source only.

For a weak source, fluctuations in the background determine the signal-to-noise ratio:

$$\frac{N_S}{\delta N_S} = \frac{(A_{eff}\Delta E F t)^{1/2}}{\omega^{1/2}(f^2 B_i / A_{eff} + j_D)^{1/2}}.$$

© Cambridge University Press • Provided by the NASA Astrophysics Data System

Scintillation detector

Illustration representing a NaI scintillation detector showing sequence of events producing output from electron multiplier and various processes which contribute to response of detector to a gamma-ray source. (Adapted from Heath, R. L., *Scintillation Spectrometry*, *USAEC Report*, IDO-16880, 1964.)

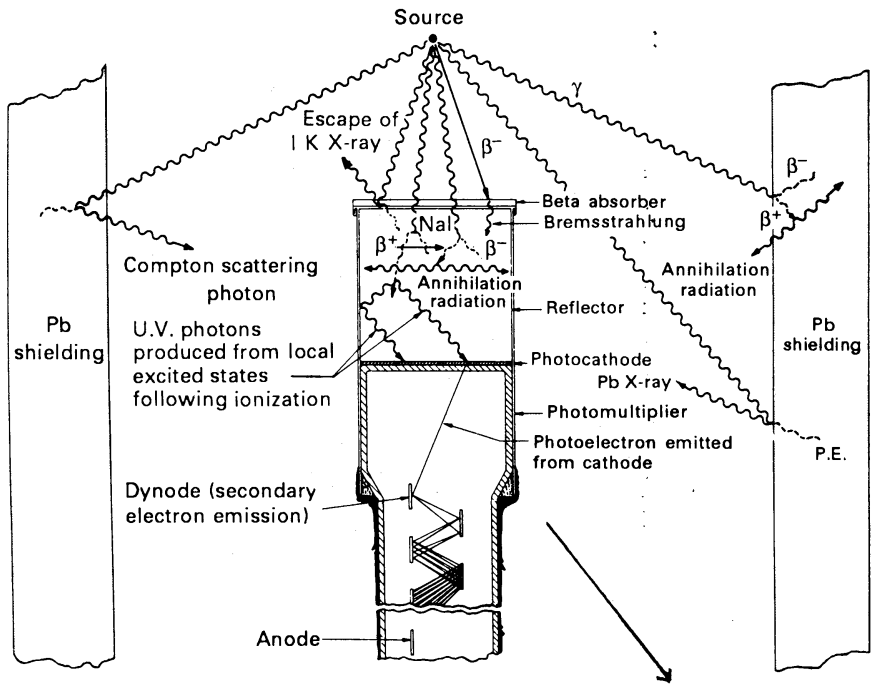

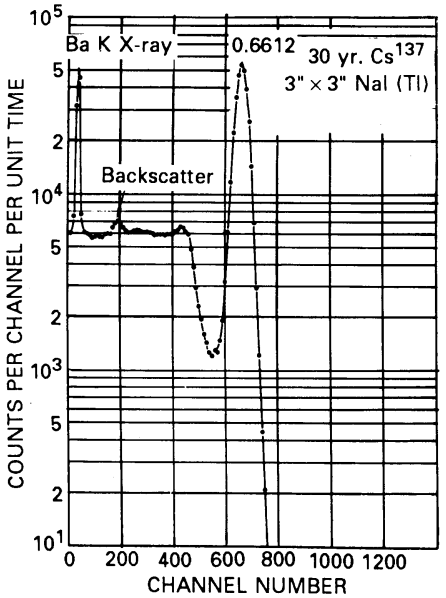

A typical pulse-height spectrum obtained with a NaI(Tl) spectrometer, illustrating the energy response of inorganic scintillators. The scale of the abscissa is 1 keV per channel.

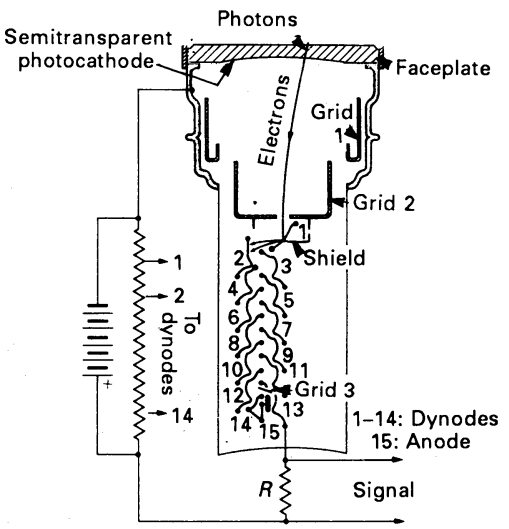

© Cambridge University Press • Provided by the NASA Astrophysics Data System

Gas proportional counter

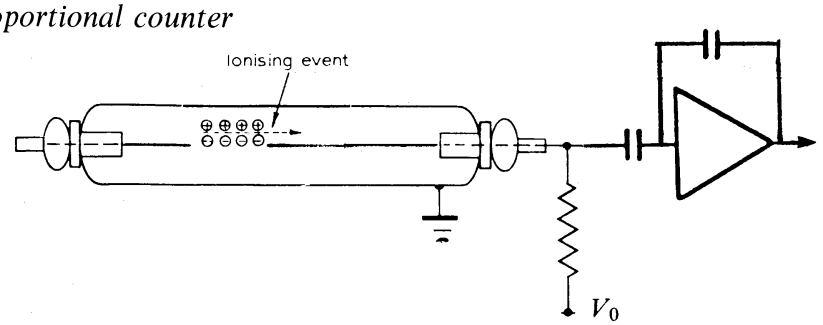

Since a proportional counter has internal gain, the system noise can be neglected and the energy resolution is:

$$(\Delta E)_{\text{FWHM}} = 2.35[(F+f)WE]^{1/2} \quad \text{eV},$$

where

E = energy deposited in counter (eV),
F = Fano factor,
f = a factor to account for variance in the gas gain,
W = mean energy to form an ion pair (eV).

As an example, for methane gas:

$F = 0.26$
$f = 0.75$
$W = 27\,\text{eV}$,

so that for a proportional counter:

$$\frac{E}{(\Delta E)_{\text{FWHM}}} = 2.6E^{1/2} \quad (\text{with } E \text{ in keV}).$$

Total number of ion pairs collected in a gas-filled chamber as a function of the voltage across electrodes of the chamber.

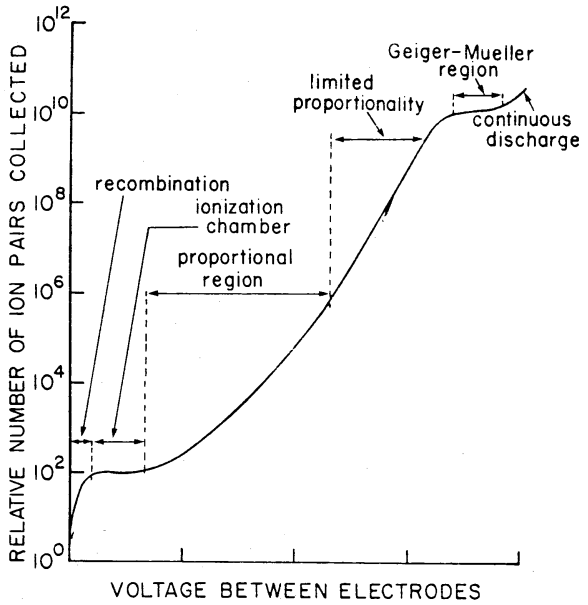

© Cambridge University Press • Provided by the NASA Astrophysics Data System

Position sensitive gas proportional detector

Readout system of detector. Incident photon is absorbed at point a; electrons drift toward anode–cathode planes. An avalanche at the anode (A) gives rise to pulse distributions at the cathodes ($K_{\parallel}$ and $K_{\perp}$). The position (X, Y) is obtained by analog summation and division. (Adapted from Bade, E. *et al.*, *Nucl. Inst. and Meth.*, **201**, 193, 1982.)

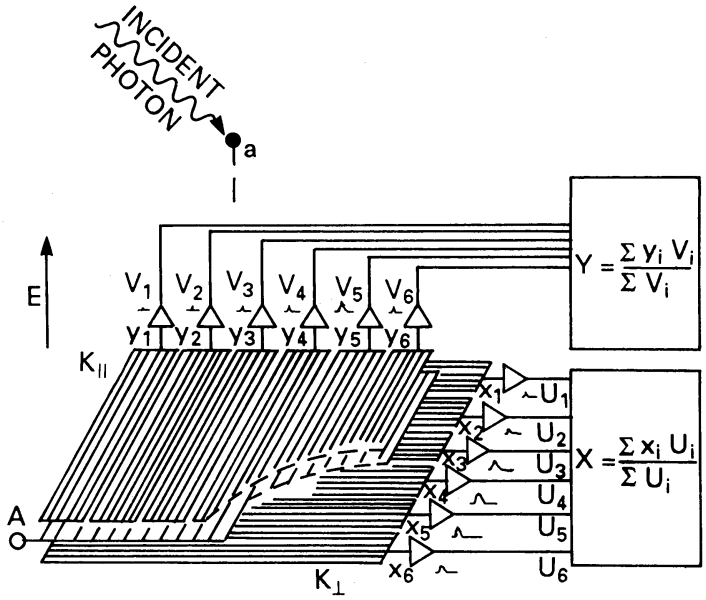

Typical performance

Spatial resolution:

0.25 mm (FWHM) at 1 keV.

Energy resolution:

$$\frac{E}{(\Delta E)_{\mathrm{FWHM}}} = 2.2E^{1/2} \quad \text{(with } E \text{ in keV)}.$$

Format:

10 cm × 10 cm.

The solid-state detector

$$(\Delta E)_{\mathrm{FWHM}} = 2.35[(\eta\sigma)^2 + (F\eta E)]^{1/2} \quad \mathrm{eV},$$

where

η = conversion factor (Si: 3.6 eV per electron–hole pair; Ge: 2.9 eV per electron–hole pair),
σ = detector rms noise (electrons),
F = Fano factor (Si: 0.14; Ge: 0.13),
E = photon or particle energy (eV).

© Cambridge University Press • Provided by the NASA Astrophysics Data System

Schematic diagram of a solid state detector. (Adapted from Enge, H., *Introduction to Nuclear Physics*, Addison-Wesley, 1966.)

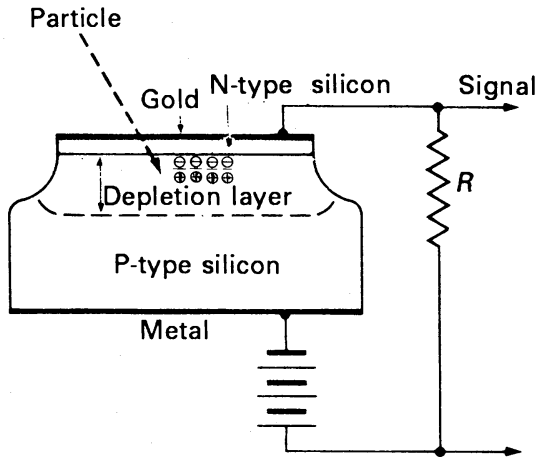

Charge-coupled device (CCD)

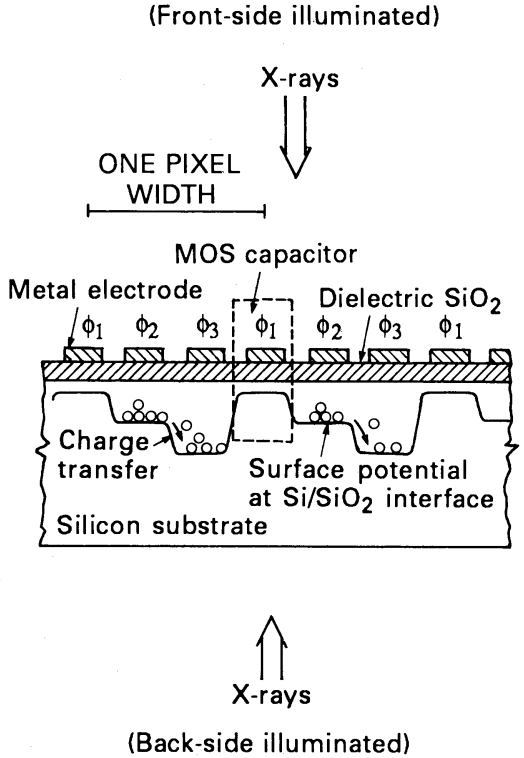

$$(\Delta E)_{\mathrm{FWHM}} = 2.35[(\eta\sigma)^2 + (\eta i_{\mathrm{d}} t)^2 + \eta FE]^{1/2} \quad \text{keV},$$

where

i_{d} = dark current (electrons s^{-1}),
σ = rms readout noise (electrons),

© Cambridge University Press • Provided by the NASA Astrophysics Data System

η = mean energy required to produce one electron–hole pair (0.0036 keV for silicon),
t = integration time (s),
F = Fano factor (~ 0.15),
E = energy of incident photon (keV).

Expected quantum efficiency (defined as the probability that an incident X-ray photon is detected as an 'event') vs. energy. The calculations consider only the interactions of X-rays in Si, for two hypothetical CCD's whose dead-layer and substrate thicknesses are separately within the range spanned by real devices. There will be a low energy cutoff (not shown) depending on the minimum signal which can be discriminated against the system noise.

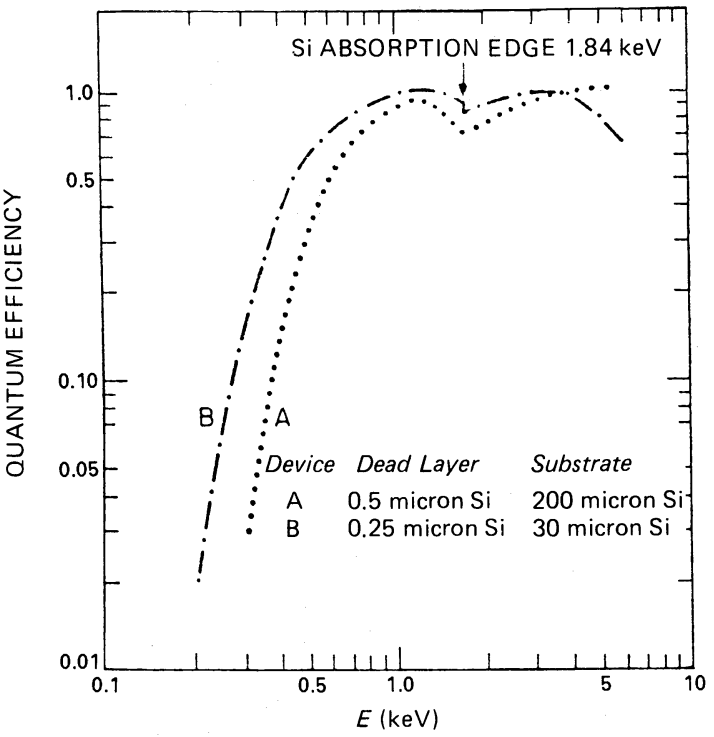

Microchannel plate detector
Typical performance
Spatial resolution:

20–30 μm (FWHM).

Quantum efficiency:

25% at 1.5 keV (CsI photocathode).

Format:

25–100 mm in diameter.

© Cambridge University Press • Provided by the NASA Astrophysics Data System

Schematic diagram of a microchannel plate detector.
(Adapted from Behr, A. in Landolt–Bornstein, subvol. 2a, Springer-Verlag, 1981.)

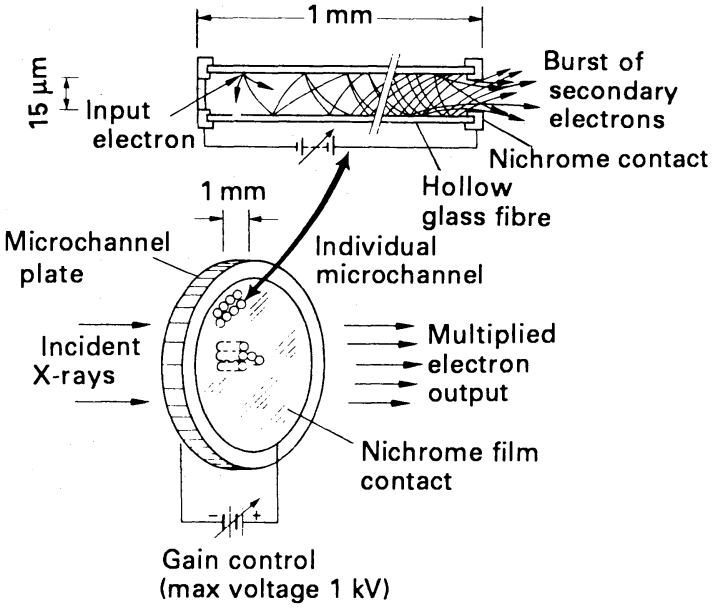

Properties of common X-ray detectors

Detector	Energy range (keV)	$\Delta E/E$[a] at 5.9 keV (%)	Dead time/event (μs)	Maximum count rate (s^{-1})
Geiger counter	3–50	none	200	10^4
Gas ionization in current mode	0.2–50	n/a	n/a	10^{11} [b]
Gas proportional	0.2–50	15	0.2	10^5
Multiwire proportional chamber	3–50	20	0.2	10^5/anode wire
Scintillation [NaI(Tl)]	3–10 000	40	0.25	10^6
Semiconductor [Si(Li)]	1–60	3.0	4–30	5×10^4
Semiconductor (Ge)	1–10 000	3.0	4–40	5×10^4

[a] FWHM.
[b] Maximum count rate density is limited by space-charge effects to around 10^{11} photons $s^{-1} cm^{-3}$.
(From Thompson, A. C. in *X-ray Data Booklet*, Lawrence Berkeley Laboratory, University of California, 1986.)

© Cambridge University Press • Provided by the NASA Astrophysics Data System

Ionization and excitation data for a number of gases

Gas	Atomic number	First ionization potential (eV)	Second ionization potential (eV)	First excited state (eV)	Principal emission wavelengths (Å)
He	2	24.48	54.40	20.9	584
				19.8 meta	3888
					5875
Ne	10	21.56	41.07	16.68	734
				16.53 meta	743
				16.62 meta	5400
					5832
					5852
					6402
Ar	18	15.76	27.62	11.56	1048
				11.49 meta	1066
				11.66 meta	6965
					7067
					7503
					8115
Kr	36	14.00	24.56	9.98	1236
				9.86 meta	5570
				10.51 meta	5870
Xe	54	12.13	21.2	8.39	1296
				8.28 meta	1470
				9.4 meta	4501
					4624
					4671
H	1	13.60		10.2	1215
					4861
					6562
N	7	14.53	29.59	6.3	1200
					4110
O	8	13.61	35.11	9.1	1302
					7771
H_2		15.4		11.2	
N_2		15.8		6.1	
O_2		12.5			
I_2		9.0		1.9	1782
					2062

(Adapted from Rice-Evans, P., *Spark, Streamer, Proportional and Drift Chambers*, The Richelieu Press, London, 1974.)

© Cambridge University Press • Provided by the NASA Astrophysics Data System

Properties of scintillation and solid-state detector materials

Material	Density ($g\,cm^{-3}$)	Band gap (eV)	λ of max. emission (Å)	Decay time[a] (μs)	Index of refraction[b]	Energy[c] (eV)	K-edge (keV)	Scintillation conversion[d] efficiency (%)	Notes
SCINTILLATORS									
NaI(Tl)	3.67	5.38	4100	0.23	1.85	—	1.07, 33.2	100	Hygroscopic
CaF_2(Eu)	3.18	—	4350	0.94	1.47	—	0.68, 4.04	50	Non-hygroscopic
CsI(Na)	4.51	5.67	4200	0.63	1.84	—	33.2, 36.0	80	Hygroscopic
CsI(Tl)	4.51	5.67	5650	1.0	1.80	—	33.2, 36.0	45	Non-hygroscopic
Plastics	1.06	—	3500–4500	0.002–0.020	Varies	—	0.284	20–30	Non-hygroscopic
Liquids	0.86	—	3500–4500	0.002–0.008	Varies	—	0.284	20–30	Non-hygroscopic
SOLID-STATE									
Si(Li)	2.35	1.21	—	—	—	3.6	1.84	—	LN_2 required during operation
Ge(Li)	5.36	0.785	—	—	—	2.9	11.1	—	LN_2 required during operation

[a] Room temperature, exponential decay constant.
[b] At emission maximum.
[c] Per electron–hole pair.
[d] Referred to NaI(Tl) with S-11 photocathode.
(Adapted from *Harshaw Scintillation Phosphors*, The Harshaw Chemical Company.)

© Cambridge University Press • Provided by the NASA Astrophysics Data System

Properties of materials used in X-ray detector systems

	Atomic number, Z	Density (STP) (g cm^{-3})	Shell energy[a] (keV)	X-ray lines[b] (keV)	Fluorescence yield[c]	Energy at which photoelectric equals Compton cross-section (keV)
PROPORTIONAL COUNTER GASES						
Methane (CH_4)	6	0.713×10^{-3}	0.284	0.277		20
Ne	10	0.901×10^{-3}	0.867	0.849, 0.858	0.01	38
Ar	18	1.78×10^{-3}	3.203	2.96	0.105	72
			(0.285, 0.246, 0.244)			
Kr	36	3.74×10^{-3}	14.32	12.64, 14.12	0.625	170
			(1.92, 1.73, 1.67)		(0.04)	
Xe	54	5.85×10^{-3}	34.56	29.67, 33.78	0.875	300
			(5.45, 5.10, 4.78)	(4.10, 4.49, 5.30)	(0.14)	
CRYSTALS						
NaI	53	3.61	33.16	28.47, 32.30	0.865	260
			(5.19, 4.86, 4.56)	(3.93, 4.22, 4.80)	(0.13)	
CsI	55	4.54	35.97	30.81, 34.99	0.885	300
				(4.28, 4.62, 5.28)	(0.15)	
Si	14	2.33	1.84	1.74, 1.83	0.04	53
Ge	32	5.36	11.10	9.88, 10.98	0.49	145
			(1.42, 1.41, 1.21)	(1.19, 1.22)	(0.01)	

© Cambridge University Press • Provided by the NASA Astrophysics Data System

Properties of materials used in X-ray detector systems (cont'd)

	Atomic number, Z	Density (STP) (g cm^{-3})	Shell energy[a] (keV)	X-ray lines[b] (keV)	Fluorescence yield[c]	Energy at which photoelectric equals Compton cross-section (keV)
WINDOWS, FILTERS						
Be	4	1.82	0.111	0.109		14
Mylar	8	1.4	0.532	0.525		
$(C_{10}H_8O_4)_n$	6		0.284	0.277		
Formvar	8	1.2[d]	0.532	0.525		
$(C_5H_7O_2)_n$	6		0.284	0.277		
Polypropylene $(CH_2)_n$	6	0.95[d]	0.284	0.277		22
Air (1.3%Ar,	18	1.29×10^{-3}	3.20	2.96	0.105	27
23.2%O,	8		0.532	0.525		
75.5%N)	7		0.400	0.392		
Mg	12	1.74	1.30	1.25, 1.30	0.02	46
Al	13	2.7	1.56	1.49, 1.55	0.03	50
Fe	26	7.87	7.11 (0.849, 0.722, 0.709)	6.40, 7.06	0.31	135
Ni	28	8.9	8.33 (1.01, 0.877, 0.858)	7.47, 8.27	0.38	140
Cu	29	8.96	8.99 (1.10, 0.954, 0.935)	8.04, 8.91	0.40	145

[a] The first line is the K-shell energy. The three L-shell energies are listed in the parentheses.
[b] The first line for each material gives $K\alpha$ and $K\beta$ energies. $L\alpha$, $L\beta$, and $L\gamma$ are listed in the parentheses.
[c] The first line is the K fluorescence yield. The L fluorescence yield is listed in the parentheses. If the fluorescence yield is less than 1% the space is left blank.
[d] Variable, depending on the detailed preparation of a batch of film.

© Cambridge University Press • Provided by the NASA Astrophysics Data System

Compton telescope for high energy gamma-rays

a) Configuration of a Compton telescope which relies on the detection of scattered photons: S, scatterer; C, collector; A_1, A_2, anticoincidence detectors. b) Basic configuration of a Compton telescope which relies on the detection of secondary electrons. (Adapted from Hillier, R., *Gamma Ray Astronomy*, Clarendon Press, 1984.)

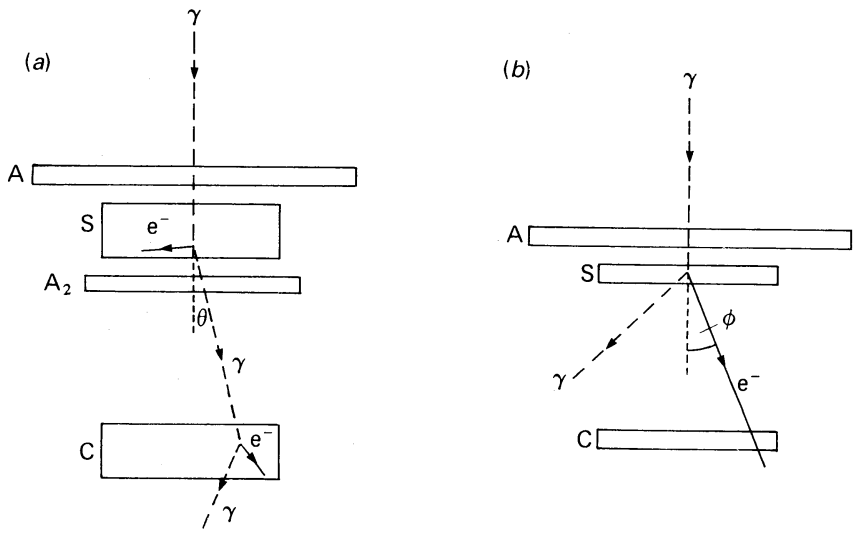

Spark chamber telescope for high energy gamma rays

Diagram showing the basic design of a spark chamber with plates (S), anticoincidence shield (A), and triggering detectors (C_1 and C_2). (Adapted from Hillier, R., *Gamma Ray Astronomy*, Clarendon Press, 1984.)

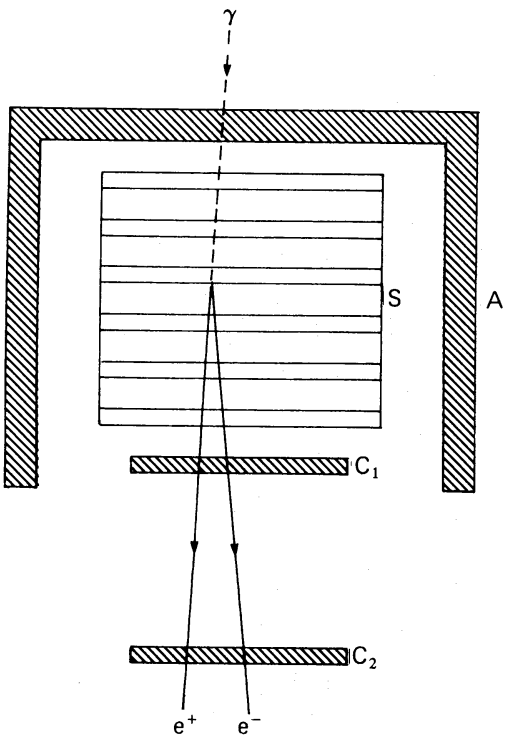

© Cambridge University Press • Provided by the NASA Astrophysics Data System

ASCII character code

This chart shows the ASCII character set and corresponding code numbers, in decimal, hexadecimal and binary form.

Decimal	Binary	Hexadecimal	ASCII character
0	00000000	00	(NUL)
1	00000001	01	(SOH)
2	00000010	02	(STX)
3	00000011	03	(ETX)
4	00000100	04	(EOT)
5	00000101	05	(ENQ)
6	00000110	06	(ACK)
7	00000111	07	(BEL)
8	00001000	08	(BS)
9	00001001	09	(HT)
10	00001010	0A	(LF)
11	00001011	0B	(VT)
12	00001100	0C	(FF)
13	00001101	0D	(CR)
14	00001110	0E	(SO)
15	00001111	0F	(SI)
16	00010000	10	(DLE)
17	00010001	11	(DC1)
18	00010010	12	(DC2)
19	00010011	13	(DC3)
20	00010100	14	(DC4)
21	00010101	15	(NAK)
22	00010110	16	(SYN)
23	00010111	17	(ETB)
24	00011000	18	(CAN)
25	00011001	19	(EM)
26	00011010	1A	(SUB)
27	00011011	1B	(ESC)
28	00011100	1C	(FS)
29	00011101	1D	(GS)
30	00011110	1E	(RS)
31	00011111	1F	(US)
32	00100000	20	(SP)
33	00100001	21	!
34	00100010	22	"
35	00100011	23	#
36	00100100	24	$
37	00100101	25	%
38	00100110	26	Et
39	00100111	27	'
40	00101000	28	(
41	00101001	29	)
42	00101010	2A	*

© Cambridge University Press • Provided by the NASA Astrophysics Data System

ASCII character code *(cont.)*

Decimal	Binary	Hexadecimal	ASCII character
43	00101011	2B	+
44	00101100	2C	,
45	00101101	2D	-
46	00101110	2E	.
47	00101111	2F	/
48	00110000	30	0
49	00110001	31	1
50	00110010	32	2
51	00110011	33	3
52	00110100	34	4
53	00110101	35	5
54	00110110	36	6
55	00110111	37	7
56	00111000	38	8
57	00111001	39	9
58	00111010	3A	:
59	00111011	3B	;
60	00111100	3C	<
61	00111101	3D	=
62	00111110	3E	>
63	00111111	3F	?
64	01000000	40	@
65	01000001	41	A
66	01000010	42	B
67	01000011	43	C
68	01000100	44	D
69	01000101	45	E
70	01000110	46	F
71	01000111	47	G
72	01001000	48	H
73	01001001	49	I
74	01001010	4A	J
75	01001011	4B	K
76	01001100	4C	L
77	01001101	4D	M
78	01001110	4E	N
79	01001111	4F	O
80	01010000	50	P
81	01010001	51	Q
82	01010010	52	R
83	01010011	53	S
84	01010100	54	T
85	01010101	55	U
86	01010110	56	V
87	01010111	57	W
88	01011000	58	X
89	01011001	59	Y
90	01011010	5A	Z

© Cambridge University Press • Provided by the NASA Astrophysics Data System

ASCII character code *(cont.)*

Decimal	Binary	Hexadecimal	ASCII character
91	01011011	5B	[
92	01011100	5C	\
93	01011101	5D	]
94	01011110	5E	^
95	01011111	5F	—
96	01100000	60	‘
97	01100001	61	a
98	01100010	62	b
99	01100011	63	c
100	01100100	64	d
101	01100101	65	e
102	01100110	66	f
103	01100111	67	g
104	01101000	68	h
105	01101001	69	i
106	01101010	6A	j
107	01101011	6B	k
108	01101100	6C	l
109	01101101	6D	m
110	01101110	6E	n
111	01101111	6F	o
112	01110000	70	p
113	01110001	71	q
114	01110010	72	r
115	01110011	73	s
116	01110100	74	t
117	01110101	75	u
118	01110110	76	v
119	01110111	77	w
120	01111000	78	x
121	01111001	79	y
122	01111010	7A	z
123	01111011	7B	{
124	01111100	7C	|
125	01111101	7D	}
126	01111110	7E	~
127	01111111	7F	(DEL)
128	10000000	80	
129	10000001	81	
130	10000010	82	
131	10000011	83	
132	10000100	84	
133	10000101	85	
134	10000110	86	
135	10000111	87	
136	10001000	88	
137	10001001	89	
138	10001010	8A	

© Cambridge University Press • Provided by the NASA Astrophysics Data System

ASCII character code *(cont.)*

Decimal	Binary	Hexadecimal	ASCII character
139	10001011	8B	
140	10001100	8C	
141	10001101	8D	
142	10001110	8E	
143	10001111	8F	
144	10010000	90	
145	10010001	91	
146	10010010	92	
147	10010011	93	
148	10010100	94	
149	10010101	95	
150	10010110	96	
151	10010111	97	
152	10011000	98	
153	10011001	99	
154	10011010	9A	
155	10011011	9B	
156	10011100	9C	
157	10011101	9D	

Boolean algebra

$A = \bar{\bar{A}}$	
$AA = A$	
$A + A = A$	
$A \times 0 = 0$	
$A + 0 = A$	
$A \times 1 = A$	
$A + 1 = 1$	
$A \times \bar{A} = 0$	
$A + \bar{A} = 1$	
$AB = BA$	Commutative law for multiplication
$A + B = B + A$	Commutative law for addition
$(AB)C = A(BC)$	Associative law for multiplication
$A + (B + C) = (A + B) + C$	Associative law for addition
$A(B + C) = AB + AC$	Left distributive law
$(B + C)A = BA + CA$	Right distributive law
$\overline{A + B} = \bar{A}\bar{B}$	De Morgan's laws
$\overline{AB} = \bar{A} + \bar{B}$	De Morgan's laws

© Cambridge University Press • Provided by the NASA Astrophysics Data System

$$AB + A\bar{B} = A$$
$$A + AB = A$$
$$(A + \bar{B})B = AB$$
$$(A + B)(A + \bar{B}) = A$$
$$(A + B)(A + C) = A + BC$$
$$A(A + B) = A$$
$$A\bar{B} + B = A + B$$
$$\bar{A}B + A\bar{B} = A \oplus B \qquad \text{Exclusive OR}$$

Logic gates

Summary of the elementary positive and negative logic gates. (The positive logic gates in the left column are equivalent to the corresponding negative gates in the right column.)

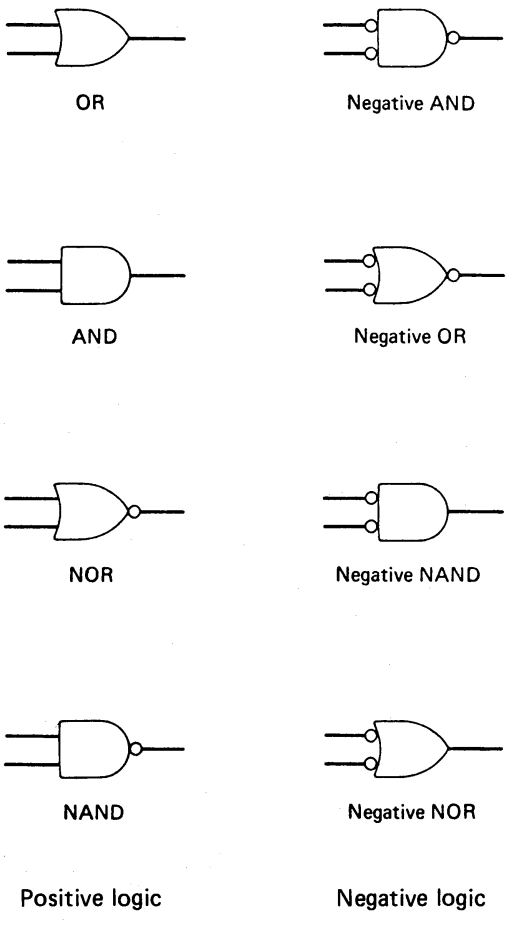

© Cambridge University Press • Provided by the NASA Astrophysics Data System

© Cambridge University Press • Provided by the NASA Astrophysics Data System

The RS-232-C standard

The RS-232-C serial interface standard defines the binary state 1 as a voltage level between −3 V and −15 V. The binary state 0 can range from +3 V to +15 V. (Adapted from Libes, S. and Garetz, M. *Interfacing to S-100/IEEE Microcomputers*, Osborne/McGraw-Hill, Berkeley, CA.)

DB-25 type connector

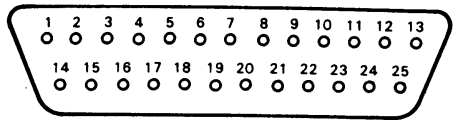

Female Connector as Viewed from Wiring Side

Pin Number	EIA Name	RS-232-C Common Mnemonic	Description
1	AA		Protective ground
2	BA	TxD	Data transmitted from terminal
3	BB	RxD	Data received from modem
4	CA	RTS	Request to send
5	CB	CTS	Clear to send
6	CC	DSR	Data set ready
7	AB		Signal ground
8	CF	DCD	Carrier detector
9	•		Reserved for Data Set Testing
10	•		Reserved for Data Set Testing
11	•		Unassigned
12	SCF		Secondary carrier detector
13	SCB		Secondary clear to send
14	SBA		Secondary transmitted data
15	DB		Transmitted bit clock, from DCE
16	SBB		Secondary received data
17	DD		Received bit clock
18	•		Unassigned
19	SCA		Secondary request to send
20	CD	DTR	Data terminal ready
21	CG		Signal quality detector
22	CE		Ring indicator (used by auto answer equipment)
23	CH/CI		Data signal rate selector
24	DA		Transmitted bit clock, from DTE
25	•		Unassigned

*Undefined

RS-232-C Connector and Pin definitions
DTE: data terminal equipment
DCE: data communications equipment

Modem-Terminal

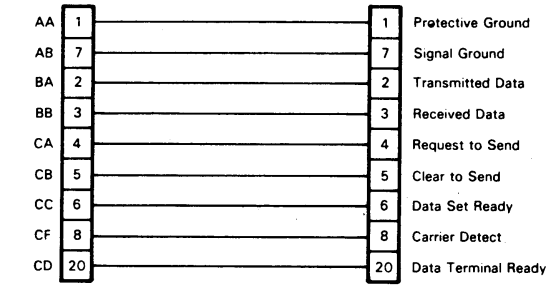

Computer-Terminal

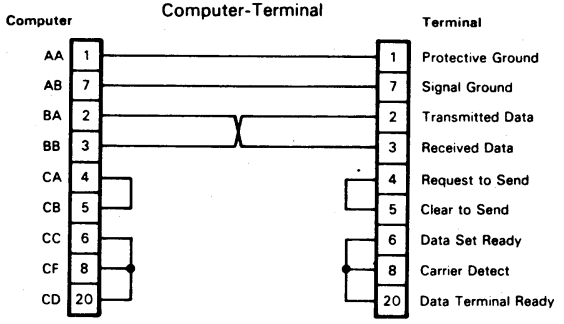

RS-232 Cable Wiring

RS-232-C Signal Level Conventions

Notation	Interchange Voltage	
	Negative	Positive
Signal Condition	Marking	Spacing
Binary State (data lines)	1	0
Function (control lines)	OFF	ON

Parallel interface

Centronics interface connector pinouts as they appear on the IBM PC's 25-pin D-shell connector. The pin connections on the printer end are the same for lines 1–14 and 19–25 but differ somewhat on the other lines, since a 36-pin connector is used there. (From Sargent, M. & Shoemaker, R., *The IBM PC from the Inside Out*, Addison-Wesley, 1986, with permission.)

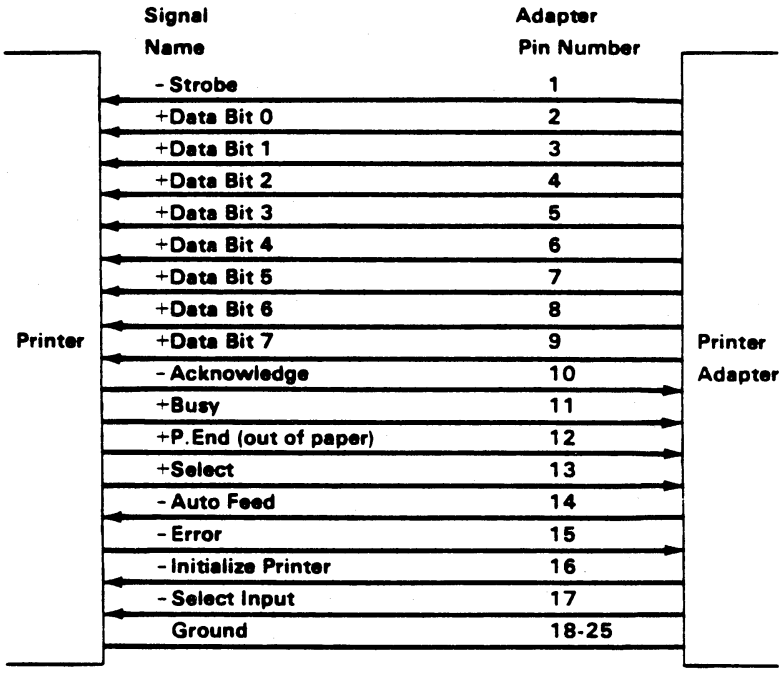

© Cambridge University Press • Provided by the NASA Astrophysics Data System

IEEE 488 interface

Example of an IEEE 488 interface bus (GPIB) configuration. (Intel Corp.)

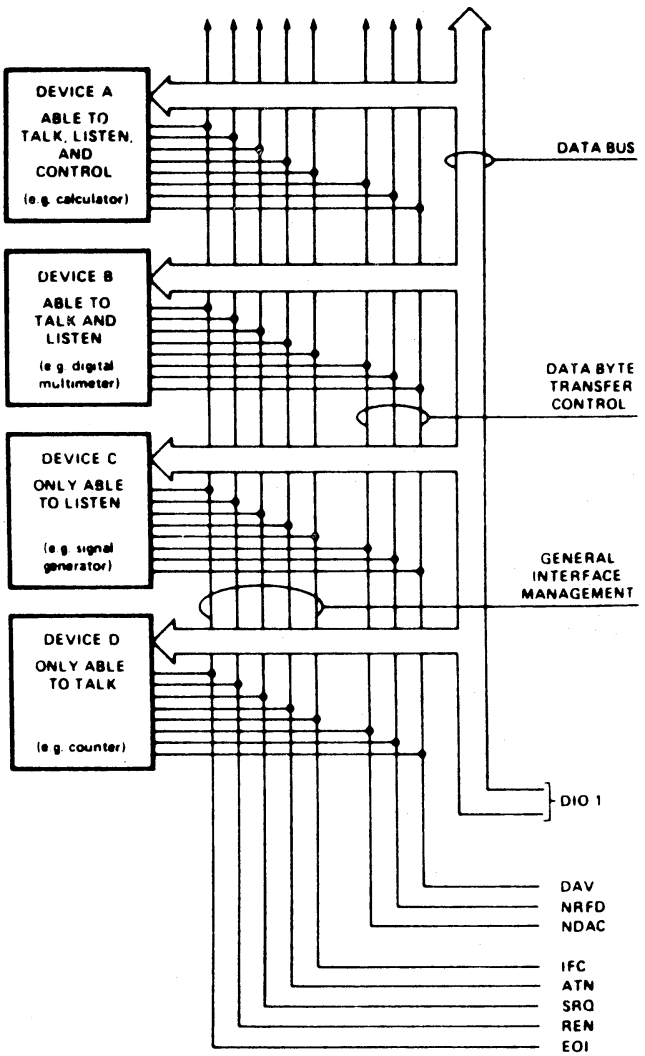

DAV data valid
NRFD not ready for data
NDAC not data accepted
IFC interface clear
ATN attention
SRQ service request
REN remote unable
EOI end or indentify

© Cambridge University Press • Provided by the NASA Astrophysics Data System

Data transmission

Data transmission nomogram.
Transmission time (s) = size (bytes)/data rate (byte s^{-1})
(1 byte = 8 bits; T1 and T3 are telephone transmission standards.)

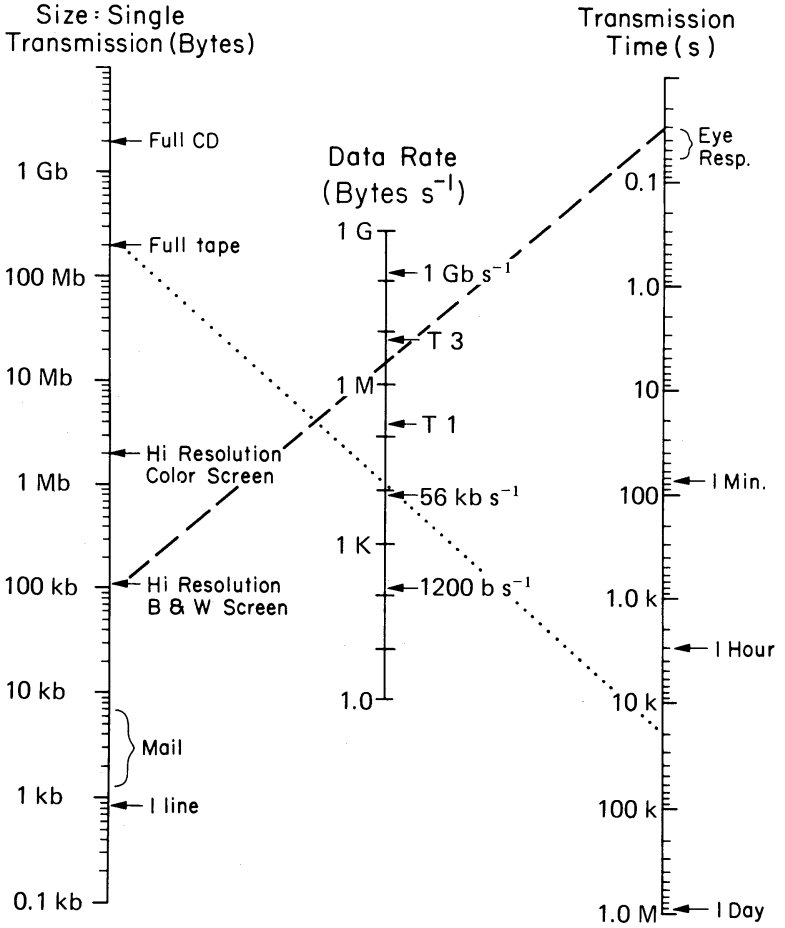

Bibliography

Techniques of Vacuum Ultraviolet Spectroscopy, Samson, J. A. R., John Wiley and Sons, 1967.

The Atomic Nucleus, Evans, R. B., McGraw-Hill Book Company, 1955.

Handbook of Chemistry and Physics, CRC Press, 1979.

Table of Isotopes, C. M. Lederer & V. S. Shirley, eds., John Wiley and Sons, 1978.

'Low energy X-ray interaction coefficients: photoionization, scattering, and reflection', Henke, B. L. *et al.*, *Atomic Data and Nuclear Data Tables*, **27**, no. 1, 1982.

Vacuum Technology and Space Simulation, NASA SP-105, US Government Printing Office, 1966.

'X-ray wavelengths', Bearden, J. A., *Rev. Mod. Phys.*, **39**, 78, 1967.

X-ray Data Booklet, Lawrence Berkeley Laboratory, PUB-490 Rev., University of California, 1986.

© Cambridge University Press • Provided by the NASA Astrophysics Data System